

Investigation of the Semi-Empirical Method for Force Limited Vibration Testing

Vijayamohan Rao Dharanipathi

A Thesis
in
The Department
of
Mechanical and Industrial Engineering

Presented in the partial fulfillment of the requirements
For the degree of Master of Applied Science (Mechanical Engineering) at
Concordia University,
Montreal, Quebec, Canada.

September 2003.

© Vijayamohan Rao Dharanipathi.

National Library
of Canada

Bibliothèque nationale
du Canada

Acquisitions and
Bibliographic Services

Acquisitions et
services bibliographiques

395 Wellington Street
Ottawa ON K1A 0N4
Canada

395, rue Wellington
Ottawa ON K1A 0N4
Canada

Your file *Votre référence*

ISBN: 0-612-83881-1

Our file *Notre référence*

ISBN: 0-612-83881-1

The author has granted a non-exclusive licence allowing the National Library of Canada to reproduce, loan, distribute or sell copies of this thesis in microform, paper or electronic formats.

L'auteur a accordé une licence non exclusive permettant à la Bibliothèque nationale du Canada de reproduire, prêter, distribuer ou vendre des copies de cette thèse sous la forme de microfiche/film, de reproduction sur papier ou sur format électronique.

The author retains ownership of the copyright in this thesis. Neither the thesis nor substantial extracts from it may be printed or otherwise reproduced without the author's permission.

L'auteur conserve la propriété du droit d'auteur qui protège cette thèse. Ni la thèse ni des extraits substantiels de celle-ci ne doivent être imprimés ou autrement reproduits sans son autorisation.

Canada

ABSTRACT

Investigation of the Semi-Empirical Method for Force Limited Vibration Testing

Vijayamohan Rao Dharanipathi

Conventional vibration testing of aerospace hardware is normally performed by controlling the acceleration input to the base of a test item to the specifications, namely the envelope of the acceleration peaks of the flight environment. This conventional approach to testing has been known for over forty years to greatly overtest the test item at its own natural frequencies. In the nineties, NASA JPL led the development and implementation of an improved method called Force Limited Vibration (FLV) testing. In addition to controlling the input acceleration, the FLV testing measures and limits the reaction forces between the test item and the shaker. This force limiting technique results in acceleration notching at predominant natural frequencies of the test item. Because of its numerous advantages, the semi-empirical method is presently the approach most widely applied to derive the force limits. Due to its partly empirical nature, the crucial coefficient, C^2 , still requires some judgment for its selection. Although the semi-empirical method is very powerful and has been implemented successfully on several space missions, there is still some work required to realize it and make it acceptable to everyone.

The objective of this study is to present a comprehensive and complete analytical and experimental investigation on the semi-empirical method. Design optimization of test item, mounting structure and fixture using finite element method, conducting in-depth analytical and experimental sensitivity studies to investigate the semi-empirical method and affecting parameters and documenting a comprehensive benchmark problems are

among the most important contributions of this thesis. More specifically, the present work investigates the range of value C^2 which might be expected for space hardware and the parameters on which it depends. Based on an evaluation of more than 70 different cases, the analytical sensitivity study shows that most of the C^2 values falls within the range of 2 to 5 found in the literature; however, there are several cases for which C^2 was higher than 5, with 5 of them being between 10 to 17. The experimental sensitivity study validates the procedures and the results obtained in the analytical sensitivity study.

ACKNOWLEDGMENT

I wish to express my highest gratitude to my supervisors Dr. Ramin Sedaghati and Dr. Yvan Soucy for their encouragement, guidance and instruction and I am fortunate to have supervisors like them. They have been supportive throughout the period of my thesis. I am thankful to Dr. Sedaghati for constantly supporting and provided helpful suggestions during the course of the study. Dr. Soucy has helped me significantly to better understand the force limited vibration-testing procedure. I am indebted to my supervisors for morally supporting me in the time of need.

I would like to thank Mr. Daniel Levesque in Canadian Space Agency (CSA), whose broad knowledge of FEM, his valuable suggestions and helpful comments made a significant impact in the current research. I also want to thank Dr. Terry Scharton formerly with Jet Propulsion Laboratory for his guidance in proper selection of mounting structure, Andre Cote formerly with EMS Technologies whose suggestions helped in estimation of total interface force, Mr. Raj Singhal of DFL for lending the required load cells for the experimentation and Philippe Tremblay of Maya Heat Transfer for providing guidance in the initial phase of the project. My thanks are extended to Mr. Ralph Nolting and Mr. Pierre Lortie of CSA who helped in manufacturing of the required structures for the completion of the project.

I want to extend my gratitude to my friends in and around Concordia who have been there for me when required the most. I personally want to thank Chandra Sekhar, Nagaraju, Laxmi Narayana, Raghu Kumar, Vamsi Mohan, Chandra Mouli, Sanjeev Kumar, Venu Madhav and Sainath.

Finally I want to thank my parents Mr. D.Venkateswara Rao and Mrs. D. Vijaya Laxmi without whose love and continuous support this would not have been possible I also extend my gratitude to my uncles Dr, C.J. Rao and Dr, C.S. Rao.

I dedicate the current work to my sister late Mrs. Hima Bindu, Y.

TABLE OF CONTENTS

| | |
|---|------|
| ABSTRACT | iii |
| ACKNOWLEDGMENTS | v |
| TABLE OF CONTENTS | vi |
| LIST OF FIGURES | ix |
| LIST OF TABLES | xiii |
| | |
| Chapter 1: INTRODUCTION | |
| 1.1 Problem Statement and Motivation | 1 |
| 1.2 State of the Art | 3 |
| 1.3 The Vibration Overtesting Problem | 9 |
| 1.3.1 Vibration Absorber Effect and its Relation to the Overtesting Problem | 11 |
| 1.3.2 Procedures to Overcome the Vibration Overtesting Problem | 16 |
| 1.4 Mechanical Impedance Characteristics | 21 |
| 1.4.1 Apparent Mass | 22 |
| 1.4.2 Effective Mass | 22 |
| 1.4.3 Residual Mass | 23 |
| 1.4.4 Relation Between Interface Force and Interface Acceleration | 25 |
| 1.5 Force Limits | 27 |
| 1.5.1 Coupled Source/Load System | 28 |
| 1.5.2 Semi-Empirical Method | 30 |
| 1.6 Present Study | 31 |
| 1.7 Thesis Organization | 32 |
| | |
| Chapter 2: DESIGN AND ANALYSIS OF STRUCTURES | 35 |
| 2.1 Design Requirements | 35 |
| 2.1.1 Test Article Requirements | 36 |
| 2.1.2 Fixture Requirements | 42 |
| 2.2 Design of Test Structures | 43 |
| 2.2.1 Test Items | 43 |

| | |
|--|-----|
| 2.2.2 Mounting Structure | 53 |
| 2.2.3 Test Fixtures | 59 |
| Chapter 3: ANALYTICAL SENSITIVITY STUDY FOR ESTIMATION OF | |
| C² PARAMETERS | 68 |
| 3.1 Description of Analytical Cases | 68 |
| 3.1.1 Naming of Cases at the System Level | 71 |
| 3.1.2 Naming of Cases at the Test Item Level | 72 |
| 3.2 Procedures for Estimating of C ² . | 75 |
| 3.3 Sensitivity Study Results | 88 |
| 3.3.1 C ² value and the Relative Parameters | 97 |
| 3.3.2 Notch Value | 105 |
| 3.4. Summary and Conclusion | 105 |
| Chapter 4: EXPERIMENTAL SENSITIVITY STUDY FOR ESTIMATION OF | |
| C² PARAMETERS | 107 |
| 4.1 Selection of Case Studies | 107 |
| 4.2 Test Procedures | 109 |
| 4.3 Description of Test Equipment | 111 |
| 4.4 Testing in X Direction | 114 |
| a) Validation of Test Fixture | 114 |
| 1) Test Description and Instrumentation | 114 |
| 2) Test Results and Comparison with Analytical Results | 116 |
| b) Driven-Based Modal Survey of Mounting Structure | 117 |
| 1) Test Description and Instrumentation | 117 |
| 2) Test Results and Comparison with Analytical Prediction | 120 |
| c) Low level Random Testing of Test Item | 123 |
| 1) Test Description and Instrumentation | 123 |
| 2) Test Results and Comparison with Analytical Prediction | 126 |
| d) System Level Random Vibration Testing | 128 |
| 1) Test Description and Instrumentation | 128 |
| 2) Test Results and Calculation of C ² Value | 130 |
| 4.5 Testing in Z Direction | 132 |

| | |
|---|-----|
| a) Validation of Test Fixture | 132 |
| 1) Test Description and Instrumentation | 132 |
| 2) Test Results and Comparison with Analytical Results | 134 |
| b) Driven-Based Modal Survey of Mounting Structure | 136 |
| 1) Test Description and Instrumentation | 136 |
| 2) Test Results and Comparison with Analytical Prediction | 137 |
| c) Low level Random Testing of Test Item | 139 |
| 1) Test Description and Instrumentation | 139 |
| 2) Test Results and Comparison with Analytical Prediction | 140 |
| d) System Level Random Vibration Testing | 142 |
| 1) Test Description and Instrumentation | 142 |
| 2) Test Results and Calculation of C^2 Value | 144 |
| 4.6 Demonstration of FLV Notching | 146 |
| 4.7 Results and Conclusion | 152 |
| | |
| Chapter 5: CONCLUSIONS AND RECOMMENDATIONS | 156 |
| 5.1 Summary | 156 |
| 5.2 Conclusion | 158 |
| 5.3 Recommendations for Future Work | 159 |
| | |
| REFERENCES | 161 |
| | |
| APPENDIX | 165 |

LIST OF FIGURES

| | | |
|-------|--|----|
| 1-1. | Simple 2 DOF coupled system and load in vibration test configuration. | 12 |
| 1-2. | System interface acceleration for Vibration Absorber Effect. | 13 |
| 1-3. | Load apparent mass for Vibration Absorber Effect. | 15 |
| 1-4. | System interface force | 15 |
| 1-5. | Physical interpretation of effective and residual mass concepts | 23 |
| 2-1. | Test item with provision for lumped masses | 45 |
| 2-2. | Simplest possible test item for vibration testing in X direction (but the X shaped stiffening member is replaced with cross member) | 50 |
| 2-3. | Robust possible structure (test item) for vibration testing in X direction | 51 |
| 2-4. | Simplest possible structure for vibration testing in Y direction | 52 |
| 2-5. | Robust possible structure for vibration testing in Y direction | 52 |
| 2-6. | Top plate of the Mounting structure, indicating the variation in thickness of the plate | 54 |
| 2-7. | Medium plate of the mounting structure, the edges were cut to increase the flexibility | 56 |
| 2-8. | Mounting Structure indicating the attachment points for the test item | 58 |
| 2-9. | Location and thickness details of the flanges | 63 |
| 2-10. | Fixture for vibration testing of test item and mounting structure in vertical direction (Z) | 67 |
| 2-11. | Fixture for testing of test item and mounting structure in the lateral directions (X & Y) | 67 |
| 3-1. | Attachment points of the test item | 70 |
| 3-2. | Description of test name at the system level | 71 |
| 3-3. | Description of test name at the test item level | 72 |

| | | |
|-------|---|-----|
| 3-4. | Finite element model of test item used to find the apparent mass, and the node simulating the fixture beneath the test item | 79 |
| 3-5. | Apparent mass of the test item for 4pt_4r_cpl_wo_z configuration | 79 |
| 3-6. | Coupled System consisting Test Item and the Mounting Structure | 81 |
| 3-7. | Acceleration input to the base of mounting structure at the coupled system level | 82 |
| 3-8. | Interface accelerations at 4 attachment points and the envelope of accelerations | 83 |
| 3-9. | Total force PSD for 4pt_4r_two_mwo for excitation in Z direction | 86 |
| 3-10. | Force at the base of the test item at the instrument level and the force limit with a C^2 value of 3.6 | 88 |
| 3-11. | The C^2 versus effective mass ratio in the lateral direction | 97 |
| 3-12. | The C^2 value versus the effective mass ratio in the vertical direction | 98 |
| 3-13. | The C^2 value versus the effective mass ratio in the lateral direction for different attachment points | 99 |
| 3-14. | The C^2 value versus the effective mass ratio in the vertical direction for different attachment points | 101 |
| 3-15. | System interface acceleration for different stiffness of the load (test item) | 104 |
| 4-1. | Test Fixture for lateral test | 116 |
| 4-2. | Acceleration response at attachment points of test item on the fixture | 117 |
| 4-3. | Mounting Structure without lumped mass in the burst random testing in the lateral direction | 119 |
| 4-4. | Mounting Structure with lumped mass in the burst random testing in the lateral direction | 119 |
| 4-5. | The FRF response of accelerometers located on the side plates of the mounting structure without lumped mass | 122 |

| | | |
|-------|--|-----|
| 4-6. | The FRF response of accelerometers located on the side plates of the mounting structure with lumped mass | 122 |
| 4-7. | Test item without lumped mass and with 8 attachment points for low level random testing in X direction | 124 |
| 4-8. | Test item with lumped mass and with 4 attachment points for low level testing in X direction | 125 |
| 4-9. | Force sensors at the attachment points to measure the apparent mass of the test item | 125 |
| 4-10. | Apparent Mass of the test item for 4pt_4r_cpl_wo configuration | 127 |
| 4-11. | System level testing of test item fixed at 4 attachment points in X direction | 129 |
| 4-12. | Force sensors and the interface accelerometers at the system level testing in X direction | 130 |
| 4-13. | Interface acceleration for 4pt_4r_two_2mwl configuration | 131 |
| 4-14. | Interface Force for 4pt_4r_two_2mwl configuration | 132 |
| 4-15. | Test fixture for Z direction and the response accelerometers | 133 |
| 4-16. | Control accelerometers location on the shaker | 134 |
| 4-17. | FRF of response accelerometers located at the attachment points of the test item on the top plate of the fixture | 135 |
| 4-18. | Mounting Structure with lumped mass in driven-base burst random testing configuration for Z direction | 136 |
| 4-19. | Control and response accelerometers for burst random testing of mounting structure for Z direction | 137 |
| 4-20. | The FRF of acceleration response of the accelerometer located on the top plate of the mounting structure without lumped mass | 138 |
| 4-21. | The FRF of acceleration response of the accelerometer located on the top plate of the mounting structure with lumped mass | 138 |

| | | |
|-------|--|-----|
| 4-22. | Test item attached at 8 attachment points without lumped mass for low level random testing in Z direction | 139 |
| 4-23. | Test item with lumped mass and attached at 4 attachment points for low-level random testing in Z direction | 140 |
| 4-24. | Apparent mass of the test item for 4pt_4r_cpl_wo configuration in z direction | 142 |
| 4-25. | Test setup and instrumentation for system level testing of 4pt_4r_two_mwl configuration | 143 |
| 4-26. | Interface accelerometers at 4-point configuration (4pt_4r_two_mwl) | 143 |
| 4-27. | Interface acceleration for 4pt_4r_two_2mwl configuration | 145 |
| 4-28. | Interface force for 4pt_4r_two_2mwl configuration | 145 |
| 4-29. | Interface accelerations for 4pt_4o_two_2mwl and the input acceleration (envelope) for testing of test item by itself | 148 |
| 4-30. | Interface force at the system level for 4pt_4o_two_2mwl configuration | 150 |
| 4-31. | Control acceleration input to the test item for 4pt_4o_ystf_wo configuration | 150 |
| 4-32. | Forces on test item for 4pt_4o_ystf_wo configuration | 151 |

LIST OF TABLES

| | | |
|-------|--|-----|
| 2-1. | Natural frequencies and effective masses of the test item with and without lumped mass | 49 |
| 2-2. | Natural frequencies of mounting structure with and without lumped mass and attached at 8 attachment points | 59 |
| 2-3. | Natural frequencies of mounting structure with and without lumped mass and attached at 16 attachment points | 59 |
| 2-4. | Natural frequencies of the test fixtures and their corresponding effective mass and the direction in which it is obtained | 66 |
| 3-1. | The possible cases for stiffening members | 74 |
| 3-2. | Impedance characteristics of the test structures at the natural frequency of the test item in the lateral directions (X and Y) | 91 |
| 3-3. | Interface acceleration and force and corresponding C^2 value in the lateral direction for $Q=50$ and 20 , i.e. $\xi = 0.01$ and 0.025 | 92 |
| 3-4. | Apparent Mass of test item at its fundamental frequency and the notch value in the lateral direction for $Q=50$ and 20 , i.e. $\xi = 0.01$ and 0.025 | 93 |
| 3-5. | Impedance characteristics of the test structures at the natural frequency of the test item in the vertical direction (Z) | 94 |
| 3-6. | Interface Acceleration and Force and corresponding C^2 value in the vertical direction for $Q=50$ and 20 , i.e. $\xi = 0.01$ and 0.025 | 95 |
| 3-7. | Apparent Mass of test item at its fundamental frequency and the notch value in the vertical direction for $Q=50$ and 20 , i.e. $\xi = 0.01$ & 0.025 | 96 |
| 3-8. | Configuration of Cases for the Figure 3-13 | 100 |
| 3-9. | Configuration of Cases for the Figure 3-14 | 102 |
| 3-10. | Comparison of C^2 value between the lateral and vertical directions | 103 |
| 4-1. | Fundamental frequency (Hz) of the mounting structure in X-direction | 120 |
| 4-2. | Fundamental frequency (Hz) of the test item in X-direction | 127 |
| 4-3. | Fundamental frequency (Hz) of the mounting structure in Z-direction | 137 |

| | | |
|------|--|-----|
| 4-4. | Fundamental frequency (Hz) of the test item in Z-direction | 141 |
| 4-5. | The acceleration input and corresponding force limit for testing of test item with FLV procedure | 149 |
| 4-6. | The C^2 values in X direction | 152 |
| 4-7. | The C^2 values in Z direction | 153 |

CHAPTER 1

INTRODUCTION

1.1. Problem Statement and Motivation

The primary goal of vibration testing of aerospace hardware is to identify problems, which if not remedied, would result in flight failures due to the extreme conditions of the launch environments. Thorough testing is essential to ensure that the system performance meets design requirements and that adequate margins are demonstrated to reduce the probability of flight/mission failures. Generally any aerospace hardware is vibration tested to 1: Determine if designs meet performance requirements, 2: Verify that the built system will function and survive the launch as it is designed, and 3: Verify design margins and system robustness.

In conventional vibration testing of aerospace hardware, the acceleration input to the base of a test item is controlled to the specifications, namely the envelope of the acceleration peaks of the flight environment. This conventional approach to testing has been known for over forty years to greatly overtest the test item at its own natural frequencies. This mainly occurs due to the impedance differences of the mounting structure between the flight and the testing environments. The penalty of overtesting with conventional vibration test appears in design and performance compromises, as well as in the high costs and schedule slippage associated with recovery from artificial test failures that would have not occurred in a flight environment.

The purpose of Force Limited Vibration (FLV) testing is to reduce the overtesting occurring during conventional vibration testing. In addition to controlling the input acceleration, the FLV testing measures and limits the reaction force between the test item and the shaker. This force limiting technique results in acceleration notching at predominant natural frequencies of the test item. The approach has been developed at NASA Jet Propulsion Laboratory (JPL) and has been used successfully during the last decade in several space missions (including complete Cassini spacecraft [1]). The FLV approach has also been validated with system level acoustic testing and with limited flight data. Other NASA centers and some U.S. companies (e.g. Orbital Sciences) have implemented FLV testing on numerous flight missions. Recently, FLV testing has been used in Canada within three space programs, i.e. SciSat-1 [2], MOST and CloudSat.

The semi-empirical method is presently the approach most widely applied to derive the force limits between the test item and the shaker. The advantages of the semi-empirical method over previously-developed more analytical techniques (the so called simple and complex two-degree-of-freedom system (TDFS) methods) are significant and have greatly contributed to the widespread acceptance of FLV technology presently taking place in the aerospace community. The two main advantages of the semi-empirical method are: (1) the simplicity of the technique as compared to the TDFS methods, and (2) there is no need of impedance information for the mounting structure.

Although the semi-empirical method seems to be very powerful and promising, there is still some work to make it acceptable to everyone. Due to its partly empirical nature, the

crucial coefficient, C^2 , which sets the force limits throughout the frequency bandwidth of excitation is based either on the extrapolation of interface forces for similar mounting structures and test items, or on comparison with results of techniques such as the TDFS methods or the limit load factors. Based on limited number of flight data, it has been observed that, in normal conditions, C^2 value as low as 2 might be chosen for complete spacecraft or strut-mounted heavier equipment, C^2 value as high as 5 might be considered for directly mounted lightweight test items. However there is not enough experimental investigation to define the range of C^2 .

The objective of the present thesis is to present a comprehensive and complete analytical and experimental investigation on the semi-empirical method. The present study provides a platform to acquire a better understanding of the semi-empirical method so that it can be used in aerospace community more comfortably.

1.2. State of the Art

As early as 1950 many pioneers of the aerospace mechanics recognized that the low mechanical impedance of lightweight mounting structures would lead to overtesting of aerospace equipment. Not much could be done efficiently until 90's to overcome the overtesting, as proper tools were not available to simulate mechanical impedance in vibration tests. It is very important to have more realistic vibration test procedures in today's faster, better and cheaper environment. For the past five decades various procedures have been proposed and implemented to overcome the vibration overtesting problem, which is summarized below.

To overcome the overtesting of mechanical equipment at the significant frequencies, which occurs due to the general procedure of overlapping the acceleration peaks, Blake [3] proposed a complex conceptual solution, where the impedance characteristics of the mounting structure are simultaneously measured by small shaker and emulated by the test shaker.

Simulating the impedance of mounting structure by employing force transducers between the test item and shaker was proposed by Morrow [4]. However exact impedance simulation of mounting structure, phase included was not, and still is not, possible at the test item level.

To overcome the overtesting two methods were proposed by Slater [5], 1) response limiting at multiple points to reduce the impact of fixture at resonances, and 2) force limiting to account for the vibration absorber effect at the test item resonances. He also proposed the maximum force limit/force limit for force limited test would be 1.5 times the product of mass and peak acceleration or input acceleration for vibration testing. This procedure later gave impetus for new method in force limited vibration test called semi empirical method. An equalizer was designed and tested for shaker by Ratz [6], which uses force feedback to simulate the mechanical impedance of the equipment mounting structure.

An experimental investigation of sinusoidal vibration test conducted on aircraft components by Painter [7] using dual control of force and acceleration. The envelopes of interface force and acceleration between the simulated equipment and aircraft fuselage control the input to the shaker. It is found that the overtesting of the equipment is reduced to a greater extent by employing the above procedure of controlling force and acceleration.

A vibration test procedure is developed by Murfin [8], which employs the dual control procedure, in which the product of input acceleration and the smoothed apparent mass obtain the force specification. This procedure is similar to the semi empirical method of force limited vibration testing, where the impedance of the mounting structure is ignored. In dual control, the force and acceleration control signals are analyzed in narrow bands, and in each band the shaker drive signal is adjusted until one or the other of the specifications is attained. This typically results in acceleration control off resonances and force control, and acceleration notches, at the resonances.

Special methods were developed by Witte and Rodman [9] and later by Hunter and Otts [10], to use simple parametric models to study the dynamic absorber effect and to smooth the apparent mass of the test item to implement the Murfin's dual control method.

A technique for obtaining an equivalent single-degree-of-freedom system (SDFS) for each eigen-vector when the dynamic characteristics of the structure are available in the form of a finite element model (FEM) or as test data was developed by Wada, Bamford,

and Garba [11]. The masses of these SDFS's are called the "effective mass" which may be defined as the mass terms in a modal expansion of the drive point apparent mass of a kinematically supported system. The effective masses are independent of the modal normalization, and the sum of the effective masses of all modes is equal to the total mass. A complementary term is the residual mass, which is defined as the difference between the total mass and the effective masses of all the modes with natural frequencies lower than the frequency of interest. The effective mass and residual mass are used to characterize the mechanical impedance of both the mounting structure and the test item for the TDFS methods for computing the force limits.

Scharton [12] describes application of force limited vibration testing to nine JPL flight hardware projects, one of which is the complete TOPEX spacecraft tested at NASA Goddard Space Flight Center. Two of the cases include validation data that show that the force limited vibration test of the components are still conservative compared with the input data obtained from vibration tests and acoustic tests at higher levels of assembly.

A method to calculate the force limits by evaluating the test item dynamic mass at the coupled system resonance frequencies by considering a Two-Degree of Freedom-System (TDFS) was developed by Scharton [13]. Application of this method to a simple (S-TDFS) and to a complex (C-TDFS) coupled oscillator system yields non-dimensional analytical results which may be used to calculate limits for future force limited vibration tests. The analysis for the simple system provides an exact, closed form result for the peak force of the coupled system and for the notch depth in the vibration test. The

analysis for the complex system provides parametric results that contain both the effective modal and residual masses of the test item and mounting structure and is therefore well suited for use with FEM models.

The Monograph for the force limited vibration testing, which discusses the history, theory and applications of FLV testing was written by Scharton [1]. The monograph also discusses the implementation of FLV on CASSINI spacecraft, for which the force limits for various parts of the spacecraft are obtained by the semi-empirical method of FLV testing, which requires only the interface accelerations/input acceleration and data from low level pre-test to obtain the apparent mass of the test item. The force limits obtained by semi empirical method are compared with the TDFS methods and the acoustic tests.

Comparison of the flight data obtained using Spacecraft Launch Acceleration Measurement (SLAM) system during the launch and the force and acceleration specifications used for testing of Cosmic Ray Isotope Spectrometer (CRIS) of Advanced Composition Explorer (ACE) spacecraft during ground level testing done by Scharton [15] confirm that the acceleration input at the ground level testing were approximately 20 dB higher than the flight data measured, and the flight force measurements agree with the force limits specified during the test level (obtained from semi empirical and simple TDFS methods).

Validation of force limiting vibration testing is done by Worth and Kaufman [16]. A simple structure was flown on a Black-Brant sounding rocket and instrumented with

force sensors and accelerometers. The results during the flight tests were compared to the predicted results, which were performed prior to the flight tests. The acceleration and force specifications for the first mode during the random tests were conservative with respect to the measured data from the flight test.

Scharton [17] compared the force limits measured on a space shuttle flight to the force specifications used during the ground level random vibration test. The flight data was in agreement with the force limits obtained using semi empirical method. The vibration loads obtained from the flight data was one and a half times less than those specified in the shuttle payload design guide.

Chang [18] derived for a simplified formula for a SDFS for predicting the structural test loads. By properly choosing the semi empirical force specification factor C^2 along the predominant resonant frequency, the force limited vibration will result in test loads comparable with the design limit loads derived from Mass Acceleration Curve.

Handbook for FLV testing written by Scharton [19] discusses the instrumentation involved in the vibration testing, methods of deriving the force limits and the implementation of FLV testing.

Second validation of FLV testing of the series of validation tests performed by Kaufman and Worth [20] in which they compared the force limits obtained by various methods with the flight data. The results indicate that the semi-empirical method (using a

surprising low C^2 value of 1) is least conservative than the rest of the methods, and 2) CTDFS was found to provide the most conservative force limits.

Amato, Pankow and Thomsen [21] implemented FLV testing on HESSI imager; the FLV reduced unnecessary overtesting and reduced the acceleration specifications at the imager resonances. The loads applied to the most of the sensitive imager components are reduced by a factor of 2 or better as compared to the acceleration controlled testing without FLV.

Vibration qualification testing of Deep Space-1 spacecraft is done by FLV testing by Chang [22]. The force limits for the test are calculated by semi empirical force limit procedure.

Soucy et al. [2] implemented FLV testing on Fourier Transform Spectrometer (FTS) instrument of the SCISAT-1, which happened to be the first vibration test implementing FLV by the Canadian space program. The values of C^2 used to test the structure in all the directions are 10, 8 and 4 in Z, Y and X directions respectively. The C^2 value in two of the three directions was above the nominal range of 2 to 5 as mentioned in most part of the literature, confirming the need for the current study of investigation of semi empirical method of FLV testing.

1.3. The Vibration Overtesting Problem

As specified earlier random vibration testing of a space structure is performed to ensure that the structure will survive the launch environment. The structure would ideally be

subjected to acceleration and forces similar to the ones encountered in the flight during the launch and sometimes with an acceptable margin. However, because of the high complexity associated with such attempts partly due to the statistical nature of the launch environment, and to controller limitation (especially for older versions), this ideal situation is not really practical and has been replaced by testing procedures which often generates high vibrations at certain critical frequencies of the test item. The conventional practice for specifying the input excitation for vibration testing is to envelop the launch interface acceleration spectra obtained normally from analytical methods such as couple load analysis [1].

The main cause of overtesting is the difference in boundary conditions between test and flight configurations. During a vibration test, the test article is usually attached to a very rigid fixture and is excited or driven along a single linear direction, with the structure being completely restrained along the other five degrees-of-freedom (d.o.f.). In the flight configuration, the test article is attached to a mounting structure, which normally exhibits some flexibility in all six d.o.f. in the frequency range of interest.

The flexibility difference in the direction of excitation is the main contributor to the overtesting phenomenon. In the flight configuration, the acceleration at the interface between the mounting structure and the test item drops at certain frequencies, resulting in valleys in the acceleration spectra. These frequencies correspond to the resonance frequencies of the test item when attached to a rigid support (as on a shaker). This phenomenon is known as the vibration absorber effect. On the other hand, during a vibration test, the

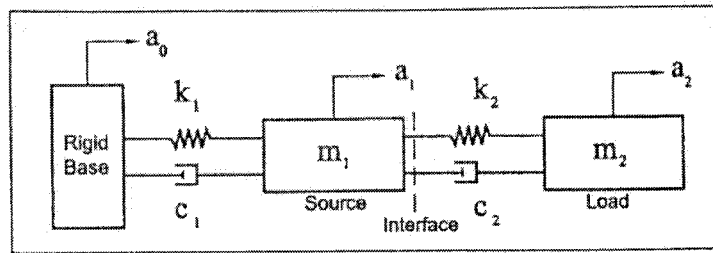
structure is excited with a specified input acceleration, which is the envelope of the flight interface acceleration, despite the amplitude drop in the flight configuration. This results in exaggerated amplification of input forces, and internal stresses, at the resonance frequencies of the test item, i.e. overtesting.

1.3.1. Vibration Absorber Effect and its Relation to the Overtesting Problem

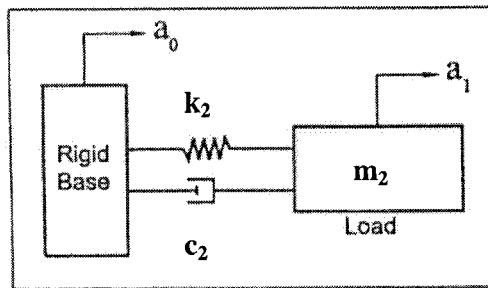
Consider the simple vibratory system of Figure 1-1 consisting of two oscillators connected in series (2 DOF system). The main oscillator (Source) is vibrated through the motion of its rigid base; the secondary oscillator (Load) is excited because of its attachment to the main one. The vibration absorber effect refers to the fact that (if the secondary oscillator is undamped) the motion of the source is zero at the resonance frequency of the load, i.e., the resonance frequency of the load when attached to the rigid base. It is important to note that this phenomenon occurs even if 1) the mass of the load is much smaller than the source, or 2) if the resonance frequencies of the two oscillators are different. It should also be noted that the vibration absorber effect also occurs in the case of the source being excited directly through a force acting on it, instead through vibration from its base. If the load has some damping instead of being undamped, the mass of the source will have some small motion at the resonance frequency of the load, instead of being at rest. In fact, the amount of motion is proportional to the damping of the load [1, 23].

The relationship of the vibration absorber effect with the vibration overtesting problem is studied by assuming that the oscillatory system of Figure 1-1 represents a vibration mode

of a flight mounting structure (source) coupled with a vibration mode of the test article (load). For example, the mounting structure could be a spacecraft and the test article could be an antenna of the spacecraft, or the mounting structure could be an antenna and the test article one of the components of the antenna.



Simple Two-Degree-of-freedom Coupled System



Load in the Vibration Test Configuration

Figure 1-1. Simple 2 DOF coupled system and load in vibration test configuration.

As a numerical example, assume that the natural frequencies of the two uncoupled oscillators are the same, the masses m_1 and m_2 are unity, the base acceleration is unity and the dynamic amplification factor Q ($Q = 1/2\xi$ where ξ is the damping ratio) of both the oscillators is 50 i.e., the damping ratio of 1%. For simplicity the excitation is considered to be sinusoidal.

The amplitude of the coupled system interface acceleration is shown in Figure 1-2. One may notice the two peak accelerations at the system resonance frequencies are located at $0.62\omega_0$ and $1.62\omega_0$ (where ω_0 is the load resonance frequency). The notch in the interface acceleration at ω_0 is clearly visible and it has a value of Q^{-1} with respect to the input acceleration. This illustrates the general dynamic absorber result, for example the frequency spectrum of acceleration at the interface between the spacecraft and instrument will have notches at the fixed-base resonance frequencies of the instrument.

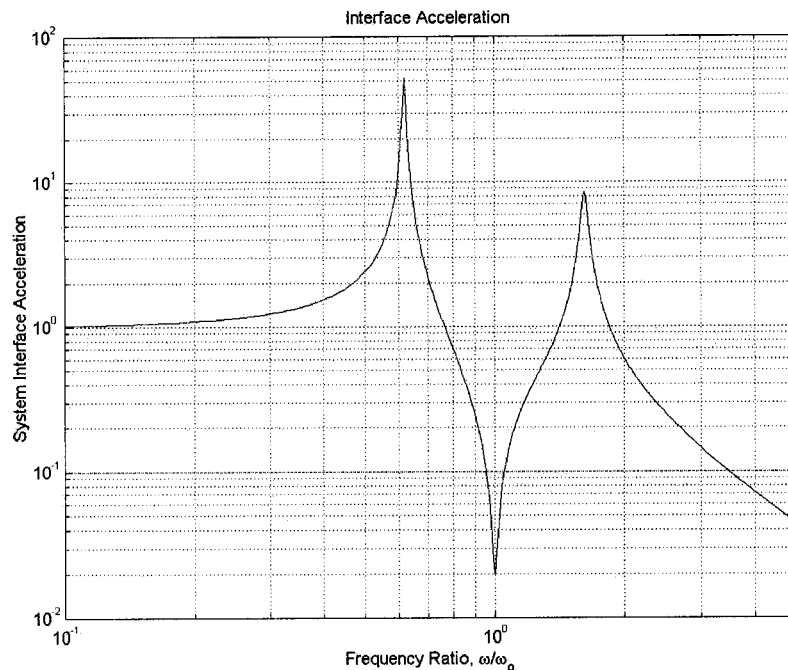


Figure 1-2. System interface acceleration.

One important characteristic of the load is the apparent mass which is the frequency response function (FRF) defined as the ratio of reaction force at its base divided by the acceleration at the same location. Independently of the structure underneath the load, the reaction force of the load is always equal to the product of its apparent mass and its base acceleration. For the numerical example considered above the apparent mass is shown in

the Figure 1-3. The abscissa is the frequency normalized by the load resonance frequency ω_0 . The apparent mass approaches the physical mass value as the frequency tends to zero, and has its peak value of Q at ω_0 .

The interface force of the coupled system (or the flight configuration) is obtained by multiplying the interface acceleration by the load apparent mass. The interface force shown in the Figure 1-4 also peaks at two resonance frequencies of the coupled system, with a maximum value of 80 occurring at $0.62\omega_0$.

The Figures 1-2,1-3 and 1-4 also illustrate the vibration-overtesting problem from enveloping the interface acceleration and how the force limiting alleviates the overtesting. In the coupled system, the interface force peak of 80 at the lower resonance frequency of $0.62\omega_0$, results from multiplication of the interface acceleration peak of 50 by the load apparent mass value of 1.6. In a conventional vibration test without force limiting, the corresponding shaker force would be of 2500, which is the interface acceleration envelope of 50 times the load apparent mass peak of 50 at the load resonance frequency ω_0 . With force limiting, the input acceleration would be notched at the load resonance frequency ω_0 to reduce the shaker force by a factor of 2500/80 or 31.25 to a value of 80, which is the maximum force produced at the coupled system level.

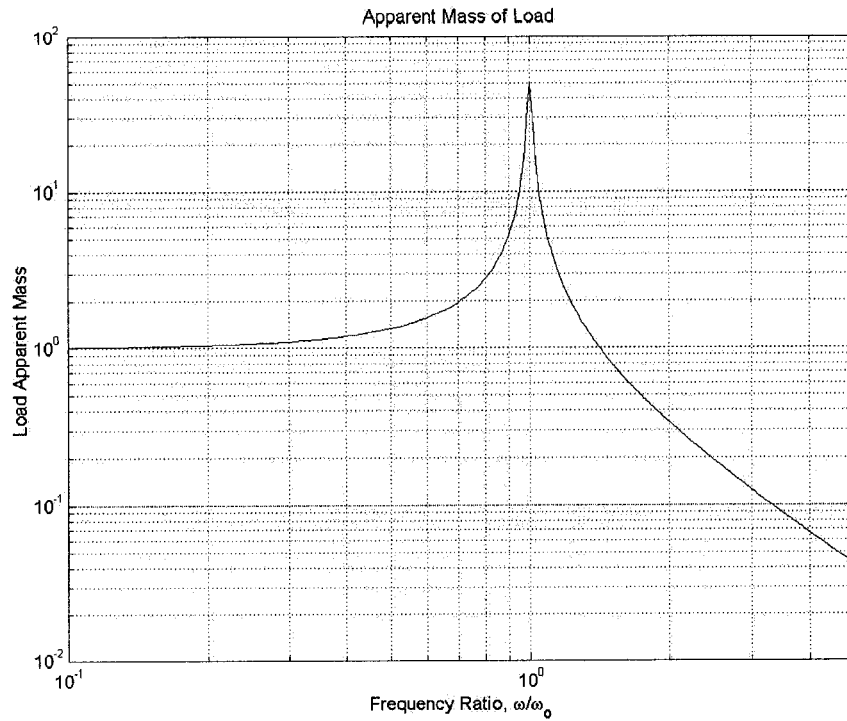


Figure 1-3. Load apparent mass.

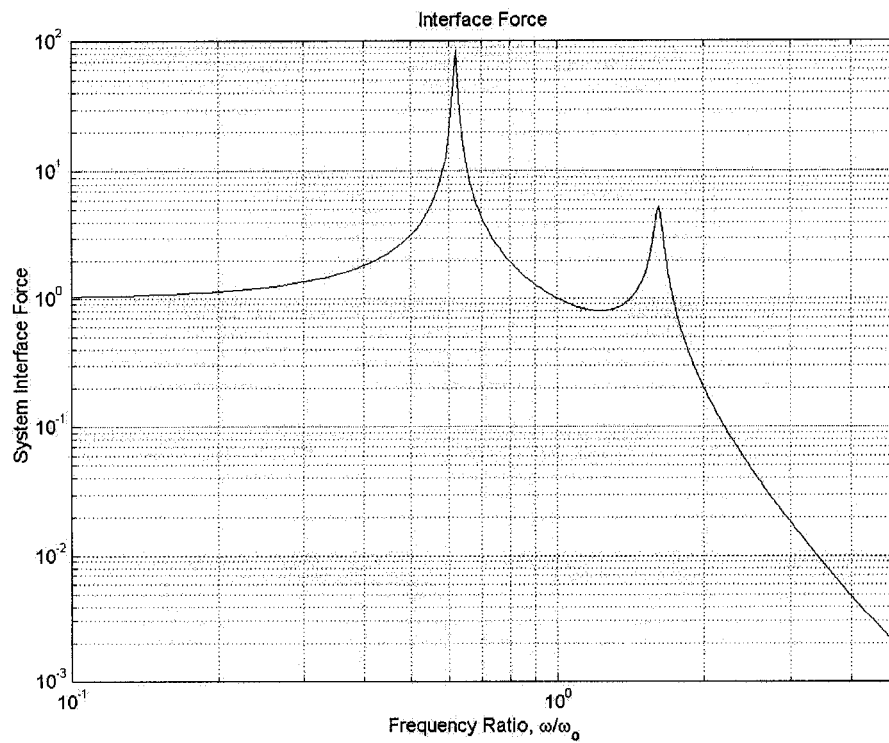


Figure 1-4. System interface force.

1.3.2. Procedures to Overcome the Vibration Overtesting Problem

There are some structures, which are still "built like brick", to survive vibration overtesting and even iterative test failure, rework and retesting scenario. This may be the cheapest way to go in some cases but the frequency in such cases is certainly much less than it should be. The two historical methods of alleviating overtesting are impedance simulation and response limiting and the recent method is the force limited vibration testing [1,19].

Impedance Simulation

In the 1960's, the personnel at NASA's Marshall Space Flight Center (MSFC) developed a mechanical impedance simulation technique called the "N plus one structure" concept, which involved incorporating a portion of the mounting structure into the vibration test. A common example would be the vibration test of an electronic board, mounted in a black box. In addition acoustic tests were conducted very often with the test items attached to the flight-like mounting structure. In all these approaches where a portion of the mounting structure or simulated mounting structure, is used as the vibration test fixture, it is preferred that the acceleration input be specified and monitored internally at the interface between the mounting structure and the test item. If instead, the acceleration is specified externally at the interface between the shaker and mounting fixture, the impedance simulation benefit is greatly decreased. When the input is defined internally, the "N plus one structure" approach is similar to the response limiting approach [1].

Mechanical impedance simulation approaches are seldom employed because they require additional hardware and therefore added expense. Two exceptions which may find acceptance in this low cost environment are: 1) deferring component testing until higher levels of assembly, e.g. the system test, when more of the mounting structure is automatically present, and 2) replacement of equipment random vibration tests with acoustic tests of the equipment mounted on a flight like plate, e.g. honeycomb [1].

Response Limiting

In order to alleviate the vibration overtesting problem many institutions have resorted for some form of response limiting for the past decades. Response limiting is analytically predicting the in-flight response at one or more critical locations on the item to be tested, and then to measure that response in the vibration test and to reduce, or notch, the acceleration input to the test item at particular frequencies. With this procedure the measured response is kept low or below the predicted limit [1,23].

The coupled load analysis for response limiting prediction is based on the Finite Element Models (FEM) of both the test article and the mounting structure. This model is typically used to design and analyze the loads in the test item. In this case the role of the test as an independent verification of the design and analysis is severely compromised. In addition, the model has to be very detailed in order to predict the in-flight response at critical locations. Thus the accuracy of the predictions is usually suspicious, particularly in the higher frequency bandwidth of the random spectrum.

In addition, it is often complicated or impossible to measure the responses at critical locations on the vibration test item. Sometimes the critical locations are not accessible, as in the case of optical and cold components. In the case of large test items, there may be many response locations of interest; hundreds of response locations may be measured in a typical spacecraft test. Since the uncertainty in the predictions of the resonance frequencies of the test on the shaker is typically 10% to 20%, any notches based on the pre-test analysis must be very wide, and may result in undertesting at frequencies other than at resonance.

There is one form of response limiting which almost represents the real conditions that exist in the launch environment, i.e. limiting the acceleration of the center-of-gravity (CG) or mass centroid of the test item [1]. By Newton's second law, the acceleration of the CG is equal to the external force applied to the body, divided by the total mass. It is indeed much easier to predict the in-flight responses of the test item CG, than the responses at other locations. The CG response is typically predicted with FEM using only a lumped mass to represent the test item, any method used to predict the in-flight interface force obviously predicts the CG acceleration as well.

However there are some problems associated with CG response limiting. First it is difficult or impossible to measure the acceleration of the CG with accelerometers in the vibration test. Some times the CG is inaccessible, or there is no physical structure at the CG location on which to mount an accelerometer. Furthermore attempts to measure the CG response overestimate the CG response at resonance, so limiting based on these

measurements will result in undertesting of test item. However, the CG acceleration is uniquely determined by dividing an interface force measurement by the total mass of the test item.

Force Limited Vibration Testing

The primary cause of the vibration overtesting is associated with the traditional practice of enveloping acceleration spectra to generate a vibration test specification. In the past overtesting, or conservatism, was typically attributed to the amount of margin that was used to envelope the spectral data or predictions. Now it is understood that the major component of the overtesting is inherent in the enveloping process itself. As mentioned earlier in the section 1.3.1, the traditional enveloping procedure completely ignores the valleys of the interface acceleration spectrum that correspond at the resonance frequencies of the test structure (vibration absorber effect) and thus it leads to the overtesting of the test structure at its own natural frequencies.

Conventional vibration tests are conducted by controlling only the acceleration input to the test item. In theory, if the frequency spectrum of the acceleration input in the test, including the peaks and valleys, were identical to that of the interface acceleration in the flight configuration, and if the boundary conditions for other degrees of freedom (rotations, etc) were the same as in the flight configuration, then the interface forces and all the responses would be the same in the test as in the flight. However, this is seldom the case, primarily due to the necessity of using a smoothed or an enveloped representation of the flight interface acceleration as the test input, and secondarily

because of frequency shifts associated with the unrealistic restraint of other degrees of freedom by the shaker mounting. It has been found that the dual control of the acceleration and the force input (force limited vibration testing) from the shaker alleviates the overtesting problem associated with the conventional vibration tests using only acceleration control.

Compared with the a point-by-point basis approach in the response limiting method, the force limiting vibration approach has the following advantages [23]:

- 1- The interface force prediction depends less or not at all on the FEM of the test item and the mounting structure. First, since the interface forces are global parameters, thus “averaged” characteristics of the structure, they can be predicted analytically with more confidence than the single point responses. Consequently, good prediction may be obtained with less detailed and smaller size finite element model. Second, since the parameters of the test and the mounting structure required for predicting force limits may be obtained experimentally, if the hardware of the mounting structure is timely available, the force limits could be predicted without the need of any finite element model. Third, at the limit, the estimation of force limits using the semi-empirical method could be done without any FEM of the test item.

- 2- Force sensors are incorporated at the interface attachments between the test article and the shaker (or fixture). These are physical locations, which are normally easily accessible.
- 3- Force limiting typically only requires one to six instrumentation channels (three forces and three moments at the interface between the test article and the shaker). Often, only the reaction force in the direction of excitation is required.
- 4- Force Limited Vibration provides a theoretically sound basis for input limiting which, once understood, should be acceptable to all parties and thus should reduce the effort of coming to an agreement on this sometimes serious issue.

1.4. Mechanical Impedance Characteristics

Estimation of force limits using coupled source-load system (Complex or Simple Two Degree of Freedom System methods) and Semi-empirical method depends on impedance information of both the load and the source, which can be obtained by finite element analysis or from the low level testing of test articles. It is to be noted that for the semi-empirical method, the only required impedance information is the impedance of the test item.

Impedance characteristics are related to input and response at single points on a structure. Strictly speaking, mechanical impedance refers to the ratio of input force divided by

response velocity. However, in the literature, the name mechanical impedance is also given to the ratios force/ displacement and force/acceleration (apparent mass).

1.4.1. Apparent Mass

Mechanical impedance as concerned to the force limited vibration is defined as the frequency response function (FRF) consisting of the ratio of response force to the input acceleration, which is also known as apparent mass or dynamic mass of the structure. The force and acceleration of the apparent mass refers to the same degree of freedom, implying that it is a drive point FRF. The apparent mass is generally a complex quantity, with magnitude and phase, but herein the term apparent mass will often be used in referring to only the magnitude. The apparent mass can vary greatly with frequency and peaks at the resonance frequencies of the structure, as seen in Figure 1-3. Therefore the apparent mass reflects the dynamic characteristics of the structure [1].

1.4.2 Effective Mass

The effective mass concept, introduced in the early seventies, is of prime importance for the dynamics related to the base excitation and modal reaction force. A physical interpretation of the effective mass has been given [1,23] by a set of parallel single degree of freedom oscillators attached to a rigid mass-less base as shown in the Figure 1-5. Each mode of vibration of the distributed structure is represented by an oscillator. The mass of each oscillator is defined by the effective mass of the mode. For each mode, the effective mass is such that the reaction force of the mode of the structure to the driven base acceleration a_0 is equal to the reaction force of the corresponding accelerator. It may be

shown [28] that, for each excitation axis, the sum of the effective mass of all the modes is equal to the total mass (or the moment of inertia) of the distributed structure.

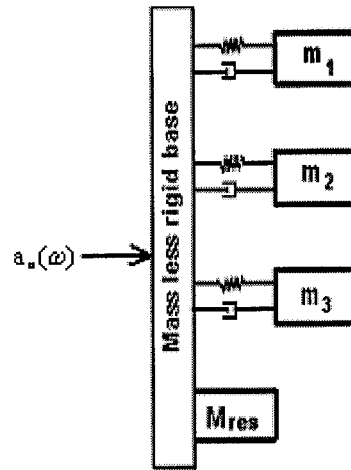


Figure 1-5. Physical interpretation of effective and residual mass concepts [21].

1.4.3 Residual Mass

Another mass quantity closely related to effective mass is the “residual mass”, which is defined as the total mass of the structure minus the effective mass of the modes which have natural frequencies below the excitation frequency. In other words, the residual mass is the sum of effective mass for all modes above the excitation frequency.

Practically it is not possible to capture all normal modes (let say l) of the structure. Assuming that in the frequency range of excitation, m normal modes exist we can define the residual mass matrix of the m^{th} mode as

$$\mathbf{M}_m^{res} = \sum_{i=m+1}^l \mathbf{M}_i^{eff} = \mathbf{M}_o - \sum_{i=1}^m \mathbf{M}_i^{eff} \quad (1-1)$$

where \mathbf{M}_o , \mathbf{M}_i^{eff} and \mathbf{M}_m^{res} are the rigid body mass matrix, effective mass matrix of the i^{th} mode and the residual mass matrix of the m^{th} mode respectively.

Considering Eq. (1-1), the residual mass of the m^{th} mode in the direction j due to an excitation in the direction k , M_{mjk}^{res} , can be written as:

$$M_{mjk}^{res} = M_{o,jk} - \sum_{i=1}^m M_{ijk}^{eff} \quad (1-2)$$

where $M_{o,jk}$ is the (j, k) term of the rigid body mass matrix, M_{ijk}^{eff} is the effective mass of the i^{th} mode in the direction j due to an excitation in the direction k and M_{mjk}^{res} is the residual mass of the m^{th} mode in the direction j due to an excitation in the direction k

Assuming the natural frequencies of the excluded modes are significantly higher than the excitation frequency, the residual mass may be interpreted as the fraction of the total structural mass, which moves with the input acceleration without any amplification factor. This is illustrated in Figure 1-5 by mass M_{res} directly attached to the rigid base. It is evident from the definitions of effective mass and the residual mass that the residual mass tends towards zero as the excitation frequency increases.

The effective mass and the residual mass of the structure are generally obtained from the analytical models, however they can also be estimated from the experimental values of the apparent mass [28].

1.4.4. Relation between the Interface force and the Interface Acceleration

Consider the based excited load system shown in the Figure 1-1. The frequency response function, $H(\omega)$, and the gain function, $|H(\omega)|$, of this system where the input is the base acceleration and the output is acceleration of the load, m_2 can be found as [25]:

$$H(\omega) = \frac{k_2 + ic_2\omega}{(k_2 - m_2\omega^2) + ic_2\omega} \quad (1-3)$$

$$|H(\omega)| = \frac{\sqrt{k_2^2 + (c_2\omega)^2}}{\sqrt{(k_2 - m_2\omega^2)^2 + (c_2\omega)^2}} \quad (1-4)$$

Considering the Eq. (1-3), the relation between output (acceleration of the load, a_2) and input (base acceleration, a_0) can be written as:

$$a_2 = H(\omega) a_0 \quad (1-5)$$

On the other hand, in random vibration, it can be easily shown that [25]

$$S_{A_2}(\omega) = |H(\omega)|^2 S_{A_0} \quad (1-6)$$

In words, the power spectral density of the response which is the acceleration of the load, S_{A_2} , equals the spectral density of the base acceleration, S_{A_0} , times the square of the gain function.

In the current study we are concerned about the interface force spectral density and the interface acceleration spectral density. It can also be observed in Figures 1-2, 1-3 and 1-4 that the interface force at any frequency is the product of apparent mass and the corresponding interface acceleration. Hence the relation between interface force and acceleration can be represented as

$$F = M_2^{app}(\omega) a, \quad (1-7)$$

where F is the interface force, $M_2^{app}(\omega)$ is the load apparent mass and a is the interface acceleration. If the above equation is expressed for a random excitation we can obtain:

$$S_{FF}(\omega) = |M_2^{app}(\omega)|^2 S_{AA}(\omega) \quad (1-8)$$

The load apparent mass is a frequency response function which includes mass, damping, and stiffness effects. The frequency dependence is shown explicitly in the above equation to emphasize that the relation between force and acceleration applies at each frequency.

1.5. Force Limits

As mentioned previously, to overcome the problems encountered in Impedance Simulation and Response Limiting, a new test method called the force limited vibration testing is used which can reduce the cost and increase the safety to critical space hardware. Force limiting is a new way of conducting vibration tests to achieve better

simulation of the flight environment, alleviating the overtesting and resultant failures inherent in conventional vibration tests.

In conventional vibration tests, only the input vibratory motion is specified. The vibration specification is derived by enveloping the peaks of the flight or higher hardware level test vibration data and ignoring the valleys, or notches, in the data, which correspond to the resonance frequencies of the test article when attached to the rigid support, which is termed as vibration absorber effect. In force limited vibration tests, both the shaker motion and reaction force are controlled to enveloped values predicted for flight. Reaction forces are measured and limited real time in the vibration tests by employing force gauges sandwiched between the test item and the shaker fixture. At test item significant resonance frequencies, the reaction forces become large and control the test, automatically putting the vibration notches back into the test. This eliminates or at least significantly reduces the major cause of overtesting, i.e. the response (impedance) mismatch between the massive rigid fixture and the relatively lightweight mounting structure aerospace hardware. More realistic testing reduces the cost, schedule and performance penalties of over-testing and over-design. In other words the Force limited vibration testing can be said to be as for the traditional vibration test specification, which is the envelope of the peak accelerations, but to notch the input at the resonance frequencies on the shaker to emulate the valleys in the flight environment.

Force Limits for the vibration tests can be obtained by one of the following two methods [1]:

1. Two-degree-of-freedom or other analytical models of the coupled source/load system together with measured or FEM effective mass data for the mounting structure and the test item,
2. A semi-empirical method based on system test data and heuristic arguments, and Quasi-static design criteria, which may be based on coupled load analysis or a simple mass acceleration curve.

The two methods are proportional to the conventional acceleration specification; any conservatism or error in the acceleration specification is carried over to the force specification. The procedure employed in the above methods is briefly described as below.

1.5.1. Coupled Source/Load System

The basic approach to calculating force limits with the coupled system model involves four steps [1]:

1. Development of a parametric model of the coupled source and the load system which might be a FEM or a multi-degree-of-freedom modal model,
2. Identification of the model parameters using measured apparent mass or FEM modal frequency and effective mass information,
3. Solution of the coupled system problem to obtain the ratio of the force frequency envelope to the acceleration envelope at the source/load interface, and

4. Multiplication of the ratio of envelopes by the acceleration specification to obtain an analogous force specification.

The method of calculating force limits using a coupled source/load model is implemented for two specific cases where the coupled system is considered as a simple and a complex two-degree-of-freedom system (TDFS).

As mentioned earlier for both the flight configuration with a coupled source and load and the vibration test configuration with an isolated load, the interface force spectral density S_{FF} is related to the interface acceleration spectral density S_{AA} according to Eq. (1-8).

Both the simple and the complex TDFS methods are derived by multiplying the conventional acceleration specification, which is assumed to properly envelope the acceleration spectral peaks, by the load apparent mass, evaluated at the coupled system resonance frequencies. A central point of this approach is that the load apparent mass must be evaluated at the coupled system, or shifted, resonance frequencies. The values of the load apparent mass at the coupled system resonance frequencies is considerably less than the peak value at the load uncoupled resonance frequency. [23]

1.5.2 Semi-Empirical Method

The basic idea behind the semi-empirical method is to properly envelop the input force spectrum at the fundamental frequency of the test item. Considering Eq. (1-10), the semi-empirical method can be expressed by the following two relations [1]

$$S_{FF}(f) = C^2 M_o^2 S_{AA}(f) \quad f < f_o \quad (1-9)$$

$$S_{FF}(f) = \frac{C^2 M_o^2 S_{AA}(f)}{(f/f_o)^n} \quad f > f_o \quad (1-10)$$

where, M_o is the physical mass of the test item, f_o is the fundamental frequency (or most significant mode in Hz), C is a constant, and n is a roll-off ratio introduced to account for the falling off of the apparent or dynamic mass above the fundamental frequency.

In Eqs. (1-11) and (1-12), the mass M_o is known, S_{AA} is defined (usually from coupled load analysis), the values of f_o and n may be obtained from finite element analysis and finalized from a low level sine or random run performed just prior the full level vibration testing.

Constant C^2 is a key parameter of the semi-empirical method, which sets the force limits throughout the complete frequency bandwidth of excitation. Some judgment should be done to choose the value of C^2 . Based on limited number of flight data, it has been observed that, in normal conditions, C^2 value as low as 2 might be chosen for complete spacecraft or strut-mounted heavier equipment, C^2 value as high as 5 might be considered for directly mounted lightweight test items [1,18].

1.6. Present Study

The present thesis constitutes a comprehensive study in the area of force limited vibration testing using semi-empirical method. Design optimization of the test item, the mounting structure and the fixture using finite element method, conducting in-depth analytical and

experimental sensitivity studies to investigate semi-empirical method and affecting parameters and documenting a comprehensive benchmark problems are among the most important contributions of this thesis.

Relatively fewer investigations have been reported in the literature on force limited vibration testing using semi-empirical method, to study the behavior of semi empirical force limiting factor C^2 and the parameters on which it depends.

Here, the test item, mounting structure and fixture has been deigned so flexibly that desired natural frequencies can be obtained at the test item and assembled structure levels. Investigation of the force limited vibration testing using semi-empirical method to this extent is unique and due to its extensive analytical and experimental studies, it can be extremely useful for the researchers and engineers in the aerospace community to better understand the semi empirical method of force limited vibration.

Current study can also be used in the future implementation of FLV testing in Canadian space programs or by the aerospace industry in general in deciding the C^2 parameter for testing any aerospace equipment depending on the number of interface points, direction and the mass ratio of the test item and the mounting structure. It also gives confidence in selection of C^2 parameter higher than 5 while implementing FLV testing using semi-empirical method.

In the following sections, same terminology as found in Force Limited Vibration literature is used. More specifically, the test item refers to the structure being subjected to FLV vibration testing, the mounting structure refers to the immediate structure to which the test item is being attached, the assembled structure is a combination of both the test item and the mounting structure. For example, in the case when the test item is an instrument, the mounting structure would be the rest of the spacecraft (without the instrument on it) and the assembled structure would be the complete spacecraft. The generic term test article (TA) or test structure refers to either the test item or the mounting structure.

1.7. Thesis Organization

The present thesis contains five chapters. Chapter 1 introduces the problem under investigation and the motivation. A historical perspective to the field of vibration testing to prevent overtesting is presented with the most important and relevant contributions to the field to date and with an in-depth review on overtesting problems and relative methods to alleviate it. The chapter concludes by identifying the most important and relevant contributions of the present study and the layout of the monogram.

Chapter 2 presents in detail the design requirements set for the test item, the mounting structure and the fixtures specifying the reasons to have a particular requirement. It then explains in detail 1) The analysis and design of test structures, 2) The flexibility of each structure indicating the frequency range the structures cover, 3) The variation in mass ratio of test item to mounting structure, 4) The stiffness variation of test item in X, Y and

Z directions, and 5) Lumped mass locations on the structures, and how the flexibility of the test item can be varied by replacing the stiffening member or by adding lumped mass.

Chapter 3 presents the analytical sensitivity study performed on the test structures (test item and mounting structure). The chapter explains in detail the guidelines set to select the cases to perform the analytical study, the probable parameters on which the semi empirical force limiting factor C^2 depends, naming of test cases for sensitivity study, and naming of test item on the basis of number and location of attachment points, stiffening member used, and the lumped mass and its location on the test item and/or mounting structure, procedure of evaluating the C^2 and notch values. It then concludes with 1) The results of the cases tabulated indicating the impedance characteristics, details at the interface of the test item and the mounting structure and C^2 value, and the notch value for each configuration of the test item and mounting structure at system level, and 2) explains in detail the variation of C^2 and notch value and the parameters on which they depend.

Chapter 4 explains the experimental sensitivity study performed on the manufactured structures, to validate the procedures and the values of C^2 obtained from analytical study. It indicates the guidelines set to pick the cases for the study from the cases in chapter 3. All the structures designed in Chapter 2 are validated and proper reasons are mentioned to defend the variation in frequency from analytical to experimental values. Towards the end of the chapter, the results with respect to C^2 parameter have been obtained from the

experimental study and compared with the analytical study in both lateral and vertical directions.

Finally, Chapter 5 concludes with a synthesis of the most important findings and contributions of the present investigation and various recommendations are put forward for future work.

CHAPTER 2

DESIGN AND ANALYSIS OF STRUCTURES

As specified earlier the main objective of the project is to investigate the range of C^2 values, which might be expected for a range of representative combination of structures. This objective is to be achieved through analytical and experimental sensitivity study of C^2 with respect to structures (test item and mounting structure) having a certain range of structural and dynamic properties, and different interfaces (Attachment Points).

2.1. Design Requirements

Some design requirements for the Test Articles (TA's) were defined in order to respect the vibration facilities at the Canadian Space Agency (CSA) and to meet the following objectives:

- Provide large enough flexibility in the key characteristics of the test articles, to allow the performance of meaningful analytical and experimental sensitivity studies of the semi-empirical method.
- Provide required limitations in order to allow performance of the experimental sensitivity study with the vibration test facilities of the CSA Space Technologies in St-Hubert, QC.
- Define the characteristics of the TA's deemed required in order to demonstrate proper relevance to typical space hardware. These characteristics are based on discussions with government and industrial partners.

A requirement containing the verb 'shall' refers to a condition, which must be met. However, a requirement containing the verb 'should' refers to a condition, which ideally would be met, but is not necessary if the implication or cost is too significant [26].

2.1.1. Test Article Requirements

Attachment Points

1. The design of both the test item and the mounting structure shall have sufficient attachment points to allow different combination of these points to be used in the various attachment configurations. The maximum number of attachment points used in the configuration shall be limited to twelve.

The maximum of twelve attachment points is related to the fact that there are presently a total of twelve triaxial force sensors available within the CSA.

2. The design of the test item shall have provision for the variation in stiffness, and to a certain extent in damping, of the attachment points between the mounting structure and the test item.

The dynamic characteristics of a test item may be significantly affected by the conditions at the boundary or the interface.

3. The means of attachment between the test articles, as well as between each of the test articles and the fixture shall be through bolts.

This requirement is based on the fact that bolts are the standard means of attachment between the various parts of the spacecraft. Also the use of bolts, as opposed to other means of attachment such as clamps, ensures a better control and repeatability of the interface characteristics. These are very suitable characteristics in the present sensitivity study, since it eliminates undesirable uncertainties in the factors affecting the interface force seen by the test item during the vibration test of the assembled structure.

4. Bolt size should normally be M6 or M8 (or its English unit equivalent), based on stress analysis of the worst-case scenarios. However bolt size shall not exceed M8.

The maximum bolt size of M8 is defined by the diameter of the triaxial force sensors, through which the bolt must pass.

5. For the test item, attachment points shall include holes through which the bolts will pass to attach the test item to the mounting structure or to the fixture.
6. For the mounting structure, attachment points of the test item include threaded holes for the attachment of the test item. The attachment points to the fixture shall include holes, through which the bolts will pass to attach the mounting structure to the fixture.

Dynamic Characteristics of the Test Articles

7. The fundamental frequency of the test item should be higher than 100 Hz and the frequency of its first three modes shall be no more than 600 Hz.

This frequency range of 100-600 Hz is fairly representative of where one might expect the first three or four modes of an instrument be located. These are normally the modes which will be affected with FLV notching. Also by having the fundamental frequency above 100 Hz, one ensures that the apparent or dynamic mass FRF reaches an asymptotic horizontal line below the lowest frequency. This simplifies the calibration of the force sensors for the experimental sensitivity study.

8. In order to simulate real life situations, at least the lower three natural frequencies of the mounting structure shall be below the fundamental frequency of the test item.

Independently of the hierarchy level (e.g. component, instrument or the sub-system or spacecraft) of the test article, the mounting structure normally exhibits more flexibility and lower fundamental frequencies than the test item. For example the fundamental frequency of the spacecraft would normally be above 25 Hz, while the fundamental frequency of an instrument could be above 100 Hz.

9. In order to simulate real-life situations, some of the design configurations shall contain several closely spaced modes for both the test item and the mounting structure and these modes shall be coupled together.

Space hardware at any hierarchy level is normally very complex and is likely to exhibit modes, which are not well-separated and even closely spaced modes. Consequently, this requirement is imposed to ensure relevance to space hardware dynamic characteristics.

10. It should be possible to modify the flexibility of both the test articles, in order to simulate a wide range of different frequency and amplitude of the most significant effective masses.

This requirement leads to a larger scope of the sensitivity study and thus brings added value to the current project.

Residual Masses of Both Test Articles

11. The design of both the test item and the mounting structure shall allow the attachment of various number of rigid masses at different locations. These rigid masses are to represent additional residual masses of the test articles.

The addition of rigid masses to both the test articles represents an easy way of increasing the residual masses. This increase of residual mass is on top of the ones associated with the modes having a frequency above the excitation frequency.

12. The ratio of added rigid masses of test item/ added rigid masses of mounting structure should cover a wide range sufficient enough to make sensitivity analysis with respect to the ratio of residual masses.
13. The added rigid masses should be fixed to either the test item or the mounting structure through bolts.

Physical Properties

14. The test articles should be easy to manufacture.

This requirement ensures that no undue delays occur in the manufacturing of the hardware required for the experimental sensitivity study.

15. The test articles and their various parts should be easy to assemble and disassemble.

This requirement is related to the fact that the experimental sensitivity study will involve several tests in various configurations and with different designs of the test articles.

16. The total mass of the test item and the fixture shall not exceed 100 lb.

17. The total mass of the test item, the mounting structure and the fixture shall not exceed 150 lb.

The above requirements (16 & 17) are based on the following assumptions. (1) The nominal force rating of the shaker at the CSA vibration test facility in St-Hubert, (2) A safety factor of 2 to account for the fact that the nominal rating of the 2000 lbf could be significantly reduced depending on the input profile, (3) an input profile having a value of 10g rms for the test item and 7g rms for the assembly. The values are representative of the level, which might be imposed on a spacecraft sub-system and spacecraft respectively.

18. The mass of the test articles should be as large as possible respecting the above requirements (16, 17).

Test articles having larger mass are likely to be more representative, at least from a mass point of view, of typical space hardware up to instrument or subsystem level.

19. Both the test articles should be made of materials representative of those typical of space hardware, such as aluminum.

2.1.2. Fixture Requirements

20. A single fixture shall be designed and used for all testing, both at the test article and assembled structure levels.

21. The fixture shall be designed to be rigid for all test configurations (including assembled structures), in the frequency range of interest (i.e., up to 2000 Hz).

22. The overall dimensions of the fixture should be such that none of its parts are hanging beyond the edge of the shaker plate or the slip table.

The purpose of this requirement is to prevent any reduction of the natural frequencies of the fixture and its rigidity, due to some of its sections not being properly fixed to the shaker plate of the slip table.

23. In order to increase the mass of the test articles, the design of the fixture may involve extrusion of material, at the expense of higher manufacturing costs.

Up to certain point, additional cost for manufacturing the fixture is considered acceptable if it results in a significant increase in the mass of the test articles.

24. The fixture shall have three sets of holes: (1) Holes with counter bore on the upper face, for the attachment of the fixture to the shaker plate or the slip table. (2) Threaded holes for the attachment of test item and (3) Threaded holes for the attachment of mounting structure.

2.2. Design of Test Structures

This section presents the nominal design of the test item, the mounting structure and the fixtures. Several iterations were performed respecting the specified design requirements and the discussions held with the engineers at CSA and JPL to arrive at the final design of structures, which are as explained in the later part of the section.

2.2.1. Test Items

The test item is considered as a hollow block, two sides of which are being removed to have easy access to all sides of the block to add additional lumped mass to achieve the requirement 11 of changing/representing additional residual mass of the test item. To have a closely space modes to simulate the real space hardware, a plate is added in the middle of the block connecting the two sidewalls. This plate also helps in adding additional lumped mass to represent the electronic components of spacecraft having higher fundamental frequency than the spacecraft by itself. To account for the large range

of values for the physical properties (Physical mass of the structure and stiffness) and dynamic properties (natural frequencies) of the test item, the test item is considered to have the maximum size depending on the dimensions of the shaker and the slip table. The variation in physical mass of the test item can be obtained by adding additional lumped mass and the stiffness can be varied by choosing the proper stiffness parameters explained in the later part of the section. Both the properties are changed respecting the dynamic and physical requirements. Frequency is a factor, which depends on both the physical properties mentioned earlier hence the range of frequency depends on the possible values for both the physical properties. The dimensions of the test item are arrived respecting the requirements of the test item (explained in the earlier section) and manufacturing cost and time involved. The mass and the frequency of the obtained structure vary by three fold the details of which are explained as below.

The test item is designed as a hollow cube of 11"x11" x11" with a wall thickness of 0.25" on each side. The dimensions of the test item are selected to meet the requirements and on the basis of the dimensions of the shaker and the slip table. The thickness of the walls is derived from static and dynamic analysis of the structure to meet the specified requirements in terms of flexibility, mass and the fundamental frequency (Req. 7 and 9). All the walls and the medium plate are considered of the same/uniform thickness to reduce the manufacturing cost and time. Such a test item could represent dynamically a small instrument of a spacecraft. As shown in the figure below two sides of the test item have been removed for easy access to the interior plate and to add additional lumped

mass so as to increase the flexibility in terms of frequency and effective mass for the fundamental frequency (Req. 10 and 11). Figure 2-1 presents a drawing of the structure.

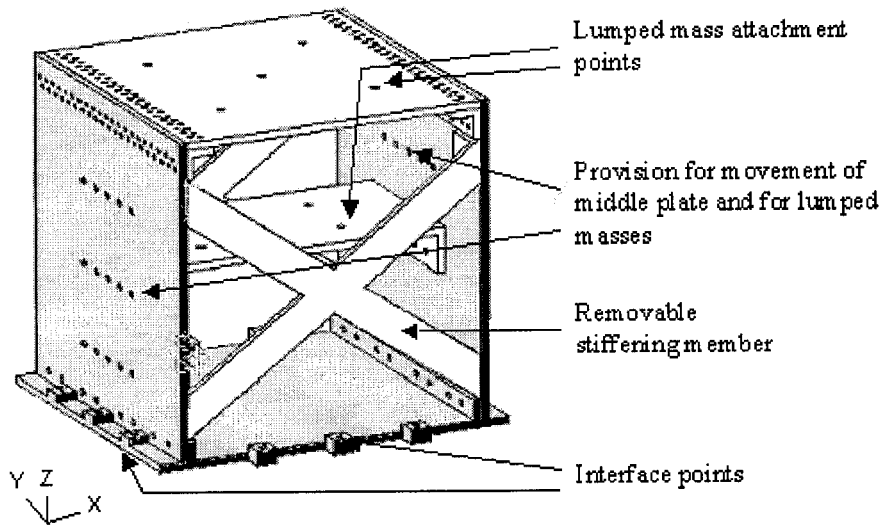


Figure 2-1. Test item with provision for lumped masses

The test item is designed as a hollow cube so that it is symmetrical and its mass is evenly distributed on all the attachment points, which vary in number from 3 to 12 as per the requirements (Req. 1). Unsymmetrical mass distribution can easily be achieved from uneven attachment of the lumped masses and the interface points.

As specified earlier, in order to meet requirements (Req. 8 to Req. 10), a middle plate of 0.25" thick and 5.5" wide is attached over the length of the test item to make a provision to add additional masses and also have its own dynamics (to improve the design flexibility), which also increases the number of cases for the sensitivity study. This plate is attached so that it can be moved along the height of the test item to further increase the design flexibility of the test item.

The fundamental frequency of the initial design of test item with four attachment points (along the side plates) and without any lumped mass was below the required 100 Hz (Req. 7). This frequency was later increased by adding quarter inch thick and an inch wide stiffening members connecting the top right corner to the bottom left corner, on either side on the block. By adopting these stiffening members, the fundamental frequency of the structure improved to 190 Hz with the same four attachment points and 200 Hz with 12 attachment points. The total mass of the test item without any lumped mass is 15.7 lb, which can be increased to a maximum of 50 lb based on the level of testing to be performed (Req. 17 and Req. 18).

The fundamental frequency with four attachment points and the maximum lumped mass of 24.2 lb (11 kg) entirely attached on the top plate was found to be 90 Hz, which is again below the requirement. Consequently in the final design, instead of a single stiffening member going on either side of the test item, an X - shaped plate is connected on either side as shown in the Figure 2-1; this improved the frequency to 105 Hz (with the attachment points on the left and right side of the stiffening members). In fact, either the single stiffening members or the X members may be used depending on the required flexibility of the test item.

However the fundamental frequency of the test item was below 100 Hz when the orientation of the attachment points is changed from the adjacent sides of the stiffening members to the same side with the same number of interface points (four attachment

points on the same side of the stiffening members). In order to increase the frequency of the structure the stiffening members mentioned above were replaced by brackets of 3/16 inch thick (4 in number attached on all corners) connecting the base and the walls of the test item as shown in the Figure 2-4, which improved the frequency to 104 Hz with all the lumped mass (worst case).

In order to simplify the manufacturing and to enhance the sensitivity study in terms of adding or removing parts to improve/reduce the stiffness and fundamental frequency, the test item is manufactured by joining different plates and bars using bolts and rivets. The lumped masses to be added are so manufactured that they can be easily assembled and disassembled. All the stiffening members/ brackets are attached to the test item by bolts so that they can be easily added or removed to the basic structure to increase or decrease the flexibility of the structure. The fundamental frequency of the structure decreases provided the stiffening member is not changed with increase in lumped mass.

The finite element tools used to arrive at the dimensions of the structures are Nastran and Patran. The model is generated in Patran. To obtain the resonance frequencies of the structure, SOL-101 is run through Nastran specifying MEFFMASS card in the case control statement to obtain the effective mass and the direction corresponding to each frequency. To perform random analysis, advanced tools of Nastran and Structural Analysis Toolkit (SATOOLS) of Maya Heat Transfer are used. Same tools are used to perform the analytical sensitivity study explained in chapter 3. To perform random test at the design level, a white noise is applied across a bandwidth of 20 Hz and 2000 Hz. The

results obtained from the Nastran are processed by the SATOOLS to obtain the stresses, forces and accelerations at the critical locations.

A static and random analysis of the system is performed to verify the stresses at 10 g rms (Req. 16) and it has been found that the structure had a Margin of Safety (M.S) of 1.5 at the attachment points, considering a safety factor of 1.25.

The margin of safety of the structure is defined as

$$M.S = \left[\frac{\sigma_{all}}{\sigma_{von} \times S.F} \right] - 1 \quad (2-1)$$

where $M.S$ is the margin of safety, $S.F$ is the safety factor, σ_{all} is the maximum allowable yield stress for the material, and σ_{von} is the maximum Von-Mises stress obtained from the results at the critical locations of the test item. The margin of safety should be more than 1 for the structure to restrain the stresses obtained during the vibration testing. The larger the value of M.S the tougher the structure is. The maximum Von-Mises is multiplied by the safety factor to account for the errors in the FEM model and the errors that occur while calculating the stresses and to obtain the maximum stresses. The value of the $S.F$ purely depends on the application of the instrument.

In order to improve the M.S and to maintain the integrity of the test item after testing at 10g rms by itself or at the system level, the thickness of the attachment points is increased from 0.25 inch to 0.5 inch. This increase in the thickness of the attachment points improved the M.S by 3 fold.

The natural frequencies of the system with minimum 4 attachment points and maximum lumped mass (worst case for Req. 7) and with maximum 12 attachment points and no lumped mass (best case) are presented in Table 2-1. The numbers inside parenthesis indicate the percentage of effective mass and the direction of the predominant motion. The results shown in the Table 2-1 confirms the flexibility of the proposed design. It is noted that the requirement of having at least 3 major modes below 600 Hz is satisfied in all the cases.

Table 2-1. Natural frequencies and effective masses of the test item with and without lumped mass

| Mode No. | Frequency (Hz) (% Eff. Mass) with max lumped mass and 4 attachment points | Frequency (Hz) (& % Eff. Mass) without lumped mass and 12 attachment points |
|-----------------|--|--|
| 1 | 97 (83 – X) | 272 (18 – Y) |
| 2 | 118 (33 – Z) | 324 (63 – X) |
| 3 | 119 (52 – Y) | 327 (19 – Z) |
| 4 | 155 (21 – Z) | 355 (28 – Y) |
| 5 | 167 (4 – X) | 450 (15 – Z) |
| 6 | 187 (17 – Y) | 460 (6 – Y) |
| 7 | 221 (5 – Y) | 621 (10 – Z) |
| 8 | 263 (5 – Z) | 815 (9 – Z) |
| 9 | 279 (7 – Z) | 1170 (31 – Z) |
| 10 | 394 (3 – Y) | - |

The variations of the structure from the simple case or most flexible structure (fundamental frequency being 97 Hz) to a robust case or rigid structure in terms of stiffness and the frequency (fundamental frequency being 270 Hz) are shown in the Figures 2-2 to 2-5. The simplest test item (with least stiffening members, fundamental frequency and mass) possible for vibration testing in X direction with all the dimensions

and the stiffness members mentioned above would be similar to Figure 2-2, but the X member would be replaced by the simple cross member connecting top right and bottom left corners on either side of the structure. This structure is used only when the test item is fixed at at least 2 attachment points on the side of the side plates. The naming of attachment points is mentioned in Section 3.2. The robust structure, which has three times higher frequency than the one mentioned above when the test item is attached at the same configuration mentioned earlier, is shown in Figure 2-3. The axes for the structure are similar to the one shown in the Figure 2-1.

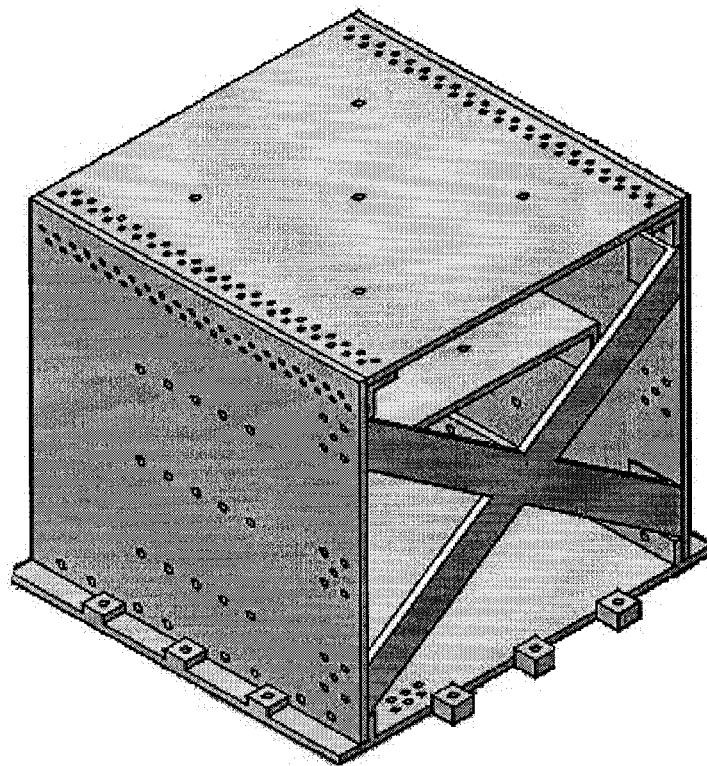


Figure 2-2. Simplest possible test item for vibration testing in X direction (but the X shaped stiffening member is replaced with cross member).

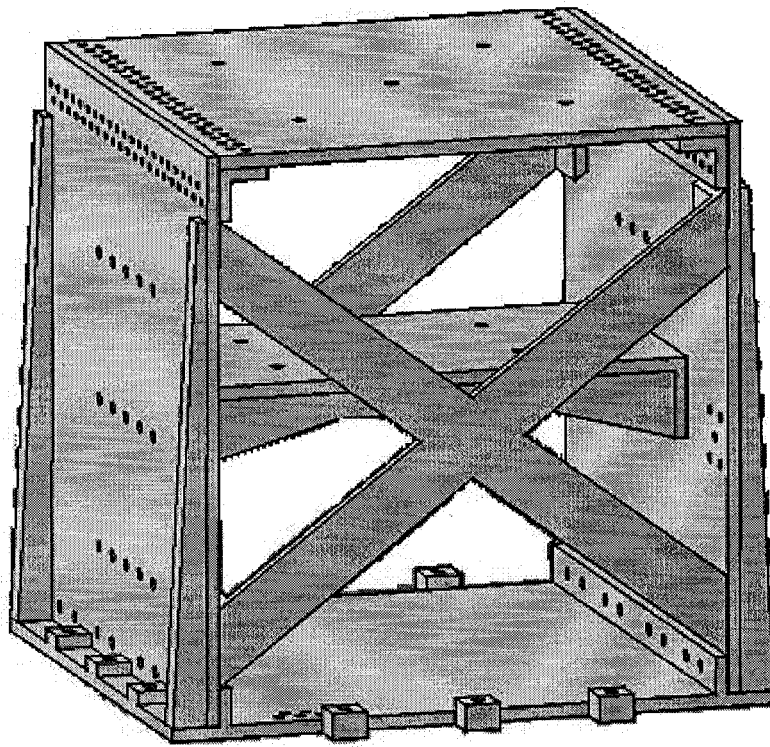


Figure 2-3. Robust possible structure (test item) for vibration testing in X direction.

Similarly when the structure is attached at the attachment points on the side of the stiffening members for vibration testing in Y direction, the simplest structure possible would include flanges as the stiffening members as shown in the Figure 2-4. The robust structure in the same configuration is shown in the Figure 2-5. there will not be much change in the frequency for both the structures but it increases by 2 fold when the test item in the figure 2-5 is attached by side stiffening members on the sides extruding outwards similar to test item in figure 2-3.

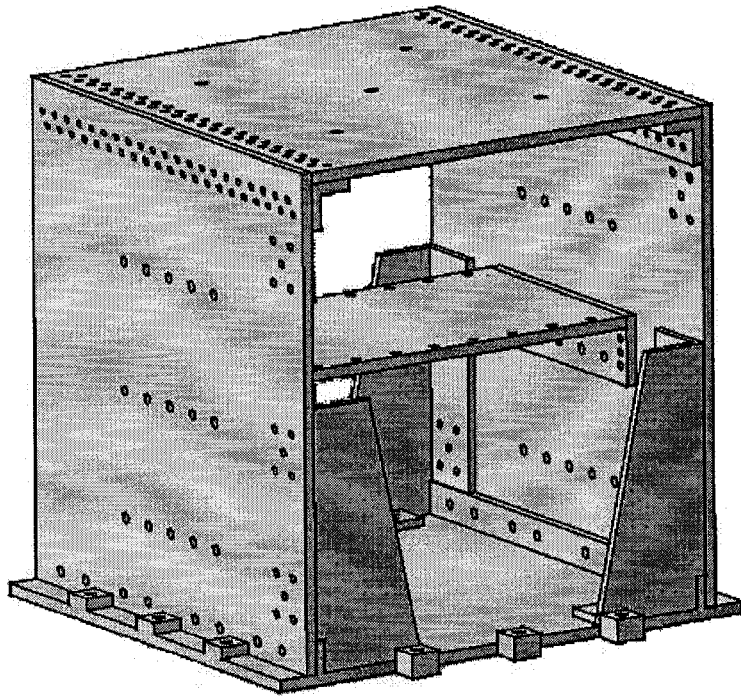


Figure 2-4. Simplest possible structure for vibration testing in Y direction.

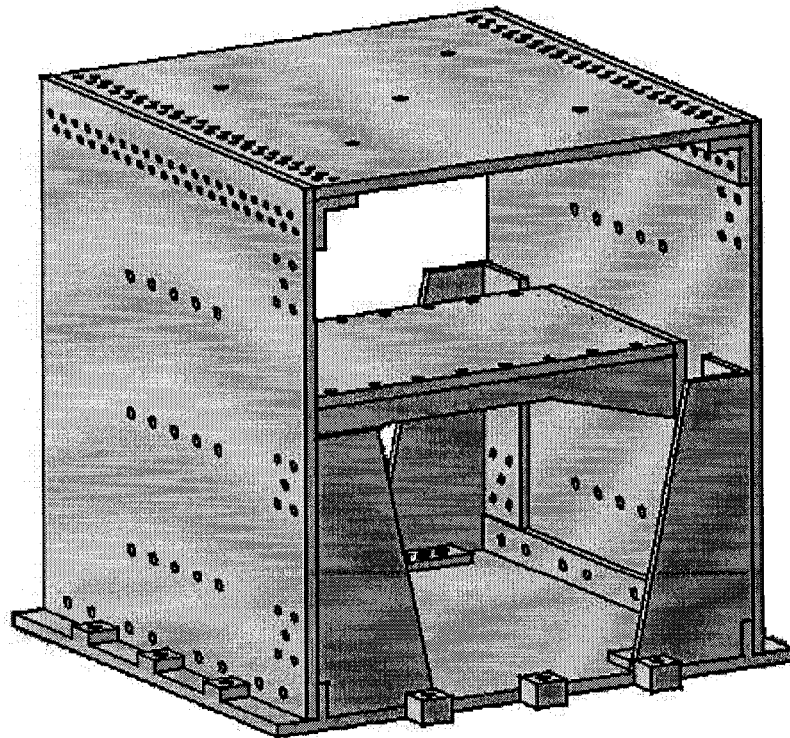


Figure 2-5. Robust possible structure for vibration testing in Y direction.

2.2.2. Mounting Structures

The mounting structure was initially considered to be a plate-like structure with varying thickness respecting the specified requirements in terms of fundamental frequency and the provision for the attachment of lumped mass to increase the residual and effective mass in the concerned bandwidth. However more investigation reveals that plate-like structures have dynamics in only one direction (normal to the plane of the plate) and may not exhibit enough dynamics at the lateral directions in the frequency range of interest. Thus they cannot be implemented for testing in the lateral directions. Furthermore, and as important if not more, plate-like structures would not easily exhibit several modes in the frequency bandwidth of interest.

After numerous simulations, the mounting structure was designed as a structure similar to the test item. However, it is much more flexible than the test item in order to increase the complexity of its own dynamics.

Taking into account of the dimensions of slip table and the test item, the mounting structure is considered to have a plate of 16"x18" mounted on walls of 5" high and 18" length plates. The thickness of the plates is selected after performing the dynamic and static analysis of the structure to satisfy the requirements in terms of fundamental frequency. To further respect the requirement of having at least three natural frequencies below the natural frequency of the test item (Req. 8), and to improve the sensitivity study, a plate of 16" x 16" is attached across the length about 2.5" from the top plate as shown in Figure 2-6. The thickness of the top plate vary from 1/8" (3.175mm) at the center

(covering the cross-section 10"x10") to 3/8" (9.525 mm) at the attachment points of the test item to the mounting structure in order to further improve the flexibility of the structure in the vertical direction (normal to the plane of plate). The details of the thickness of the top plate are as follows:

- Center area of 6" x 6" has a thickness of 0.25 in or 6.35 mm.
- An area of 10" x 10" minus the above area has a thickness of 0.125 in or 3.18 mm.
- Area under the attachment points of the test item 13" x 13" minus 10" x 10" has a thickness of 0.375 in or 9.53 mm.
- Rest of the plate has a thickness of 0.188 in or 4.76 mm.

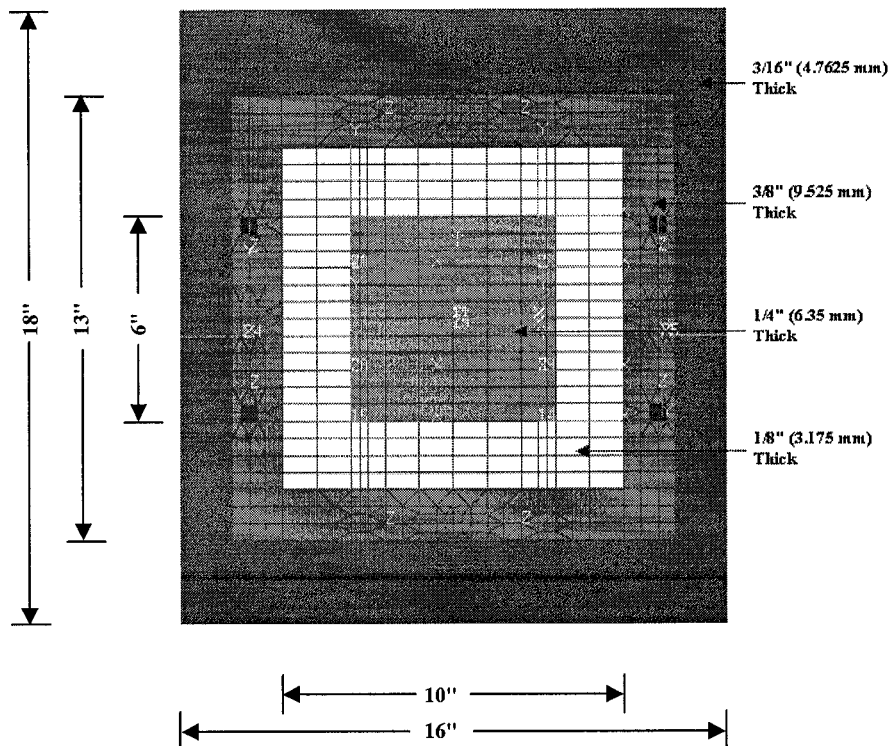


Figure 2-6. Top plate of the Mounting structure, indicating the variation in thickness of the plate.

The thickness of the sidewalls connecting the top plate to the legs also varies across the height, to reduce the frequency in the lateral and vertical directions. The details of thickness of the sidewalls and the medium plate (achieved after multiple iterations checking the frequencies, the stresses for the assumed test level and the mass of the structure) are as follows: The thickness of the plate (sidewall) at the point of attachment to the top plate is 3/16" (4.763 mm) up to a depth of 1" (25.4 mm). This feature will increase the strain energy at the attachment points of two plates, which in turn reduces the frequency in the vertical direction for the top plate (as most of the strain energy for the frequency involving the top plate in the vertical direction will be located at the attachment point of top and side plates, reducing the thickness reduces the stiffness and increases the strain energy). The rest of the sidewall plate has a thickness of 0.25" (6.25 mm) to account for the stresses and frequencies in the lateral direction. The thickness of the medium plate is 3/16" (4.7625 mm) in order to have the maximum flexibility, to allow for the additional frequencies and to take the maximum lumped mass at the maximum possible test level (10 g rms). However with this thickness considered for the medium plate, the frequency of the mounting structure involving the middle plate was found to be above the fundamental frequency of the test item, thus violating the requirement of having multiple modes below the fundamental frequency of the test item. In order to reduce the stiffness or increase strain energy of the plate, the attachment points between the side and the medium plates or the area connecting the two plates is reduced by removing the material of 4" x 8" on either side of the medium plate connecting the sidewalls, again taking care of the stresses at the attachment points

(elements connecting the middle plate to side plate) which will increase due to reduced contact area. Figure 2-7 shows the final dimensions of the middle plate achieved.

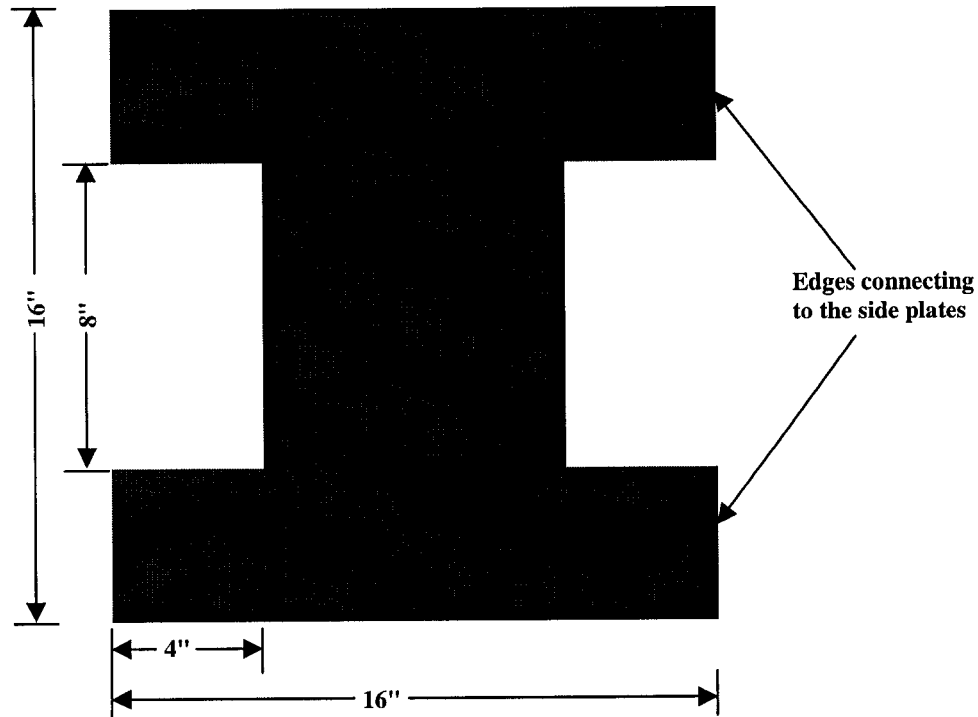


Figure 2-7. Medium plate of the mounting structure, the edges were cut to increase the flexibility.

The legs for the structure stretch across the length with a thickness of 0.5" (12.7 mm). In the first part of the analysis it was considered the legs to be extended away from the sidewalls in the outward direction to a distance of 1". But when the structure with the maximum lumped mass and the test item sitting on it was tested at 7 g RMS the margin of safety was below 1. In order to account for higher stress levels and to improve the M.S of the entire structure, the legs were considered to extend on both sides of the sidewalls to a distance of 1".

Almost the entire mounting structure (except medium plate) is manufactured using 7075 grade aluminum while regular 6061 grade is used for manufacturing the test item and the medium plate of the mounting structure. Because of the higher yield strength of the 7075 material compared to the 6061, the M.S of the structure is improved without increasing the mass of the structure, as the density of both the materials is same.

Although the proposed mounting structure with all the above mentioned dimensions has the required frequencies below the fundamental frequency of the test item and respects almost all the dynamic and static/physical requirements, the weight of the mounting structure is below the weight of the test item. In order to increase the weight of the structure, a brass plate of 3 kg and 6"x6"x0.7" in dimension is attached at the center of the top plate (facing the medium plate so as to have a flat top surface for easy attachment of test item). This also helps in further reduction of fundamental frequency and generates multiple modes below the natural frequency of the test item. Considering the brass plate the mounting structure weighs 22.8 lb (10.34 kg) and with adding 27 - 32 lb (12.25-14.52 kg) in terms of lumped mass, it can go up to a maximum of 50 - 55 lb (22.7 – 25 kg), thus respecting the Req. 17. The structure has a provision of adding additional mass on all the plates.

As there is no requirement on the number of attachment points for the mounting structure, 16 attachment points are considered, which can be altered depending on the testing acceleration and related stresses of the coupled system. The mounting structure with the achieved dimensions is shown in the Figure 2-8.

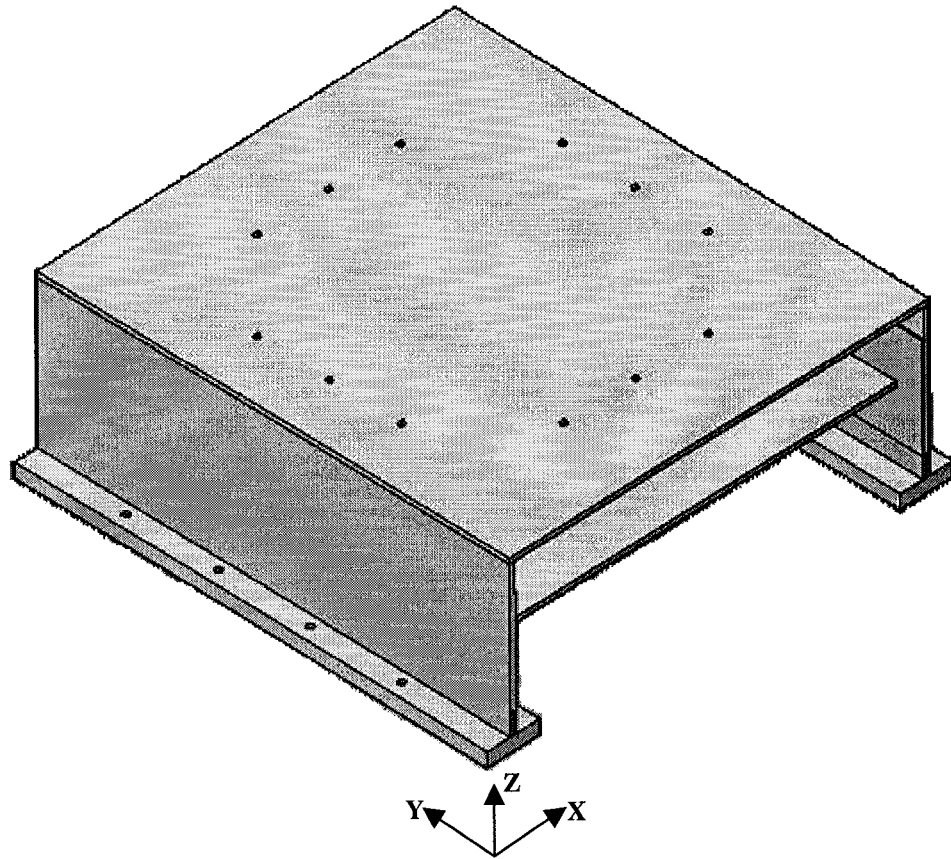


Figure 2-8. Mounting Structure indicating the attachment points for the test item.

The natural frequencies of the mounting structure with lumped masses (split evenly between the top and middle plates and attached at the center) and without lumped masses for 8 and 16 attachment points are indicated in the Tables 2-2 and 2-3, respectively. It is evident that the first three frequencies of the mounting structure are well below the fundamental frequency of the test item (Req. 8).

Table 2-2. Natural frequencies of mounting structure with and without lumped mass and attached at 8 attachment points

| Mode No. | Frequency (Hz) Without lumped mass and 8 attachment points | Frequency (Hz) With lumped mass and 8 attachment points |
|----------|--|---|
| 1 | 54 (80 - X) | 35 (85 - X) |
| 2 | 83 (48 - Z) | 45 (29 - Z) |
| 3 | 116 (14 - Z) | 61 (43 - Z) |
| 4 | 262 (3 - Z) | 215 (4 - X) |
| 5 | 332 (3 - X) | 248 (13 - Y) |
| 6 | 387 (14 - Y) | 290 (10 - Y) |
| 7 | 560 (42 - Y) | 337 (4 - X) |
| 8 | 626 (2 - X) | 366 (50 - Y) |
| 9 | 704 (3 - Z) | 405 (7 - Y) |
| 10 | 739 (2 - Z) | 509 (4 - Z) |

Table 2-3. Natural frequencies of mounting structure with and without lumped mass and attached at 16 attachment points

| Mode No. | Frequency (Hz) Without lumped mass and 16 attachment points | Frequency (Hz) With lumped mass and 16 attachment points |
|----------|---|--|
| 1 | 83 (47 - Z) | 45 (29 - Z) |
| 2 | 105 (76 - X) | 62 (42 - Z) |
| 3 | 116 (13 - Z) | 70 (78 - X) |
| 4 | 263 (2 - Z) | 219 (5 - X) |
| 5 | 339 (4 - X) | 249 (9 - Y) |
| 6 | 398 (5 - Y) | 293 (4 - Y) |
| 7 | 707 (2 - Z) | 380 (6 - X) |
| 8 | 741 (1 - Z) | 399 (1 - Y) |
| 9 | 790 (30 - Y) | 401 (2 - X) |
| 10 | 812 (7 - X) | 454 (44 - Y) |

2.2.3 Test Fixtures

According to the design requirements, both test articles should have the same fixture.

Knowing that the shaker has a 14 in diameter, the fixture is considered to have a base of 14 in diameter, the maximum possible so as to provide the maximum rigidity to the base.

Meanwhile considering the required dimensions for the test item and the mounting structure as explained in Sections 2.2.1 and 2.2.2 and dimension of the slip table (20" x 20"), the top face of the fixture has a dimension of 20" x 20" in order to accommodate the mounting structure which has a base dimension of 18" x 18".

Once the dimensions of the top and the bottom plates (thickness not included) of the fixture are finalized. The height and location of the flanges between these two plates should be obtained taking into account the length of the bolts to be used to fix the fixture to the shaker and the slip table. The thickness and number of flanges, the thickness of the top and the bottom plate should provide sufficient rigidity to the fixture that the fundamental frequency will always be above 2000 Hz (at least 1500 Hz) even when both the test structures are sitting on it. In order to have sufficient space between the top and the bottom plate of the fixture to screw the bolts, the height of the flanges was considered as 3.125" (79.375mm).

To perform the initial analysis and to obtain the fundamental frequencies of the structure, the bottom plate, top plate and the flanges are considered to be 3/4" (19.05 mm), 1/4" (6.35 mm) and 1/4" (6.35 mm) respectively. 8 flanges considered for the initial analysis, which are 45 deg apart from each other. The flanges have different dimensions in terms of length as, the rectangular plate has maximum length (14.14") at the diagonal (at 45 deg) and the minimum length (10") at 0 deg. The angles for the fixing the flanges are decided with respect to the top plate. If you draw two line bisecting the width and length of the top plate making it in to 4 equal squares, if one of the line is considered as 0 deg

then the rest will be at 90, 180 and 270 in the anti-clockwise direction from the initial point. The base plate is fixed at the maximum number of attachment points possible (20 attachment points) as provided by the shaker and the slip table to find the fundamental frequency of the fixture in all the three directions (X, Y and Z). The fundamental frequency of the fixture with the mentioned dimensions was found to be just above 500 Hz in all the three directions.

In order to increase the frequency it is considered to increase the number and thickness of the flanges. The number of flanges is doubled and they are attached at every 22.5 deg as shown in Figure 2-9, and the thickness of the flanges is increased to 0.5 in (12.7 mm). Although with this provision the frequency has increased, the fixture is found to be not sufficiently rigid to have a fundamental frequency above 1000 Hz. The mode shape of the fundamental frequency of the fixture was moving up and down in the vertical direction at the largest flange (which is at an angle of 45 deg or the diagonal of the plate) since major part of the flange was hanging without much support from the base plate. The reasons for this mode shape are 1) The flange is considered as a tapered beam extending from the base plate to the edge of the top plate reducing along the height maintaining the thickness, 2) To provide a provision for the bolts to fix the base plate to the shaker plate or the slip table a slot is made on the flanges at 0 and 45 deg apart from thereon. Thus, the flanges at these locations have less stiffness or the maximum strain energy, which affect the frequency of the fixture. To further increase the stiffness of the fixture and to increase the frequency (or to reduce the strain energy at the critical points), the flanges at the 0 and 45 deg are considered to have variable thickness across the length.

After an extensive analysis the final dimensions obtained for the plates forming the fixture are as follows:

- The flanges located at the 0, 90, 180 and 270 deg are considered as 1.25” (31.75 mm) thick till the edge of the base plate and 0.875” (22.225 mm) from the end of the base plate till the end of the top plate.
- The thickness of the flanges at 22.5 and 45 deg apart from there after (8 in number) are uniform throughout the length, each of them have a thickness of 0.875” (22.25 mm).
- The flanges at 45 deg and 90 deg apart till 315 deg (4 in number) are 1.25” (31.75 mm) thick to a length of 4.5” (114.3 mm) from the end near to the center of the bottom plate and 0.75” (19.05 mm) thick there after till the end of the flange.
- Both the base plate and the top plate should have a thickness of 1” (25.4 mm) in order to obtain the frequencies in the desired range of above 1500 Hz.

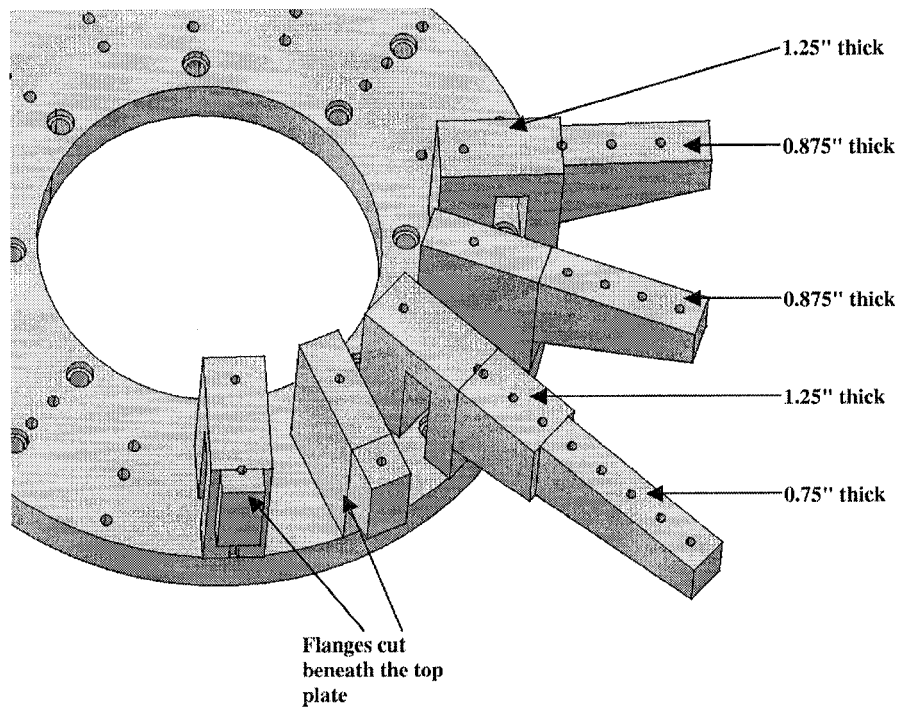
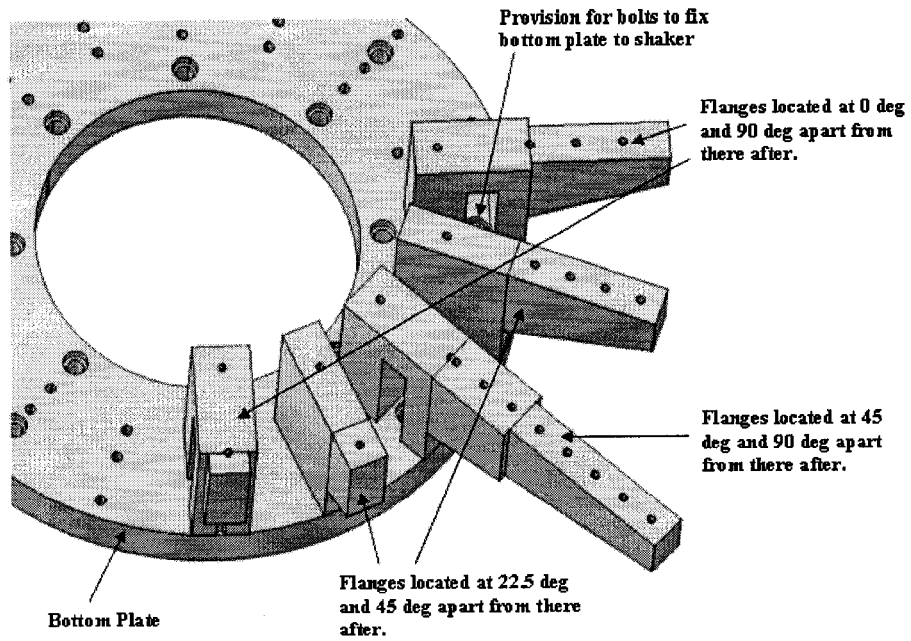


Figure 2-9. Location and thickness details of the flanges.

The frequency of the fixture with the above dimensions was found to be 1035 Hz and 1185 Hz in the lateral and the vertical directions respectively. But the effective mass associated with the above frequencies was below 10% of the total mass of the structure indicating the importance (or lack of it) of the mode. It is also observed that the sum of effective masses of the frequencies below 3000 Hz was below 50% of the total mass in the vertical direction and was 90% in both the lateral directions, which indicates the fixture is less rigid in the lateral direction compared to the vertical direction.

When the modal analysis of the fixture is repeated with the addition of lumped mass (representing the mass of the test item and the mounting structure) at the point of attachment of test item and the mounting structure, it was found that the frequency in the lateral directions was 530 Hz and 950 Hz in the vertical direction.

Once the dimensions of the fixture were finalized (satisfying the requirement of having frequencies above 1500 Hz), it was decided to reduce the mass of the fixture so that the test item and the mounting structure can include maximum possible lumped mass to account for the sensitivity analysis and also provide a large range of mass ratio for both structures. In order to achieve that, pockets were made on both the base plate and the top plate. A 3.5 in diameter circular pocket was extruded from the base plate and a 4.5 in square pocket was extruded from the top plate. Since the mounting structure has the attachment points only in one direction and the fixture is used only for vertical direction, there is no point of having a rectangular shape for the top plate; hence the material excess to the attachment points of the test item was removed from both the top plate and from

the corresponding flanges (located at 0 deg and 22.5 deg) beneath the top plate, it can be observed in Figure 2-9 that two of the flanges are smaller in size than the rest of them. However the material of the flanges extruding towards the center of the bottom plate is not removed as it provides the stiffness/rigidity to the flange in reducing the displacement of the top plate, which in turn increases the strain energy and frequency corresponding to the motion of the top plate. The total mass of the structure after removal of the excess material is found to be 52 lb. There was not much change in the frequency of the fixture in the desired direction of excitation, i.e. in the vertical direction. Figure 2-10 presents the entire assembly of the flanges, top plate and the base plate.

As mentioned above, the fixture presented in the earlier paragraph is not rigid enough in the lateral directions due to the drop in the frequency of the fixture in the lateral directions upon adding test item and mounting structure to it. Therefore it was decided to have separate fixtures for vertical and lateral directions. The fixture described above is used in the vertical direction due to its rigidity in that direction. The fixture for the lateral direction consists of a simple plate having the same dimensions as the top plate of the earlier fixture i.e., 20" x 20" in cross-section and 1" in thickness for the initial analysis. The frequency of the plate was found to be above 2000 Hz in both the lateral directions. Since the weight of slip table and bullnose (connecting the shaker to the slip table) add to the weight of the structures while testing the test item by itself and at system level in the lateral direction, it was decided to have the least possible weight for the fixture in the lateral direction. The thickness of the fixture is decided on the basis of the bolt (3/16" dia alloy steel) used to fix the fixture to the slip table with the counter bore hole, and the

minimum thickness required to hold the M6 bolt connecting the test item and the mounting structure to it. The thickness of the plate (lateral fixture) was chosen to be 0.625 in (15.875 mm). The frequency of the fixture shown in Figure 2-11 with the above-mentioned dimensions in the vertical direction was 1250 Hz and the frequency of the structure in the lateral direction was well above 2000 Hz. The weight of the structure with the dimensions mentioned is 24.4 lb (11.06 Kg).

Although the requirement 20 is not met in terms of having same fixture for all tests, both at the test article and the assembled structures level, the rest of the fixture requirements were all met providing the least possible mass for the fixtures (both lateral and vertical). The resonance frequencies of both fixtures are indicated in the Table 2-4.

Table 2-4. Natural frequencies of the test fixtures and their corresponding effective mass and the direction in which it is obtained.

| Mode No. | Frequency of fixture for vibration testing in vertical direction. | Frequency of fixture for vibration testing in lateral direction. |
|-----------------|--|---|
| 1 | 1033 (13 – X) | 1254 (15 – Z) |
| 2 | 1035 (21 – X) | 2412 (15 – Z) |
| 3 | 1082 (12 – Y) | 2486 (29 – Z) |
| 4 | 1086 (6 – X, 3 – Y) | - |
| 5 | 1093 (3 – Y, 0.6 – Z) | - |
| 6 | 1185 (12 – Z) | - |
| 7 | 1322 (14 – Z) | - |
| 8 | 1758 (6 – X, 5 – Y) | - |
| 9 | 1806 (11 – X) | - |
| 10 | 1861 (26 – Y) | - |

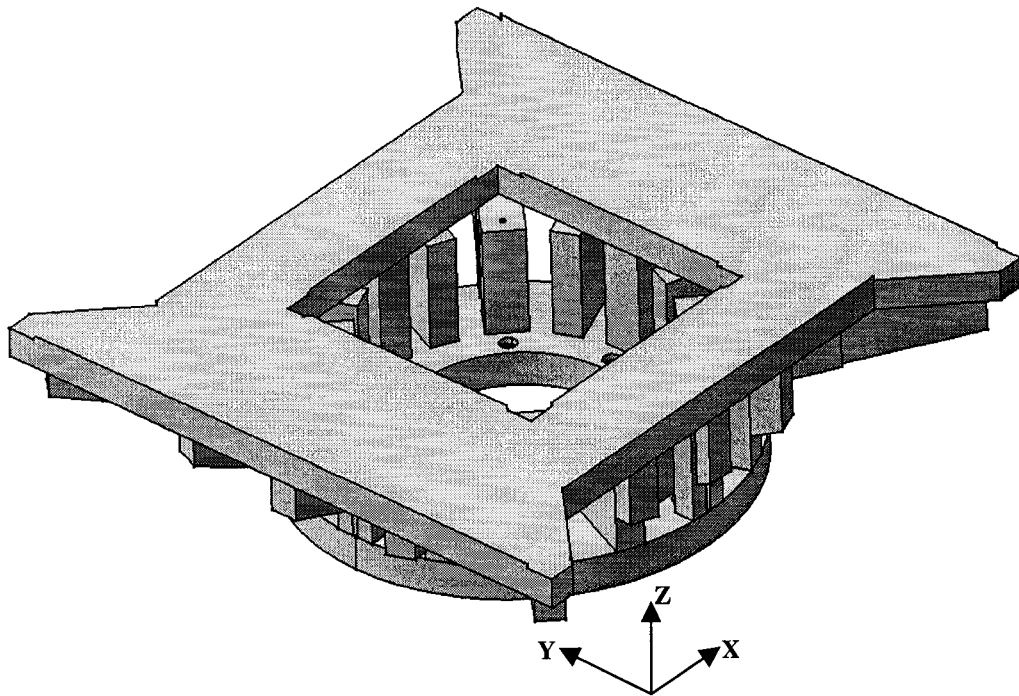


Figure 2-10. Fixture for vibration testing of test item and mounting structure in vertical direction (Z).

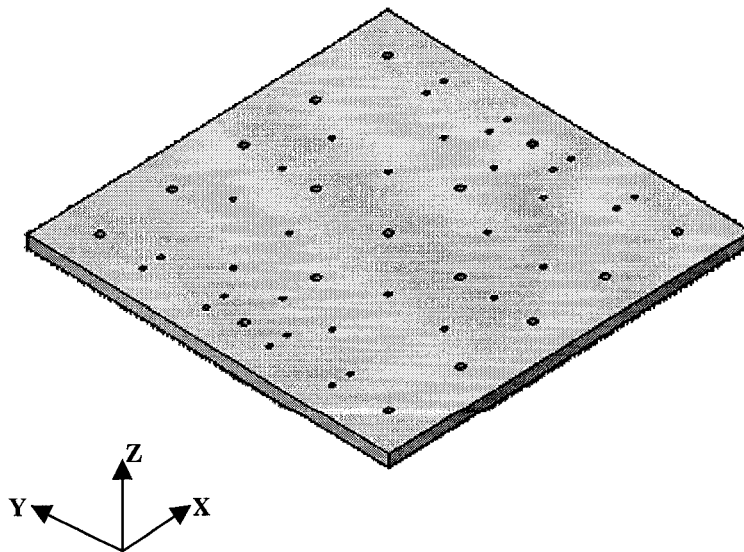


Figure 2-11. Fixture for testing of test item and mounting structure in the lateral directions (X & Y).

CHAPTER 3

ANALYTICAL SENSITIVITY STUDY FOR ESTIMATION OF C^2 PARAMETERS

As it was noticed in Chapter 2, the design of the test item and mounting structure are flexible enough to have a large variety of cases for the analytical sensitivity study. This section describes in detail 1) the guidelines and/or justifications for the selected cases in order to perform the analytical sensitivity study, 2) procedures of evaluating C^2 value, 3) sensitivity study results and finally 4) summary and concluding remarks. In the present study, some of the cases that may not be employed in real life situations are also considered in order to verify and get a broader idea on the behavior of C^2 and the parameters on which it depends.

The details of the finite element tools used to perform the coupled load analysis of the test structures are Nastran/Patran and SATOOLS of Maya Heat Transfer the details of which are mentioned in the chapter 2.

3.1. Description of Analytical Cases

Proper guidelines have been devised to select the cases for the analytical sensitivity study without duplicating the test structures (test items or mounting structures) and the assembled structures. These guidelines are related to:

- 1) Number of attachment / interface points for each structure,
- 2) Position of attachment points,
- 3) Fundamental frequency of the test structures,

- 4) Stiffness of the test structures,
- 5) Damping of the test structures,
- 6) Direction of the excitation, and
- 7) The mass-ratio of test items and mounting structure.

As mentioned earlier in the requirements and the design of test item in Chapter 2, the numbers of attachment points may vary from 3 to 12 (maximum number of force sensors available in the CSA). However any test hardware (similar to the considered test item) in real life are hardly fixed at 3 attachment points, which might occur only during the launch environment when one of the attachment points fails during the launch. Once the numbers of attachment points are finalized, the positions of the attachment points are considered. The test item can be fixed either on the same side as the side plates in which the attachment points have more stiffness or on the side of the stiffening member, which would provide the flexible attachment points and the most flexible structure. However it can be improved by adding the flanges that can ameliorate the test item in terms of stiffness as shown in the Figures 2-4 and 2-5. A proper name has been devised for the future case studies according to the attachment points and their position. The attachment points on the side of the side plates are named as Real attachment points (they are named Real attachment points since in the real life, structures similar to the test items would be attached at these points to conduct testing or for launch due to the stress considerations). The attachment points on the side perpendicular to the side plates are called Ortho attachment points (they are name Ortho since they are orthogonal to the real attachment

points). These attachment points are clearly illustrated in the test item shown in the Figure 3-1.

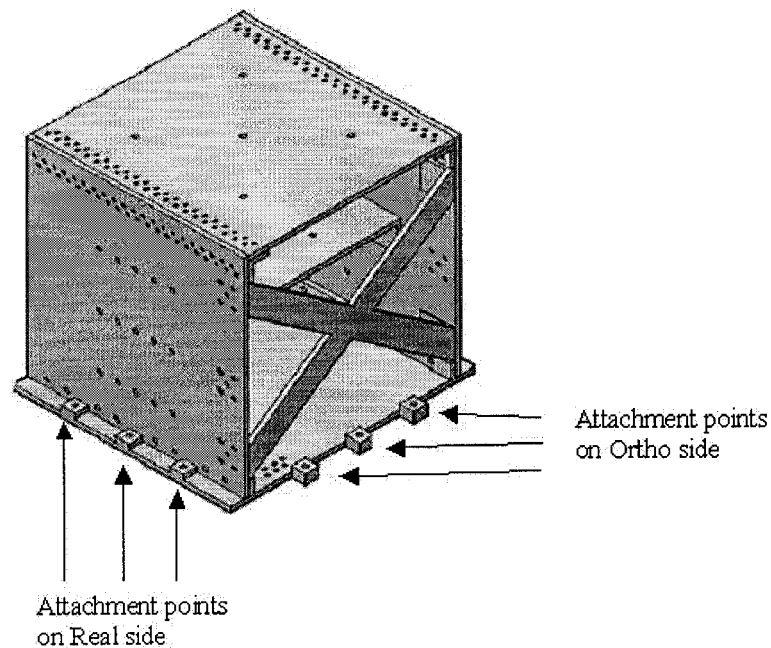


Figure 3-1. Attachment points of the test item

Next factor considered to identify the different cases is frequency, which is a major factor in describing the flexibility of the structure, which further depends on the number of attachment points and their position, the stiffness of the test item, i.e., the stiffness members used, and the number of lumped masses. The frequency factor is considered in identifying the case by taking into account the difference in fundamental frequencies of the test structures. Stiffness is one of the major factors that affect the flexibility of the test item, hence depending on the amount of lumped mass added to the structure and the fundamental frequency of the test item required, the stiffness members are changed accordingly. For the current analytical sensitivity study, only two values of viscous damping are assumed $\xi = 0.01$ and $\xi = 0.025$ ($Q=50$ and $Q=20$, respectively).

3.1.1. Naming of Cases at System Level

As explained before, due to the extensive benchmark case studies in the present research, proper naming of the cases is essential. A proper naming at the system level has been devised according to the factors affecting the flexibility of the structure (as mentioned in Section 3.1) or the possible parameters affecting the value of constant C^2 . An example of the possible case is shown in Figure 3-2.

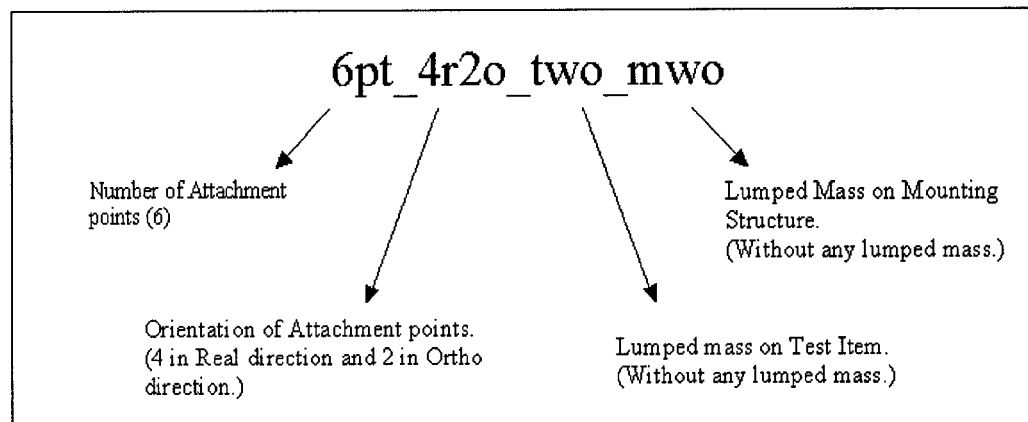


Figure 3-2. Description of test name at the system level

As illustrated in Figure 3-2, the first parameter specifies the number of the attachment points. The position of the attachment points can be identified by the second parameter, and the third and the fourth parameters indicate the lumped mass on the test item and the mounting structure, respectively. The details in the bracket shown in the Figure 3-2 indicate the values in the considered example i.e., the test item is connected to the mounting structure through 6 interface points, their position is 4 in the Real direction and 2 in Ortho direction and both the test item and the mounting structure are the basic structures without any lumped masses. The possible position of the attachment points is either on Real side or the Ortho side. However for the test item attached at 4 interface

points, one point on each side, the case is named as 4pt_oes_two_mwo and so on, where " oes " is read as "one attachment point on each side". The possible values for the 3rd and 4th parameters in the test name are two, twl and mwo, mwl respectively, where two and mwo indicates test item and mounting structure without any lumped mass, and twl and mwl indicates the test item and the mounting structure with lumped mass.

3.1.2. Naming of Cases at the Test Item Level

Naming of test cases at the test item level indicates the attachment points and the lumped mass on the test item. However this is not enough in recognition of test item that is used for testing at the test item level. Hence the proper naming of the test item is also devised to indicate the stiffness member/members used to control the fundamental frequency of the test item, which also controls the mass of the structure but to a little extent. The figure shown in the Figure 3-3 is an example of test item's naming, which can be one of the possible cases studied at the test item level. The example considered is the same test item considered at the system level explained in section 3.1.1.

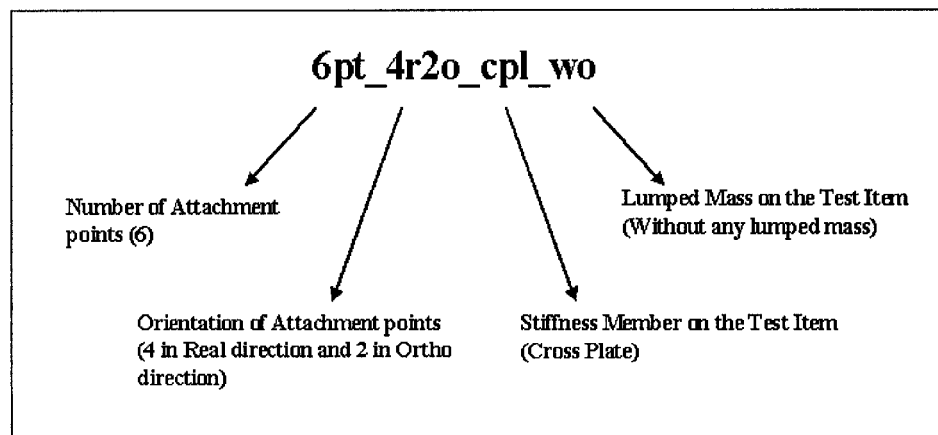


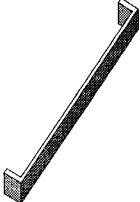
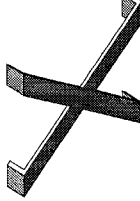
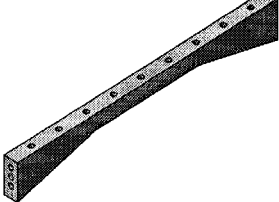


Figure 3-3. Description of test name at the test item level.

As it is clear from Figure 3-3, the first parameter indicates the number of attachment points, the second parameter specifies the position of attachment points, the third parameter points to the stiffness member used, and the fourth parameter represents the lumped mass on the test item and in some cases also represents the location of the lumped masses.

The possible cases for the third parameter, i.e. the stiffness member used, are indicated in the Table 3-1. It is noted that the possible cases for the stiffening members is the member specified in the Table 3-1 or a combination of two or more members. If the test item has all the possible stiffening members, for instance, the X-plate, Side stiff and the Medium Stiff plates, the parameter would be ASTF indicating all stiffness members have been used. There are couples of cases where this situation has been studied.

It also exist the possible cases for the fourth parameter, which indicates the lumped mass and its location. The possible location of the lumped mass would be on the top plate or middle plate or on the sides of the test item. When the lumped mass is added only on the top plate the value for the fourth parameter would be TPL, similarly for middle plate it will be MPL. In the present study there are no cases when the test item is loaded with the lumped mass only on the side plates. However the value of WL indicates that the test item is loaded on all the possible locations, i.e., top, medium and the side plates. The test name remains the same for testing of test item in lateral and vertical directions. A parameter is added at the end of the name to indicate the direction of excitation as 6pt_4r2o_cpl_wo_z, where the test item is excited in the Z direction.

Table 3-1. The possible cases for stiffening members.

| Stiffness Member Name | Stiffness Member Picture |
|--|---|
| <p>Cross Plate, attached on either side of the test item. The short form would be CPL. Most of the cases without lumped mass are with CPL as stiffening member.</p> |  |
| <p>X – Plate, attached on either side of the test item. The short form would be XPL. Most of the cases with lumped mass will include XPL as stiffening member.</p> |  |
| <p>Medium Stiff plate, this will be connected to the middle plate and the side plate to stiffen the middle plate. The short form would be MSTF. Whenever connected 2 plates will be connected.</p> |  |
| <p>Side Stiffening member, 4 of such members will be connected to the side plates on all the edges. The short form of the member would be SSTF.</p> |  |
| <p>Y – Stiff member. Most of the time this member is used to test the test item in Y direction as the structure is weak when connected in ortho direction only. They improve the stiffness and the fundamental frequency. Each time 4 of these members are attached connecting the bottom and the side plates.</p> |  |

3.2. Procedures for Estimation of C^2

Constant C^2 is a key parameter of the semi-empirical method, which sets the force limits throughout the complete frequency bandwidth of excitation. Some judgment should be used to choose the value of C^2 . Based on limited number of flight data, it has been observed that, in normal conditions, C^2 value as low as 2 might be chosen for complete spacecraft or strut-mounted heavier equipment, C^2 value as high as 5 might be considered for directly mounted lightweight test items. For the past decade many flight hardware have been tested with the semi-empirical method of force limited vibration technique, and there were cases when C^2 value above 5 was used to test the equipment. (Research in force limited vibration testing using semi-empirical method to understand the behavior of C^2 value and its relative parameters has not been reported yet. One objective of the current study is to perform in-depth study on the behavior of C^2 , and the parameters on which it depends.

Selection of the value of C^2 may be based on any, or a combination, of the following criteria [2]:

- 1) Extrapolation of interface force data for similar mounting structures and test items. The similarity of the test structures (test item and the mounting structure) is based on the individual mass or the mass ratio of test structures, resonance frequency or the bandwidth of the resonance frequency of both the test structures.
- 2) Comparison with force limits at the fundamental frequency derived from the simple and/or complex TDFS methods, when such predictions are available. Normally, this comparison is not readily available when the test item is the

complete spacecraft. It is noted that the estimation of C^2 value using Simple or Complex TDFS techniques requires the impedance characteristics of the test item and the mounting structure in the frequency bandwidth of the fundamental frequency of the test item [1].

- 3) Comparison with design limit load. The selection of C^2 should ensure that the limit load is not exceeded. [18]
- 4) Selection of a value for C^2 should result in a level of notching at the fundamental frequency equivalent to or below the notching level provided by the mechanical impedance correction technique [27].
- 5) Observation of low-level force spectral density. This data may be used as a guideline for a range of acceptable C^2 values.
- 6) Comparison with interface force between the test item and the mounting structure for the launch configuration or for the next higher hardware level, normally obtained from coupled load analysis. The force limits should obviously not be lower than the interface force to avoid any undertesting. This is the method employed in the current study for the evaluation of C^2 parameter. Coupled load analysis of the finite element models of the test structures is performed to obtain the interface acceleration and force PSD's. Once the PSD's are obtained the semi empirical formula is used to find the corresponding C^2 value, which would be rounded to the next higher integer to be conservative. The detailed procedure adopted for the calculation or evaluation of C^2 parameter using the above method is explained in the following paragraphs.

As it may be seen from the previous paragraphs, several options are available for the selection of the C^2 constant. In fact, the level of conservatism of the force limits depends on the selected value for C^2 .

As it was mentioned earlier, the current investigation is based on the coupled load analysis of the test structures for estimation of C^2 value. Over 70 cases are studied, which are identified/selected on the basis of the factors mentioned in Section 3.1. The extracted results are tabulated with respect to the values of C^2 and the resulted amount of input notching at the fundamental frequency of the test item for each individual case.

The procedure of estimation of C^2 value is now described in an example case study, where the test item is fixed at 4 attachment points oriented in the real direction with cross-plate as the stiffening member and without any lumped mass on the test item and the mounting structure and excited in the Z direction (Vertical axis). Hence the names of the tests at the system and the test item level are 4pt_4r_two_mwo and 4pt_4r_cpl_wo_z respectively.

To obtain the fundamental frequency and the apparent mass of the test item in the specified configuration and direction of excitation, a random white noise acceleration with PSD of $1 \text{ g}^2/\text{Hz}$ over a frequency range of 20 Hz to 2000 Hz (equivalent to 42 g rms) has been applied to the base of the test item when it is sitting on a rigid base (shaker). To simulate the rigid structure (fixture) beneath the test item, a node is created below the test item (sufficient distance from the base plate) and is connected to the

attachment points using the rigid-bar elements and the input is given to the node, which is constrained in all the 6 DOF as shown in the Figure 3-4. The apparent mass of the test item and its resonant frequency are shown in the Figure 3-5, which is obtained by taking the reaction force at the base node connecting all the attachment points. There is always a possibility that the obtained results may not represent the true structure, in the sense that not enough significant modes are recovered. To verify the accuracy of the results obtained, the asymptotic value of the apparent mass at the low frequencies is examined. This value should be at least 90% of the mass of the test item, i.e., at least 90% of the mass of the structure is retrieved at the base node (which is the case for most of the structures in the frequency bandwidth of 20 H to 2000 Hz). For the current example where the test item weighs 15.7 lb (7.12 kg), the asymptotic value of the apparent mass is found to be 14.7 lb (6.7 kg), which is approximately 94% of the total mass of the test item. Hence the obtained values represent the true structure in term of the amount of effective mass recovered.

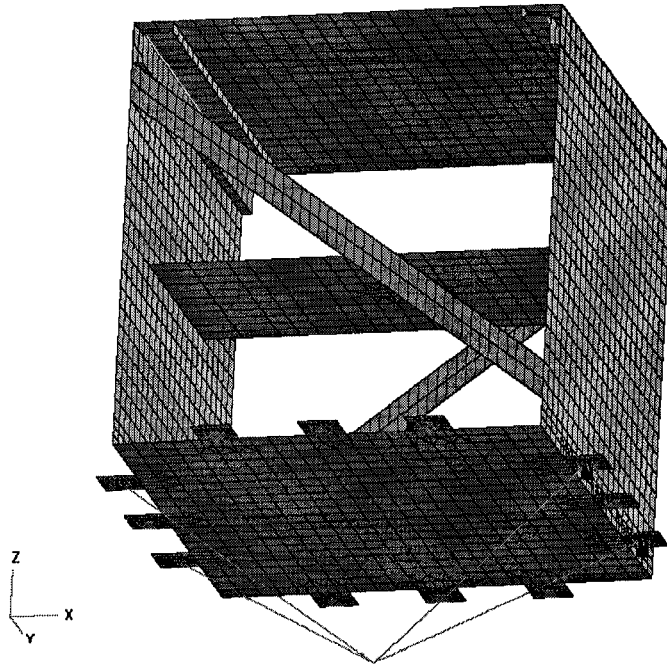


Figure 3-4. Finite element model of test item used to find the apparent mass, and the node simulating the fixture beneath the test item.

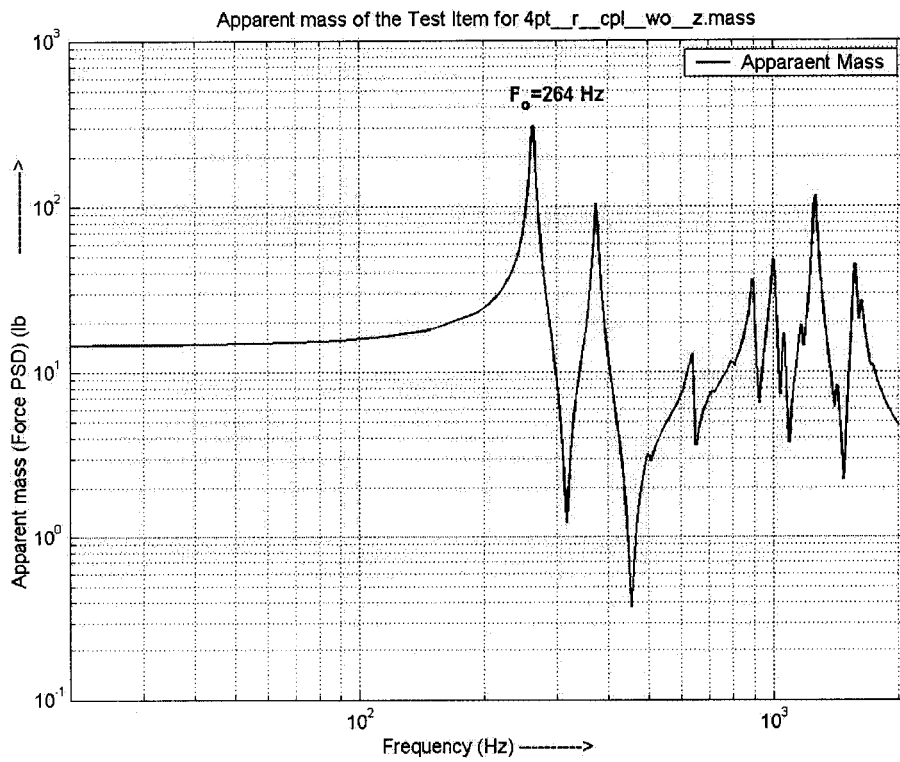


Figure 3-5. Apparent mass of the test item for 4pt_4r_cpl_wo_z configuration.

Once the test item natural frequencies and the impedance characteristics are obtained, coupled load analysis of the system is performed. For the coupled load analysis the test item is attached to the mounting structure at the same attachment points that are used in the evaluation of apparent mass and the impedance characteristics of the test item using bar element with the dimensions and properties of M6 alloy steel bolt. The bar element is connected to the Multi Point Constraint elements of both the test item and the mounting structure at the attachment points. It is noted that the MPC element is created at the attachment points connecting the nodes along the diameter of the hole with the one at the center of the attachment point, which forms one of the end point of the bar element. The same procedure is also employed to simulate the fixture below the mounting structure as done for test item to obtain the apparent mass. The nodes of attachment between the test structures and the simulation of rigid fixture below the mounting structure is shown in the Figure 3-6. The mass of test item and the mounting structure are 15.7 lb (7.12 kg) and 22.9 lb (10.4 kg), respectively.

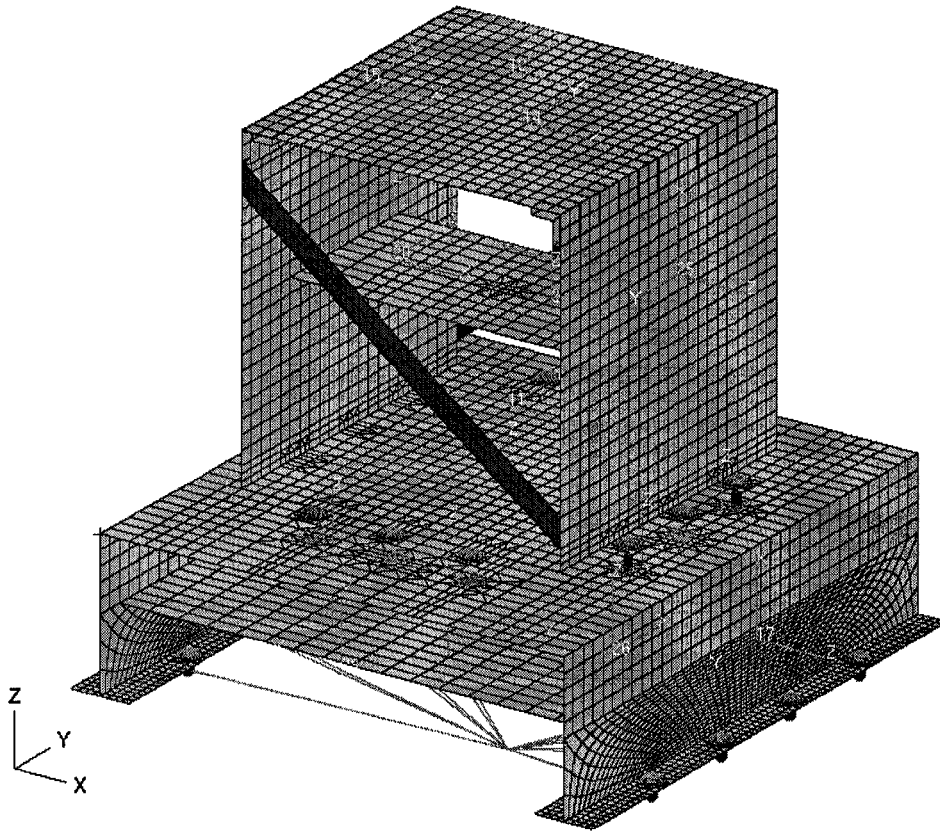


Figure 3-6. Coupled System consisting Test Item and the Mounting Structure.

Using the NASTRAN finite element solver and its random vibration module, the coupled system environment is imposed at the base of the mounting structure. The acceleration input applied to the system is based on the data extracted from the NASA GEVS standard [29] for the acceptance level vibration test performed on structures 50 lb (22.7 kg) or below. This input spectrum has an RMS value of 10.0 g. For the analysis of the present example, it is assumed that the test structures have an amplification factor of 50 ($Q=50$) i.e., a damping ratio of 0.01. The Acceleration PSD input to the coupled system is shown in the Figure 3-8. Having applied the acceleration input, the interface acceleration between the test item and the mounting structure has been computed at the attachment/interface points. The acceleration computed at the attachment points are

illustrated in the Figure 3-8. Since the test item is symmetrical and the mass is evenly distributed on the attachment points, the accelerations at all the attachment points overlap each other. One might observe that the level of acceleration in the Figure 3-8 is quite high which is mainly due to the low damping assumed for both the test structures and the conservative levels imposed by the GEVS.

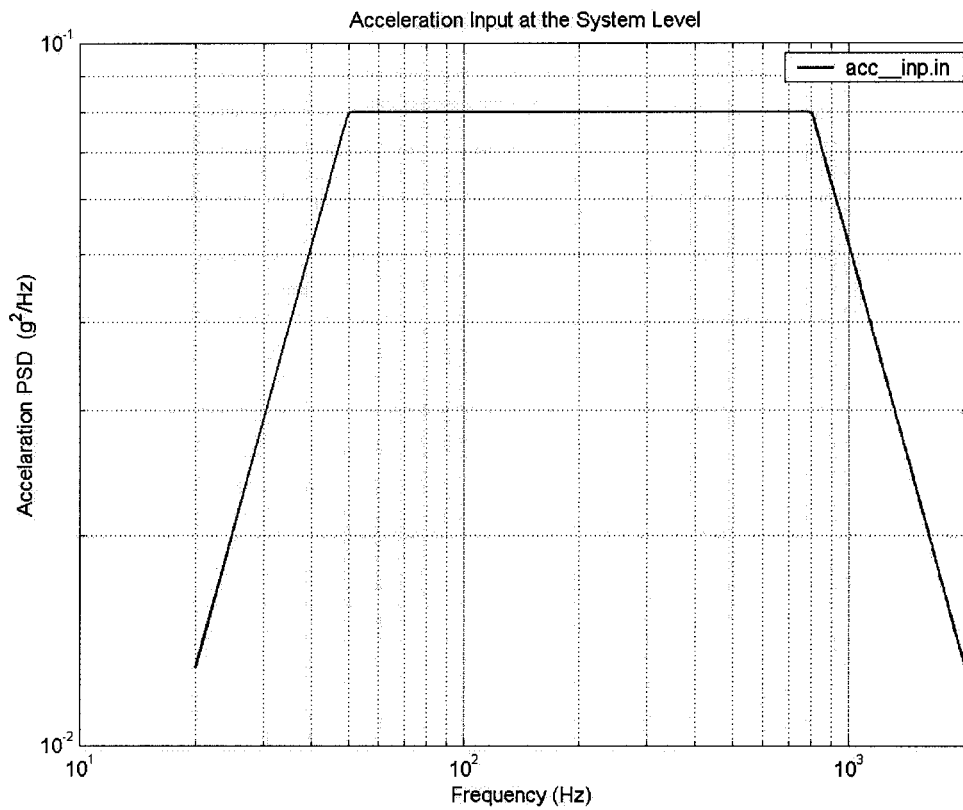


Figure 3-7. Acceleration input to the base of mounting structure at the coupled system level.

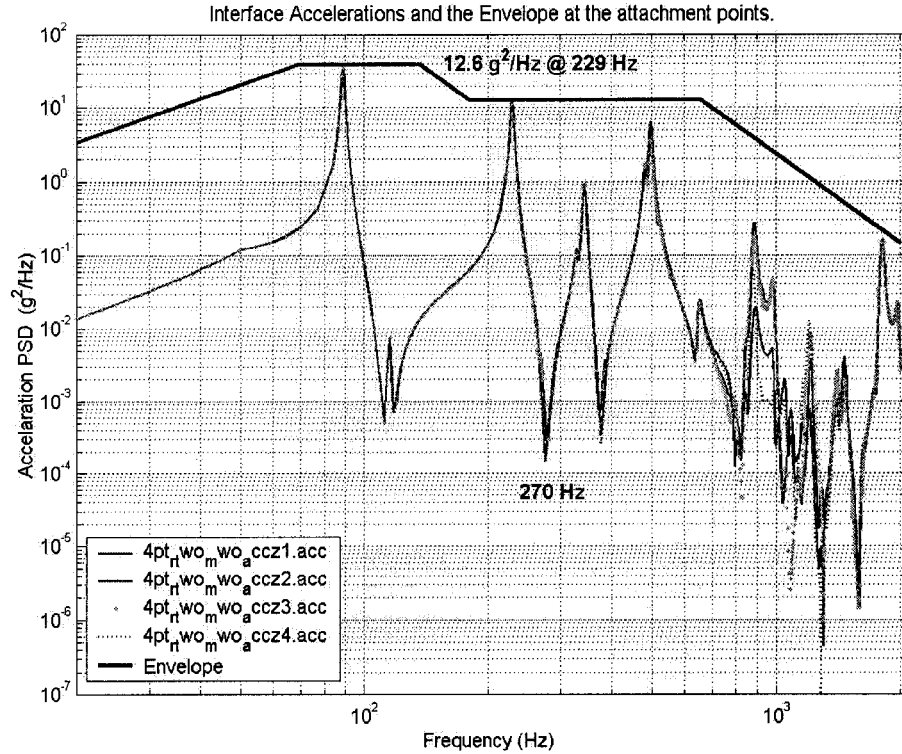


Figure 3-8. Interface accelerations at 4 attachment points and the envelope of accelerations.

The value of the C^2 parameter is obtained from Eq. (1-11) which is rewritten here as

$$C^2 = \frac{S_{FF}(f_{maxf})}{S_{AA}(f_{maxa}) \times M_o^2} \quad (3-1)$$

where, $S_{AA}(f_{maxa})$ is the maximum value of all the interface point accelerations at frequency f_{maxa} occurring at the highest of the two peaks adjacent to the anti-resonance (the fundamental frequency of the test item). In the present example, the anti-resonance occurs at 270 Hz, and the maximum acceleration having a value of $12.6 \text{ g}^2/\text{Hz}$ occurs at 229 Hz. Comparing the Figures 3-5 and 3-8 reveals that the anti-resonance occurs at a slightly different frequency than the fundamental mode of the test item. This is mainly due to the differences in boundary conditions between the test item level and the system level configurations. This selection for the acceleration value implies that, in the

frequency range of interest, the enveloping process for defining the input environment for testing the test item perfectly envelopes the highest peak of the interface accelerations directly relevant to the fundamental mode of the test item by itself. For frequencies away from the fundamental frequency of the test item, the acceleration envelope is defined by simply loose enveloping of the maximum interface accelerations. The acceleration envelope to be used as the input environment for the test item is also shown in the Figure 3-8.

$S_{FF}(f_{\max f})$ corresponds to the value of the interface force PSD calculated at the frequency $f_{\max f}$ occurring at the higher of the two peaks adjacent to the anti-resonance (the fundamental frequency of the test item by itself). The definition of the interface force PSD will be discussed later. For the majority of cases, the frequencies $f_{\max a}$ and $f_{\max f}$ are the same, implying that the maximum acceleration and force are occurring at the same system level mode.

The values of acceleration and force as defined previously leads to an exact value for the estimation of C^2 parameter. This value is exact in the sense that the application of Eq. (1-11) using this value of C^2 together with the acceleration envelope covering the fundamental frequency of the test item will result in a force limit PSD value equal to the maximum interface force at the system level. This implies that no over-testing or under-testing is involved in the process. Consequently, the selection of any C^2 larger than this exact value would lead to overtesting of the test item. Furthermore, if the acceleration

enveloping process led to an input acceleration higher than the maximum peak value discussed earlier, overtesting would be presented, even if the 'exact' C^2 value was used.

The interface force in the coupled system is shown in the Figure 3-9. The interface force is obtained by adding the forces at each of the interface points, at each frequency. Since the interface force at each of the attachment point is in the form of PSD, they cannot be added directly to represent the total force PSD, hence the total force PSD is the square of the sum of square-root of each individual force PSD, i.e.,

$$T.F(PSD) = \left[\sum_{i=1}^n \sqrt{F_i(PSD)} \right]^2 \quad (3-2)$$

where $T.F$ is the total PSD force at the interface level, n is the number of attachment points and F_i is the individual force PSD at each attachment point.

Figure 3-9 may not represent true interface force in terms of value at all the frequencies except the value at the natural frequencies of the test item. The reason for the this statement is that the forces are added by making an assumption that they will always be in phase, which certainly is not true at all the frequencies, however most often they will be in phase at the resonance frequency at the system level (f_{maxf}) which is used for computing the value of C^2 . It has been verified for the current example that all interface forces is in phase. This has also been verified care for other case studies by checking the mode shape of the test structures and the phase of the force at the concerned frequency. For the few cases when some of the interface forces are not in phase with the rest of

them, this is taken into account by subtracting the corresponding terms in the above equation.

For the current example, the application of this process would lead to the following value for C^2 :

$$C^2 = \frac{1.11 \times 10^4}{[15.7^2 \times 12.6]} = 3.6. \quad (3-3)$$

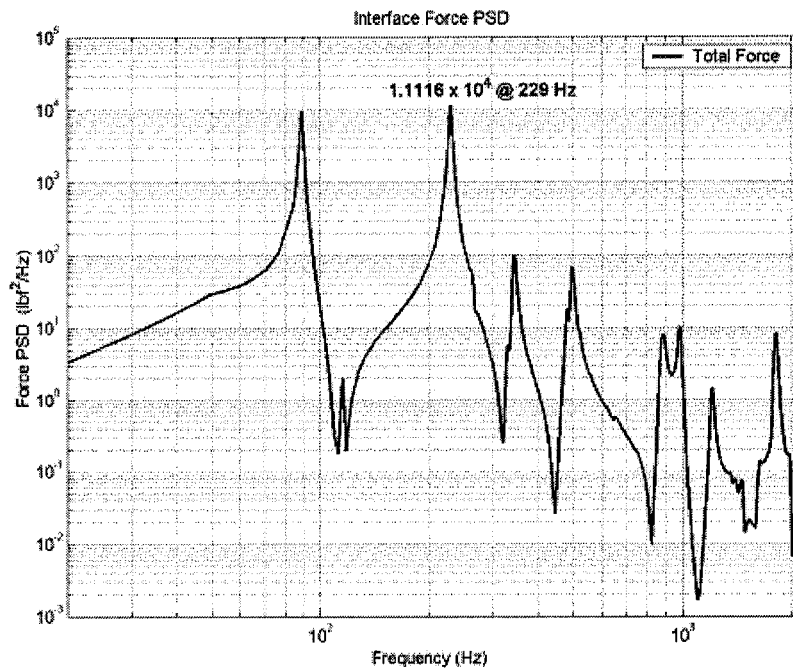


Figure 3-9. Total force PSD for 4pt_4r_two_mwo for excitation in Z direction.

Having obtained the value of C^2 , now the test item may be tested by itself. The acceleration envelope of the interface accelerations forms the input environment for the test item. The interface force obtained at the base of the test item at the instrument level with the acceleration envelope as an input to the test item is shown in the Figure 3-10. Figure 3-10 also indicates the force limit without any conservatism considered, shown as

the horizontal line. It should be noted that this line does not represent the force limits computed for the whole frequency bandwidth of excitation. It is only the value corresponding to the fundamental mode. It can be observed that at the fundamental frequency, the force is approximately 100 times more than the one obtained at the system level. During the actual force limited vibration test, the acceleration input is notched at the fundamental frequency where the force at the base of the test item crosses the force limit line by some notching factor. The value of notching at the fundamental frequency can be obtained by dividing the force obtained at the system level (i.e. force limit) with the product of maximum interface acceleration and the apparent mass at the fundamental frequency, i.e., the value of notching is a function of frequency as well. For the current example the notch value is

$$N = 10 \times \log \left[\frac{S_{FF}(\text{with FLV})}{S_{FF}(\text{Without FLV})} \right] = 10 \times \log \left[\frac{1.1116 \times 10^4}{[307.9^2 \times 12.6]} \right] = -20.3 \text{ dB} \quad (3-4)$$

where, “ S_{FF} without FLV” is the product of the maximum of the apparent mass occurring at the fundamental frequency and the input acceleration at the same frequency. In the considered example the apparent mass of the test item at the fundamental frequency is 307.9 lb (139.7 kg), the input acceleration is 12.6 g^2/Hz , and the force at the natural frequency is 1.11×10^4 lb^2/Hz , and “ S_{FF} with FLV” is the force limit.

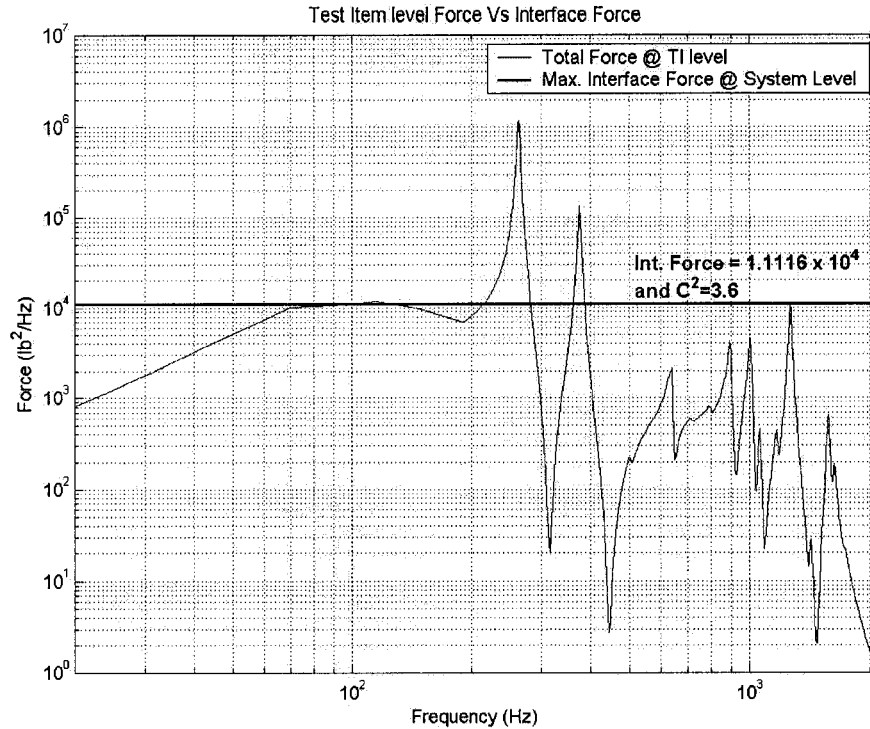


Figure 3-10. Force at the base of the test item at the instrument level and the force limit with a C^2 value of 3.6

3.3 Sensitivity Study Results

As mentioned earlier, there are about 70 cases considered for the sensitivity study in all the directions of excitation (X, Y and Z directions), which are selected on the basis of the factors specified in Section 3.1. These cases studies should be extremely useful to realize the in-depth concept of the semi-empirical method and can be interpreted as the benchmark problems, which can be a helpful reference to research community and test engineers involving in this field.

The results indicating the impedance characteristics, C^2 and notching values are tabulated separately in Tables 3-2 to 3-7 for Lateral (X and Y directions) and Vertical directions (Z direction). The physical mass and effective masses of test item and mounting structure at

the natural frequency of the test item for different configurations are shown in Tables 3-2 and 3-5. The C^2 and notching values are given in Tables 3-3 and 3-4 for lateral directions and in Tables 3-6 and 3-7 for vertical direction.

The apparent mass of the test item is found using the procedure mentioned in Section 3.2, while the effective mass of the test structures (test item and mounting structure) are found by the FEM solver (NASTRAN) by running solution SOL101 or modal analysis by including MEFFMASS card in the case control statements, which gives the effective mass in each direction for all the modes. The effective mass in the 1/3rd octave band is found by adding all the effective masses in that particular bandwidth. The points of attachment play a major role in the effective mass of the mounting structure. As mentioned in the literature [11] for coupled load analysis of the test item and the mounting structure (CTDFS method), the mounting structure is attached only to the test item. The attachment is also only with the residual masses of both the structures, i.e., the residual mass of test item is connected to the residual mass of the mounting structure. Hence the mounting structure is attached at the attachment points of the test item on it, rather than the real attachment points at its base to find the effective mass in the 1/3rd octave bandwidths. But the test item is attached at the logical or natural attachment points. The values of C^2 and the amount of notching are found according to the procedure explained in the previous section.

The results are tabulated separately for impedance characteristics, C^2 and notching. The physical mass and effective masses of test item and mounting

Not many cases were studied in the Y direction. This can be attributed for the following reasons:

- 1) The mounting structure is flexible at the attachment points of the test item, so the fundamental mode of the test item when sitting on the mounting structure was overlapped by the mode at the coupled system level making it impossible to pick the peak adjacent to the anti-resonance in the acceleration spectral density curve, which determines the input acceleration to the test item when tested by itself. It was also impossible to evaluate the interface force due to overlapping of modes at the coupled system level.
- 2) The fundamental frequency of the test item was below the fundamental frequency of the mounting structure when connected at the attachment points in the Ortho direction.

The cases with excitation in the Y direction included in the study are performed by considering the Y-Stiff members.

Same acceleration input as shown in the Figure 3-7 is given to the base of the mounting structure for all cases for the sake of uniformity, although the input acceleration level should change with the mass of the test structures according to GEVS acceptance level of testing.

Table 3-2. Impedance characteristics of the test structures at the natural frequency of the test item in the lateral directions (X and Y).

| Case No. | Case Name | Physical Mass (lb) | | Freq. (Hz) | Effective Mass (lb) | | |
|---|----------------------|--------------------|------|------------|---------------------|-----|-----------------|
| | | T.I | M.S | T.I | T.I | M.S | Ratio (T.I/M.S) |
| Cases Evaluated in the X direction | | | | | | | |
| 1 | 3pt_2r1o_twl_mwl | 43.2 | 61.5 | 117 | 35.1 | 0.0 | 351000 |
| 2 | 3pt_2r1o_two_mwo | 15.7 | 21.9 | 180 | 9.7 | 0.0 | 96800 |
| 3 | 3pt_3r_twl_mwl | 43.2 | 61.5 | 120 | 34.3 | 0.3 | 135.8 |
| 4 | 3pt_3r_two_mwo | 15.7 | 21.9 | 188 | 9.5 | 0.4 | 22.1 |
| 5 | 4pt_oes_twl_mwl | 43.2 | 61.5 | 118 | 35.2 | 0.6 | 60.0 |
| 6 | 4pt_oes_two_mwo | 15.7 | 21.9 | 185 | 10.0 | 0.7 | 14.0 |
| 7 | 4pt_4r_twl_mwl | 43.2 | 61.5 | 121 | 33.3 | 0.0 | 333000 |
| 8 | 4pt_4r_two_mwo | 15.7 | 21.9 | 190 | 9.7 | 0.0 | 97000.0 |
| 9 | 6pt_2r4o_twl_mwl | 43.2 | 61.5 | 120 | 35.2 | 0.7 | 51.0 |
| 10 | 6pt_2r4o_two_mwo | 15.7 | 21.9 | 189 | 9.8 | 0.8 | 12.2 |
| 11 | 6pt_4r2o_twl_mwl | 43.2 | 61.5 | 122 | 33.3 | 0.0 | 332700.0 |
| 12 | 6pt_4r2o_two_mwo | 15.7 | 21.9 | 192 | 9.9 | 0.0 | 99200 |
| 13 | 6pt_6r_twl_mwl | 43.2 | 61.5 | 122 | 33.1 | 0.0 | 330800 |
| 14 | 6pt_6r_two_mwo | 15.7 | 21.9 | 191 | 9.7 | 0.0 | 97300 |
| 15 | 8pt_6o2r_twl_mwl | 43.2 | 61.5 | 120 | 35.2 | 0.7 | 51.0 |
| 16 | 8pt_6o2r_two_mwo | 15.7 | 21.9 | 187 | 9.8 | 0.8 | 12.2 |
| 17 | 12pt_twl_mwl | 43.2 | 61.5 | 125 | 33.1 | 0.0 | 331200.0 |
| 18 | 12pt_two_mwo | 15.7 | 21.9 | 197 | 9.6 | 0.0 | 96200.0 |
| 19 | 4pt_4r_astf_twl_mwl | 45.4 | 61.5 | 153 | 35.2 | 0.0 | 1850 |
| 20 | 4pt_4r_astf_two_mwo | 18.9 | 21.9 | 317 | 11.6 | 1.1 | 10.9 |
| 21 | 4pt_oes_astf_twl_mwl | 45.4 | 61.5 | 148 | 37.5 | 0.0 | 375000 |
| 22 | 4pt_oes_astf_two_mwo | 18.9 | 21.9 | 298 | 9.4 | 0.5 | 17.5 |
| 23 | 4pt_4r_two_mwl | 15.7 | 62.5 | 190 | 9.7 | 0.0 | 97500.0 |
| 24 | 6pt_6r_two_mwl | 15.7 | 62.5 | 191 | 9.7 | 0.0 | 2027.0 |
| 25 | 8pt_4r4o_two_mwo | 15.7 | 22.9 | 196 | 9.6 | 0.0 | 96500.0 |
| 26 | 8pt_4r4o_twl_mwl | 43.2 | 62.5 | 101 | 36.2 | 0.0 | 362000.0 |
| Cases Evaluated in the Y direction | | | | | | | |
| 27 | 4pt_4o_twl_mwl | 42.6 | 61.5 | 104 | 30.1 | 0.0 | 301000.0 |
| 28 | 4pt_4o_two_mwo | 16.2 | 21.9 | 188 | 7.7 | 0.0 | 77400.0 |
| 29 | 6pt_6o_twl_mwl | 42.6 | 61.5 | 104 | 30.1 | 0.0 | 301000.0 |
| 30 | 6pt_6o_two_mwo | 16.2 | 21.9 | 188 | 7.4 | 0.0 | 73700.0 |
| 31 | 6pt_2r4o_two_mwo | 16.2 | 21.9 | 190 | 7.6 | 0.0 | 76500.0 |

Note: T.I and M.S indicate Test Item and Mounting Structure, respectively.

Table 3-3. Interface acceleration and force and corresponding C^2 value in the lateral direction for $Q=50$ and 20 , i.e. $\xi = 0.01$ and 0.025 .

| Case No. | Case Name | Interface Acc. (g^2/Hz) | | Interface Force (lb_f^2/Hz) | | C^2 | |
|---|----------------------|-----------------------------|--------|---------------------------------|---------|-------|------|
| | | Q=50 | Q=20 | Q=50 | Q=20 | Q=50 | Q=20 |
| Cases Evaluated in the X direction | | | | | | | |
| 1 | 3pt_2r1o_twl_mwl | 0.74 | 0.13 | 3720.0 | 620.0 | 2.7 | 2.6 |
| 2 | 3pt_2r1o_two_mwo | 0.69 | 0.10 | 764.6 | 126.0 | 4.5 | 5.4 |
| 3 | 3pt_3r_twl_mwl | 0.73 | 0.12 | 3900.0 | 632.0 | 2.9 | 2.7 |
| 4 | 3pt_3r_two_mwo | 0.62 | 0.09 | 792.0 | 125.0 | 5.2 | 5.4 |
| 5 | 4pt_oes_twl_mwl | 0.62 | 0.11 | 4400.0 | 776.0 | 3.8 | 3.8 |
| 6 | 4pt_oes_two_mwo | 0.50 | 0.08 | 1325.0 | 220.0 | 10.8 | 11.0 |
| 7 | 4pt_4r_twl_mwl | 0.85 | 0.14 | 5148.0 | 823.0 | 3.2 | 3.1 |
| 8 | 4pt_4r_two_mwo | 0.64 | 0.12 | 880.0 | 140.0 | 5.6 | 4.7 |
| 9 | 6pt_2r4o_twl_mwl | 0.66 | 0.12 | 4050.0 | 771.0 | 3.3 | 3.6 |
| 10 | 6pt_2r4o_two_mwo | 0.54 | 0.08 | 1200.0 | 205.0 | 9.0 | 10.1 |
| 11 | 6pt_4r2o_twl_mwl | 0.66 | 0.10 | 4200.0 | 750.0 | 3.4 | 3.9 |
| 12 | 6pt_4r2o_two_mwo | 0.58 | 0.09 | 1710.0 | 300.0 | 12.0 | 13.2 |
| 13 | 6pt_6r_twl_mwl | 1.00 | 0.15 | 5040.0 | 833.0 | 2.7 | 2.9 |
| 14 | 6pt_6r_two_mwo | 0.72 | 0.11 | 850.0 | 136.0 | 4.8 | 4.9 |
| 15 | 8pt_6o2r_twl_mwl | 0.62 | 0.10 | 5000.0 | 900.0 | 4.3 | 4.6 |
| 16 | 8pt_6o2r_two_mwo | 0.50 | 0.08 | 1450.0 | 250.0 | 11.8 | 13.1 |
| 17 | 12pt_twl_mwl | 0.73 | 0.11 | 2310.0 | 400.0 | 1.7 | 1.9 |
| 18 | 12pt_two_mwo | 0.59 | 0.09 | 760.0 | 124.0 | 5.3 | 5.9 |
| 19 | 4pt_4r_astf_twl_mwl | 0.28 | 0.05 | 1120.0 | 185.0 | 1.9 | 1.8 |
| 20 | 4pt_4r_astf_two_mwo | 0.01 | 0.07 | 6.4 | 50 | 3.1 | 1.9 |
| 21 | 4pt_oes_astf_twl_mwl | 3.83 | 0.66 | 10480.0 | 1780.0 | 1.3 | 1.3 |
| 22 | 4pt_oes_astf_two_mwo | 0.04 | 0.04 | 25.4 | 16.0 | 1.6 | 1.2 |
| 23 | 4pt_4r_two_mwl | 0.16 | 0.05 | 630.0 | 107.0 | 16.5 | 8.7 |
| 24 | 6pt_6r_two_mwl | 0.18 | 0.05 | 630.0 | 107.0 | 14.1 | 8.7 |
| 25 | 8pt_4r4o_two_mwo | 0.05 | 0.019 | 60.8 | 18.0 | 5.4 | 3.8 |
| 26 | 8pt_4r4o_twl_mwl | 163.38 | 27.164 | 428500.0 | 72000.0 | 1.4 | 1.4 |
| Cases Evaluated in the Y direction | | | | | | | |
| 27 | 4pt_4o_twl_mwl | 0.83 | 0.13 | 3490.0 | 570.0 | 2.3 | 2.4 |
| 28 | 4pt_4o_two_mwo | 0.80 | 0.11 | 750.0 | 120 | 3.6 | 4.2 |
| 29 | 6pt_6o_twl_mwl | 0.82 | 0.14 | 3370.0 | 542.0 | 2.3 | 2.1 |
| 30 | 6pt_6o_two_mwo | 0.79 | 0.12 | 660.0 | 112.0 | 3.2 | 3.6 |
| 31 | 6pt_2r4o_two_mwo | 0.51 | 0.08 | 3100.0 | 500.0 | 23.2 | 24.9 |

Table 3-4. Apparent Mass of test item at its fundamental frequency and the notch value in the lateral direction for Q=50 and 20, i.e. $\xi = 0.01$ and 0.025.

| Case No. | Case Name | Apparent Mass (lb) | | S _{FF} with out FLV (lbf ² /Hz) | | Notch Value (dB) | |
|---|----------------------|--------------------|-------|---|------------|------------------|------|
| | | Q=50 | Q=20 | Q=50 | Q=20 | Q=50 | Q=20 |
| Cases Evaluated in the X direction | | | | | | | |
| 1 | 3pt_2r1o_twl_mwl | 1754.5 | 702.9 | 2272000.0 | 62200.0 | 27.9 | 20 |
| 2 | 3pt_2r1o_two_mwo | 484.1 | 193.8 | 162300.0 | 3580.0 | 23.3 | 14.5 |
| 3 | 3pt_3r_twl_mwl | 1683.6 | 675.5 | 2077500.0 | 56400.0 | 27.3 | 19.5 |
| 4 | 3pt_3r_two_mwo | 473.6 | 189.8 | 138800.0 | 3400.0 | 22.4 | 14.4 |
| 5 | 4pt_oes_twl_mwl | 1756.7 | 703.0 | 1913000.0 | 53760.0 | 26.4 | 18.4 |
| 6 | 4pt_oes_two_mwo | 502.2 | 201.1 | 126000.0 | 3280.0 | 19.8 | 11.7 |
| 7 | 4pt_r_twl_mwl | 1663.0 | 665.7 | 2350700.0 | 63500.0 | 26.6 | 18.9 |
| 8 | 4pt_r_two_mwo | 487.4 | 195.2 | 152000.0 | 4570.0 | 22.4 | 15.1 |
| 9 | 6pt_2r4o_twl_mwl | 1760.4 | 704.4 | 2042200.0 | 57000.0 | 27.0 | 18.7 |
| 10 | 6pt_2r4o_two_mwo | 489.4 | 196.0 | 129600.0 | 3200.0 | 20.3 | 11.9 |
| 11 | 6pt_4r2o_twl_mwl | 1803.7 | 721.0 | 2159900.0 | 53100.0 | 27.1 | 18.5 |
| 12 | 6pt_4r2o_two_mwo | 495.9 | 198.5 | 142650.0 | 3550.0 | 19.2 | 10.8 |
| 13 | 6pt_6r_twl_mwl | 1652.3 | 661.5 | 2730000.0 | 67300.0 | 27.3 | 19.1 |
| 14 | 6pt_6r_two_mwo | 486.4 | 194.7 | 171000.0 | 4300.0 | 23.0 | 15.0 |
| 15 | 8pt_6o2r_twl_mwl | 1759.8 | 704.0 | 1920000.0 | 51550.0 | 25.8 | 17.6 |
| 16 | 8pt_6o2r_two_mwo | 489.0 | 195.7 | 119600.0 | 2953.0 | 19.2 | 10.7 |
| 17 | 12pt_twl_mwl | 1650.8 | 661.9 | 1989000.0 | 49770.0 | 29.3 | 21.0 |
| 18 | 12pt_two_mwo | 480.9 | 192.6 | 135260.0 | 3154.0 | 22.5 | 14.0 |
| 19 | 4pt_4r_astf_twl_mwl | 1760.6 | 704.8 | 879000.0 | 25330.0 | 28.9 | 21.3 |
| 20 | 4pt_4r_astf_two_mwo | 577.9 | 232.4 | 1940.0 | 3780.0 | 24.8 | 18.9 |
| 21 | 4pt_oes_astf_twl_mwl | 1873.2 | 748.5 | 13440000.0 | 369800.0 | 31.1 | 23.2 |
| 22 | 4pt_oes_astf_two_mwo | 472.3 | 193.0 | 9700.0 | 1453.0 | 25.8 | 19.5 |
| 23 | 4pt_4r_two_mwl | 487.4 | 195.2 | 36800.0 | 1900.0 | 17.7 | 12.5 |
| 24 | 6pt_6r_two_mwl | 486.4 | 194.7 | 42600.0 | 1900.0 | 18.3 | 12.5 |
| 25 | 8pt_4r4o_two_mwo | 481.1 | 193.1 | 10500.0 | 700.0 | 22.4 | 16.0 |
| 26 | 8pt_4r4o_twl_mwl | 1799.4 | 724.5 | 528995000.0 | 14260000.0 | 30.9 | 23.0 |
| Cases Evaluated in the X direction | | | | | | | |
| 27 | 4pt_4o_twl_mwl | 1079.4 | 469.7 | 962800.0 | 28700.0 | 24.4 | 17.0 |
| 28 | 4pt_4o_two_mwo | 368.4 | 147.8 | 108600.0 | 2400.0 | 21.6 | 13.0 |
| 29 | 6pt_6o_twl_mwl | 1067.3 | 469.7 | 934100.0 | 30900.0 | 24.4 | 17.6 |
| 30 | 6pt_6o_two_mwo | 368.8 | 148.0 | 107450.0 | 2600.0 | 22.1 | 13.6 |
| 31 | 6pt_2r4o_two_mwo | 384.7 | 154.2 | 75500.0 | 1830.0 | 13.9 | 5.6 |

Table 3-5. Impedance characteristics of the test structures at the natural frequency of the test item in the vertical direction (Z).

| Case No. | Case Name | Physical Mass (lb) | | Freq. (Hz) | Effective Mass (lb) | | |
|----------|-----------------------|--------------------|------|------------|---------------------|------|-----------------|
| | | T.I | M.S | T.I | T.I | M.S | Ratio (T.I/M.S) |
| 1 | 3pt_3r_twl_mwl | 43.2 | 61.5 | 127 | 13.1 | 2.6 | 5.0 |
| 2 | 3pt_3r_two_mwl | 15.7 | 61.5 | 261 | 6.7 | 8.3 | 0.8 |
| 3 | 3pt_3r_two_mwo | 15.7 | 21.9 | 261 | 6.7 | 2.5 | 2.6 |
| 4 | 4pt_oes_twl_mwl | 43.2 | 61.5 | 126 | 14.0 | 0.2 | 62.0 |
| 5 | 4pt_oes_two_mwl | 15.7 | 61.5 | 287 | 5.5 | 6.4 | 0.9 |
| 6 | 4pt_oes_two_mwo | 15.7 | 21.9 | 287 | 5.5 | 0.0 | 55500.0 |
| 7 | 4pt_4r_twl_mwl | 43.2 | 61.5 | 127 | 12.3 | 2.7 | 4.6 |
| 8 | 4pt_4r_two_mwl | 15.7 | 61.5 | 264 | 6.4 | 17.8 | 0.4 |
| 9 | 4pt_4r_two_mwo | 15.7 | 21.9 | 264 | 6.4 | 2.8 | 2.3 |
| 10 | 6pt_2r4o_twl_mwl | 43.2 | 61.5 | 126 | 14.0 | 0.2 | 76.6 |
| 11 | 6pt_2r4o_two_mwo | 15.7 | 21.9 | 290 | 3.7 | 0.0 | 36500.0 |
| 12 | 6pt_4r2o_twl_mwl | 43.2 | 61.5 | 127 | 12.5 | 0.5 | 22.8 |
| 13 | 6pt_4r2o_two_mwl | 15.7 | 61.5 | 296 | 3.6 | 7.6 | 0.5 |
| 14 | 6pt_4r2o_two_mwo | 15.7 | 21.9 | 296 | 3.6 | 10.4 | 0.3 |
| 15 | 6pt_6r_twl_mwl | 43.2 | 61.5 | 127 | 11.8 | 0.0 | 118000.0 |
| 16 | 6pt_6r_two_mwl | 15.7 | 61.5 | 265 | 6.2 | 17.3 | 0.4 |
| 17 | 6pt_6r_two_mwo | 15.7 | 21.9 | 265 | 6.2 | 2.9 | 2.1 |
| 18 | 8pt_6o2r_twl_mwl | 43.2 | 61.5 | 126 | 14.0 | 0.1 | 161.1 |
| 19 | 8pt_6o2r_two_mwl | 15.7 | 61.5 | 290 | 3.6 | 0.6 | 6.2 |
| 20 | 8pt_6o2r_two_mwo | 15.7 | 21.9 | 290 | 3.6 | 0.0 | 35800.0 |
| 21 | 12pt_twl_mwl | 43.2 | 61.5 | 128 | 12.1 | 0.6 | 20.0 |
| 22 | 12pt_two_mwl | 15.7 | 61.5 | 299 | 3.1 | 1.6 | 2.0 |
| 23 | 12pt_two_mwo | 15.7 | 21.9 | 299 | 3.1 | 10.0 | 0.3 |
| 24 | 4pt_4o_twl_mwl | 42.6 | 61.5 | 104 | 32.2 | 1.2 | 26.9 |
| 25 | 4pt_4o_two_mwl | 16.2 | 61.5 | 224 | 12.6 | 0.0 | 126430.0 |
| 26 | 4pt_4o_two_mwo | 16.2 | 21.9 | 224 | 12.6 | 0.0 | 126430.0 |
| 27 | 6pt_6o_twl_mwl | 42.6 | 61.5 | 104 | 32.2 | 1.2 | 26.9 |
| 28 | 6pt_6o_two_mwl | 16.2 | 61.5 | 224 | 12.7 | 0.0 | 127000.0 |
| 29 | 6pt_6o_two_mwo | 16.2 | 21.9 | 224 | 12.7 | 0.0 | 127000.0 |
| 30 | 6pt_2r4o_two_mwl | 16.2 | 61.5 | 300 | 3.4 | 7.6 | 0.5 |
| 31 | 6pt_2r4o_two_mwo | 16.2 | 21.9 | 300 | 3.4 | 10.4 | 0.3 |
| 32 | 4pt_oes_ms_tt_mwl | 21.8 | 61.5 | 151 | 8.6 | 0.0 | 86200.0 |
| 33 | 4pt_oes_ms_two_mwl | 16.5 | 61.5 | 292 | 6.0 | 6.4 | 0.9 |
| 34 | 4pt_oes_msstf_two_mwl | 17.9 | 61.5 | 298 | 3.5 | 6.4 | 0.5 |
| 35 | 4pt_4r_astf_twl_mwl | 45.4 | 61.5 | 200 | 18.1 | 0.0 | 181100.0 |
| 36 | 4pt_4r_astf_two_mwo | 18.9 | 21.9 | 310 | 6.8 | 8.1 | 0.8 |
| 37 | 4pt_oes_astf_twl_mwl | 45.4 | 61.5 | 196 | 19.4 | 25.4 | 0.8 |
| 38 | 4pt_oes_astf_two_mwo | 18.9 | 21.9 | 319 | 5.4 | 0.0 | 53600.0 |
| 39 | 8pt_4r4o_two_mwo | 15.7 | 22.9 | 299 | 3.2 | 11.0 | 0.3 |
| 40 | 8pt_4r4o_twl_mwl | 43.2 | 62.5 | 127 | 11.8 | 0.9 | 13.4 |

Table 3-6. Interface Acceleration and Force and corresponding C^2 value in the vertical direction for $Q=50$ and 20 , i.e. $\xi = 0.01$ and 0.025 .

| Case No. | Case Name | Interface Acc. (g^2/Hz) | | Interface Force (lb_f^2/Hz) | | C^2 | |
|----------|-----------------------|--------------------------------|------|------------------------------------|---------|-------|------|
| | | Q=50 | Q=20 | Q=50 | Q=20 | Q=50 | Q=20 |
| 1 | 3pt_3r_twl_mwl | 3.55 | 0.56 | 22000.0 | 3680.0 | 3.3 | 3.5 |
| 2 | 3pt_3r_two_mwl | 9.51 | 1.64 | 3830.0 | 870.0 | 1.6 | 2.2 |
| 3 | 3pt_3r_two_mwo | 13.93 | 2.38 | 10000.0 | 1630.0 | 2.9 | 2.8 |
| 4 | 4pt_oes_twl_mwl | 3.85 | 0.55 | 2625.0 | 72.0 | 0.4 | 0.1 |
| 5 | 4pt_oes_two_mwl | 15.28 | 2.45 | 5625.0 | 1040.0 | 1.5 | 1.7 |
| 6 | 4pt_oes_two_mwo | 14.59 | 2.27 | 6926.0 | 1130.0 | 1.9 | 2.0 |
| 7 | 4pt_4r_twl_mwl | 0.21 | 0.04 | 1480.0 | 270.0 | 3.8 | 3.8 |
| 8 | 4pt_4r_two_mwl | 14.39 | 2.50 | 11300.0 | 1910.0 | 3.2 | 3.1 |
| 9 | 4pt_4r_two_mwo | 12.60 | 2.10 | 11100.0 | 1735.0 | 3.6 | 3.4 |
| 10 | 6pt_2r4o_twl_mwl | 0.40 | 0.06 | 1185.0 | 210.0 | 1.6 | 1.8 |
| 11 | 6pt_2r4o_two_mwo | 12.99 | 2.11 | 6590.0 | 1077.0 | 2.1 | 2.1 |
| 12 | 6pt_4r2o_twl_mwl | 3.05 | 0.59 | 2700.0 | 475.5 | 0.5 | 0.4 |
| 13 | 6pt_4r2o_two_mwl | 12.36 | 1.90 | 6200.0 | 1050.0 | 2.0 | 2.2 |
| 14 | 6pt_4r2o_two_mwo | 43.83 | 7.35 | 7100.0 | 1175.0 | 0.7 | 0.6 |
| 15 | 6pt_6r_twl_mwl | 0.33 | 0.06 | 1000.0 | 200.0 | 1.6 | 1.9 |
| 16 | 6pt_6r_two_mwl | 14.85 | 2.37 | 12000.0 | 2000.0 | 3.3 | 3.5 |
| 17 | 6pt_6r_two_mwo | 13.00 | 2.12 | 11300.0 | 1830.0 | 3.5 | 3.5 |
| 18 | 8pt_6o2r_twl_mwl | 0.72 | 0.15 | 1077.0 | 120.0 | 0.8 | 0.4 |
| 19 | 8pt_6o2r_two_mwl | 4.50 | 0.76 | 1345.0 | 300.0 | 1.2 | 1.6 |
| 20 | 8pt_6o2r_two_mwo | 13.20 | 2.07 | 6380.0 | 1035.0 | 2.0 | 2.0 |
| 21 | 12pt_twl_mwl | 1.36 | 0.20 | 2237.0 | 400.0 | 0.9 | 1.1 |
| 22 | 12pt_two_mwl | 5.75 | 1.02 | 3173.5 | 530.0 | 2.2 | 2.1 |
| 23 | 12pt_two_mwo | 28.85 | 4.79 | 6600.0 | 1190.0 | 0.9 | 1.0 |
| 24 | 4pt_4o_twl_mwl | 52.80 | 8.54 | 158600.0 | 25700.0 | 1.7 | 1.7 |
| 25 | 4pt_4o_two_mwl | 8.00 | 1.26 | 13300.0 | 2130.0 | 6.4 | 6.5 |
| 26 | 4pt_4o_two_mwo | 7.45 | 1.22 | 12300.0 | 2030.0 | 6.3 | 6.4 |
| 27 | 6pt_6o_twl_mwl | 51.21 | 8.05 | 154100.0 | 25600.0 | 1.7 | 1.8 |
| 28 | 6pt_6o_two_mwl | 8.15 | 1.30 | 13100.0 | 2180.0 | 6.1 | 6.4 |
| 29 | 6pt_6o_two_mwo | 7.66 | 1.26 | 12530.0 | 2080.0 | 6.3 | 6.3 |
| 30 | 6pt_2r4o_two_mwl | 10.36 | 1.75 | 8900.0 | 1070.0 | 3.3 | 2.3 |
| 31 | 6pt_2r4o_two_mwo | 19.57 | 3.16 | 6570.0 | 1070.0 | 1.3 | 1.3 |
| 32 | 4pt_oes_ms_tt_mwl | 2.93 | 0.43 | 2100.0 | 350.0 | 1.5 | 1.7 |
| 33 | 4pt_oes_ms_two_mwl | 15.67 | 2.68 | 6800.0 | 1170.0 | 1.6 | 1.6 |
| 34 | 4pt_oes_msstf_two_mwl | 17.05 | 2.92 | 8110.0 | 1400.0 | 1.5 | 1.5 |
| 35 | 4pt_4r_astf_twl_mwl | 1.10 | 0.72 | 9600.0 | 1600.0 | 4.2 | 1.1 |
| 36 | 4pt_4r_astf_two_mwo | 20.41 | 3.32 | 16000.0 | 2600.0 | 2.2 | 2.2 |
| 37 | 4pt_oes_astf_twl_mwl | 4.50 | 1.97 | 2000.0 | 1560.0 | 0.2 | 0.4 |
| 38 | 4pt_oes_astf_two_mwo | 18.10 | 2.89 | 10100.0 | 1620.0 | 1.6 | 1.6 |
| 39 | 8pt_4r4o_two_mwo | 37.67 | 6.1 | 7840.0 | 1260.0 | 0.8 | 0.8 |
| 40 | 8pt_4r4o_twl_mwl | 1.03 | 0.2 | 2900.0 | 480.0 | 1.5 | 1.6 |

Table 3-7. Apparent Mass of test item at its fundamental frequency and the Notch Value in the vertical direction for Q=50 and 20, i.e. $\xi = 0.01$ and 0.025.

| Case No | Case Name | Apparent Mass (lb) | | S _{FF} with out FLV (lb ² /Hz) | | Notch Value (dB) | |
|---------|-----------------------|--------------------|--------|--|-----------|------------------|------|
| | | Q=50 | Q=50 | Q=50 | Q=20 | Q=50 | Q=20 |
| 1 | 3pt_3r_twl_mwl | 636.8 | 271.47 | 1441000.0 | 41270.0 | 18.2 | 10.5 |
| 2 | 3pt_3r_two_mwl | 290.2 | 129.06 | 801100.0 | 27300.0 | 23.2 | 15.0 |
| 3 | 3pt_3r_two_mwo | 290.2 | 129.06 | 1174000.0 | 39700.0 | 20.7 | 13.9 |
| 4 | 4pt_oes_twl_mwl | 706.1 | 294.65 | 1921400.0 | 47500.0 | 28.6 | 28.2 |
| 5 | 4pt_oes_two_mwl | 191.2 | 82.55 | 558700.0 | 16700.0 | 20.0 | 12.1 |
| 6 | 4pt_oes_two_mwo | 191.2 | 82.55 | 533600.0 | 15400.0 | 18.9 | 11.4 |
| 7 | 4pt_r_twl_mwl | 620.2 | 265.83 | 80800.0 | 2680.0 | 17.4 | 10.0 |
| 8 | 4pt_r_two_mwl | 307.9 | 126.69 | 1363000.0 | 40200.0 | 20.8 | 13.2 |
| 9 | 4pt_r_two_mwo | 307.9 | 126.69 | 1194000.0 | 33700.0 | 20.3 | 12.9 |
| 10 | 6pt_2r4o_twl_mwl | 704.3 | 295.51 | 198400.0 | 5410.0 | 22.2 | 14.1 |
| 11 | 6pt_2r4o_two_mwo | 184.1 | 78.79 | 440300.0 | 13100.0 | 18.2 | 10.9 |
| 12 | 6pt_4r2o_twl_mwl | 595.4 | 249.17 | 1082000.0 | 36400.0 | 26.0 | 18.8 |
| 13 | 6pt_4r2o_two_mwl | 178.4 | 74.85 | 393250.0 | 10670.0 | 18.0 | 10.1 |
| 14 | 6pt_4r2o_two_mwo | 178.4 | 74.85 | 1394400.0 | 41200.0 | 22.9 | 15.4 |
| 15 | 6pt_6r_twl_mwl | 594.2 | 256.16 | 116500.0 | 3870.0 | 20.7 | 12.8 |
| 16 | 6pt_6r_two_mwl | 301.6 | 123.26 | 1350700.0 | 36000.0 | 20.5 | 12.5 |
| 17 | 6pt_6r_two_mwo | 301.6 | 123.26 | 1182500.0 | 32200.0 | 20.2 | 12.5 |
| 18 | 8pt_6o2r_twl_mwl | 704.6 | 295.51 | 357400.0 | 13000.0 | 25.2 | 20.4 |
| 19 | 8pt_6o2r_two_mwl | 180.5 | 77.50 | 146600.0 | 4570.0 | 20.4 | 11.8 |
| 20 | 8pt_6o2r_two_mwo | 180.5 | 77.50 | 430000.0 | 12420.0 | 18.3 | 10.8 |
| 21 | 12pt_twl_mwl | 608.1 | 295.10 | 502900.0 | 17420.0 | 23.5 | 16.4 |
| 22 | 12pt_two_mwl | 155.1 | 65.39 | 138250.0 | 4350.0 | 16.4 | 9.1 |
| 23 | 12pt_two_mwo | 155.1 | 65.39 | 693700.0 | 20500.0 | 20.2 | 12.3 |
| 24 | 4pt_4o_twl_mwl | 1123.6 | 484.99 | 66660000.0 | 2008700.0 | 26.2 | 18.9 |
| 25 | 4pt_4o_two_mwl | 602.8 | 240.93 | 2907000.0 | 73400.0 | 23.4 | 15.4 |
| 26 | 4pt_4o_two_mwo | 602.8 | 240.93 | 2707000.0 | 70800.0 | 23.4 | 15.4 |
| 27 | 6pt_6o_twl_mwl | 1110.9 | 484.99 | 63203000.0 | 1893000.0 | 26.1 | 18.7 |
| 28 | 6pt_6o_two_mwl | 606.7 | 243.02 | 3001300.0 | 768000.0 | 23.6 | 15.5 |
| 29 | 6pt_6o_two_mwo | 606.7 | 243.02 | 2820800.0 | 74300.0 | 23.5 | 15.5 |
| 30 | 6pt_2r4o_two_mwl | 174.1 | 73.15 | 314300.0 | 9360.0 | 15.5 | 9.4 |
| 31 | 6pt_2r4o_two_mwo | 174.1 | 73.15 | 593500.0 | 16900.0 | 19.6 | 12.0 |
| 32 | 4pt_oes_ms_tt_mwl | 430.3 | 134.85 | 542400.0 | 7860.0 | 24.1 | 13.6 |
| 33 | 4pt_oes_ms_two_mwl | 208.5 | 89.02 | 681300.0 | 21200.0 | 20.0 | 12.6 |
| 34 | 4pt_oes_msstf_two_mwl | 178.1 | 74.85 | 541080.0 | 16300.0 | 18.2 | 10.7 |
| 35 | 4pt_4r_astf_twl_mwl | 904.0 | 363.66 | 900573.0 | 95200.0 | 19.7 | 17.8 |
| 36 | 4pt_4r_astf_two_mwo | 335.7 | 135.18 | 2300000.0 | 60700.0 | 21.6 | 13.7 |
| 37 | 4pt_oes_astf_twl_mwl | 972.3 | 390.43 | 4253800.0 | 300700.0 | 33.3 | 22.9 |
| 38 | 4pt_oes_astf_two_mwo | 269.1 | 110.06 | 1310800.0 | 35060.0 | 21.1 | 13.4 |
| 39 | 8pt_4r4o_two_mwo | 163.4 | 68.92 | 1005910.0 | 29020.0 | 21.1 | 13.6 |
| 40 | 8pt_4r4o_twl_mwl | 594.5 | 248.16 | 363300.0 | 9850.0 | 21.0 | 13.1 |

3.3.1. C^2 Value and the relative parameters

It can be observed from the results shown in the Tables 3-3 and 3-6 that most of the time the value of C^2 respected the range specified in the literature [11,16], i.e., between 2 and 5. Although there are cases where the value of C^2 was below 2, however it rarely occurs that any space hardware is tested below a C^2 of 2. On the other hand, there are different cases where the C^2 was above 5. However, with one exception, all C^2 values are below 17. It is important to note that the C^2 values fall within such a narrow range, despite the fact that the ratio of effective masses covers a range of several orders of magnitude. To realize the value of C^2 and its dependent parameters, a graph of C^2 values versus the effective mass ratio of test item to mounting structure in the lateral and vertical direction of excitation is plotted as shown in Figures 3-11 and 3-12.

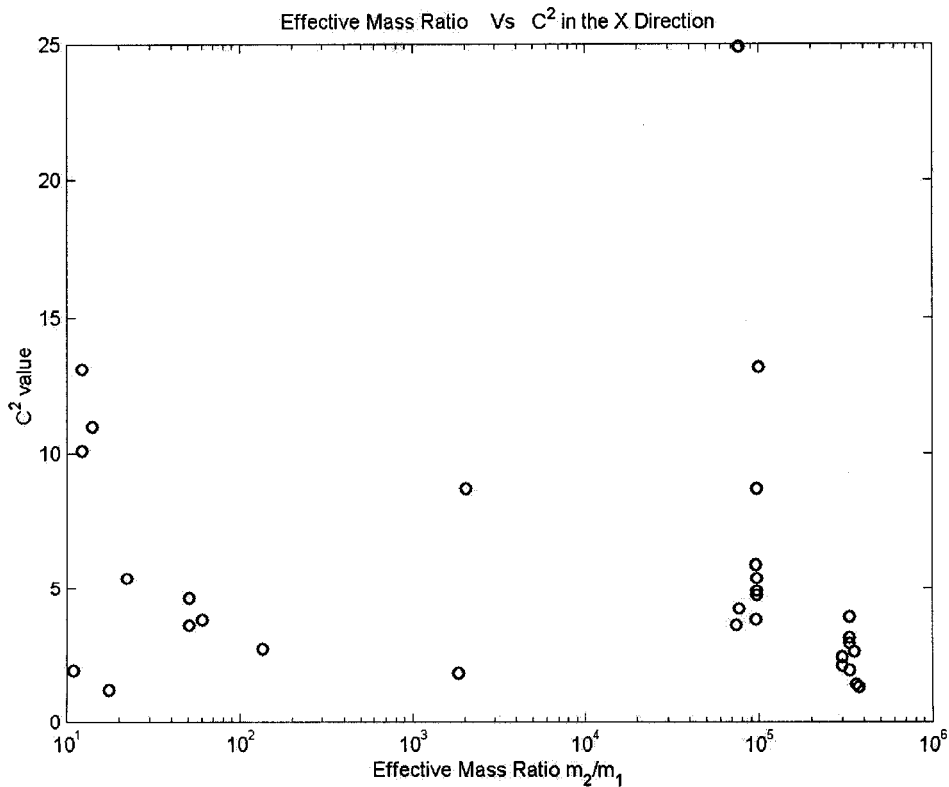


Figure 3-11. The C^2 versus effective mass ratio in the lateral direction.

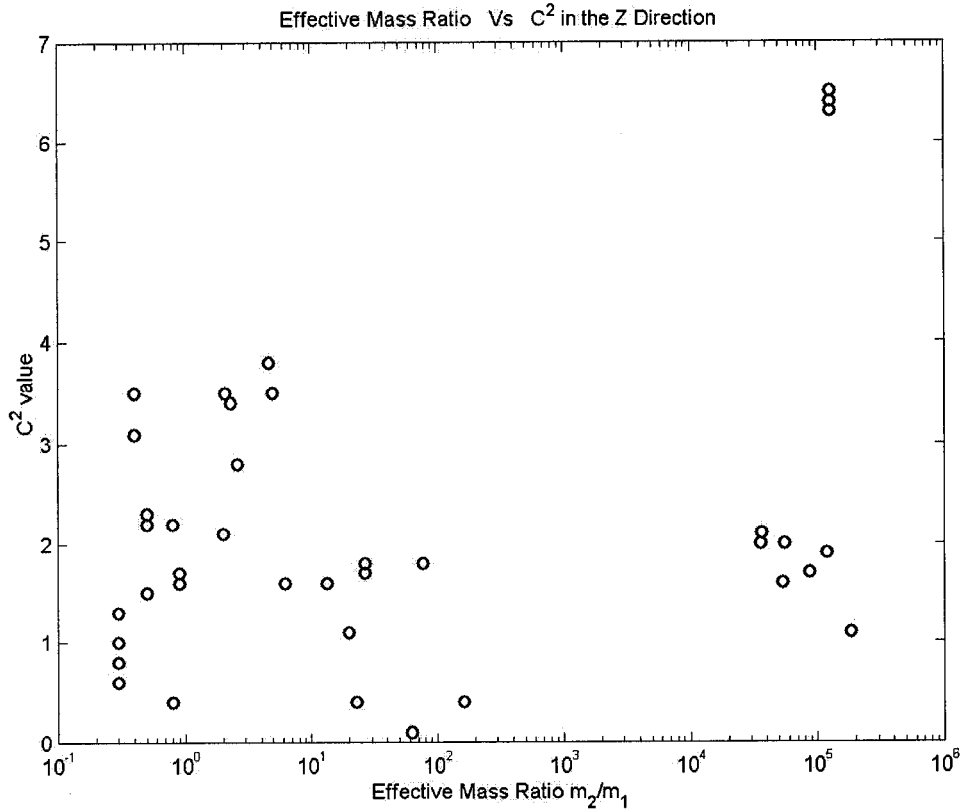


Figure 3-12. The C^2 value versus the effective mass ratio in the vertical direction.

It can be seen that the data for C^2 values are quite scattered. Thus no pertinent information can be extracted from Figures 3-11 and 3-12. In another attempt, the variation of C^2 with respect to the effective mass ratio for different number and position of attachment points has been investigated. This variation for lateral and vertical directions are shown in the Figures 3-13 and 3-14.

C² Value in Lateral Directions

It can be observed from Figure 3-13 that for the lateral direction the C^2 value decreases with increasing the effective mass ratio for a particular number of attachment points and their position. This can be attributed to the fact that the test item is connected to the mounting structure as a cantilever, and the increase in effective mass ratio happens for

higher mass on test item at its fundamental frequency, since this generally occurs when the test item is loaded with lumped masses as shown in Table 3-2. Due to the higher effective mass ratio predominant vibration absorber effect can be observed at the fundamental frequency of the test item, which may lead to the reduction of forces at the interface between the test item and the mounting structure. However since the test item also acts as cantilever, there is always a possibility of having higher deflection and acceleration at the attachment points. The increase in acceleration and drop in the force at the interface will cause the lower C^2 values. For example for a simple 2 d.o.f system, with the increase in vibration absorber effect and keeping the mass ratio constant, the acceleration at the interface increases while the force decreases. Hence the C^2 decreases with increasing vibration absorber effect, which in the above case occurs for higher effective mass ratios of the test structures.

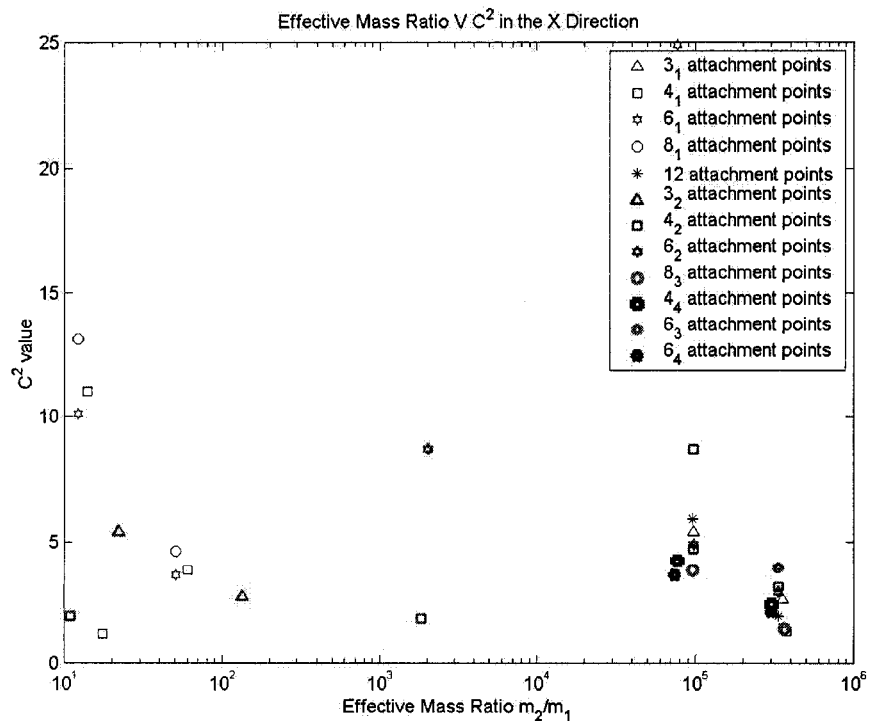


Figure 3-13. The C^2 value versus the effective mass ratio in the lateral direction for different attachment points.

Not much could be elaborated regarding the behavior of the C^2 value with respect to the number of attachment points, i.e., increase in attachment points at a constant effective mass ratio. The data achieved from the current study is not sufficient to arrive at any conclusion regarding the dependence of C^2 value on the number of attachment points at constant effective mass ratio. However when comparing with respect to the number of attachment points, the position of attachment points has to be taken into account as some of the attachment points are more flexible compared to the others.

As mentioned earlier, the location of attachment points is to be consistent when comparing the value of C^2 in terms of number of attachment points. For example, the test item attached at 3 points all in the real direction should be compared with the results of the 4 and 6-point attachment all in the real direction. This means that in Figure 3-13, case 3_2 should be compared with 4_2 , and 6_2 . The configuration of cases in Figure 3-13 is accomplished according to the number/position of the attachment points given in the Table 3-8 which is basically extracted from Table 3-2.

Table 3-8. Configuration of Cases for the Figure 3-13.

| | |
|-------------|----------------|
| 3pt_2r1o.. | 3 ₁ |
| 3pt_3r.. | 3 ₂ |
| 4pt_oes... | 4 ₁ |
| 4pt_4r... | 4 ₂ |
| 4pt_4o.. | 4 ₄ |
| 6pt_2r4o... | 6 ₁ |
| 6pt_6r.. | 6 ₂ |
| 6pt_4r2o... | 6 ₃ |
| 6pt_6o.. | 6 ₄ |
| 8pt_2r6o.. | 8 ₁ |
| 8pt_4r4o... | 8 ₃ |

C^2 Value in Vertical Direction

It can be observed from Figure 3-14 that the C^2 values are scattered and it is not evident to draw any specific conclusion for the behavior of C^2 parameter with respect to effective mass ratio and the number of attachment points and their position. The C^2 value is increasing with increase in effective mass ratio for some cases and is decreasing for some others.

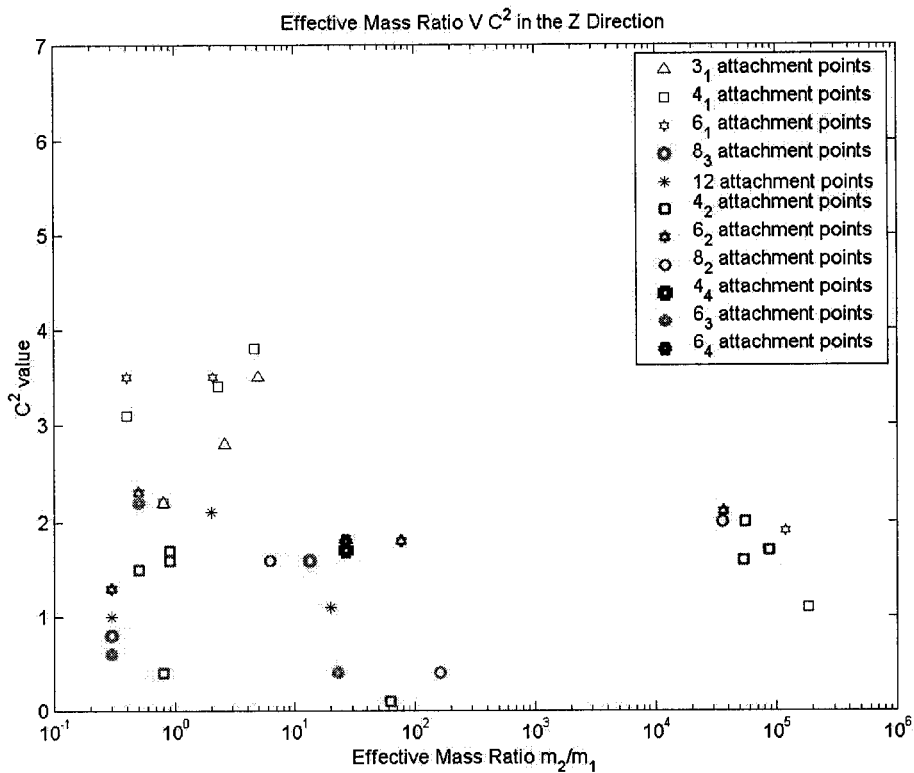


Figure 3-14. The C^2 value versus the effective mass ratio in the vertical direction for different attachment points.

The relationship between the case name with respect to the number/position of attachment points in Table 3-5 for the vertical direction and the same in Figure 3-15 is shown in Table 3-9. For a specific number of attachment points, Figure 3-15 shows that the position of the attachment points plays a major role, as it can be seen that when the

attachment points include the flexible points on the mounting structure, the C^2 has low value compared to the one attached at rigid points.

Table 3-9. Configuration of Cases for the Figure 3-14

| | |
|-------------|----------------|
| 3pt_3r_.. | 3 ₁ |
| 4pt_4r_.. | 4 ₁ |
| 4pt_oes_.. | 4 ₂ |
| 4pt_4o_.. | 4 ₄ |
| 6pt_6r_.. | 6 ₁ |
| 6pt_2r4o_.. | 6 ₂ |
| 6pt_4r2o_.. | 6 ₃ |
| 6pt_6o_.. | 6 ₄ |
| 8pt_6o2r_.. | 8 ₂ |
| 8pt_4r4o_.. | 8 ₃ |

Comparison of C^2 Value Between the Lateral and Vertical Directions

It can be observed from the results shown in Table 3-10 that most of the time (21 of 29 cases) the value of C^2 in the vertical direction is lower than the values in the lateral direction. However there are cases when the C^2 value is higher in vertical direction.

Table 3-10. Comparison of C^2 value between the lateral and vertical directions

| Case Name | C^2 in X direction (Q=50, Q=20) | | C^2 in Z direction (Q=50, Q=20) | |
|----------------------|--------------------------------------|------|--------------------------------------|-----|
| | | | | |
| 3pt_3r_twl_mwl | 2.9 | 2.7 | 3.3 | 3.5 |
| 3pt_3r_two_mwo | 5.2 | 5.4 | 2.9 | 2.8 |
| 4pt_oes_twl_mwl | 3.8 | 3.8 | 0.4 | 0.1 |
| 4pt_oes_two_mwo | 10.8 | 11.0 | 1.9 | 2.0 |
| 4pt_4r_twl_mwl | 3.2 | 3.1 | 3.8 | 3.8 |
| 4pt_4r_two_mwo | 5.6 | 4.7 | 3.6 | 3.4 |
| 6pt_2r4o_twl_mwl | 3.3 | 3.6 | 1.6 | 1.8 |
| 6pt_2r4o_two_mwo | 9.0 | 10.1 | 2.1 | 2.1 |
| 6pt_4r2o_twl_mwl | 3.4 | 3.9 | 0.5 | 0.4 |
| 6pt_4r2o_two_mwo | 12.0 | 13.2 | 0.7 | 0.6 |
| 6pt_6r_twl_mwl | 2.7 | 2.9 | 1.6 | 1.9 |
| 6pt_6r_two_mwo | 4.8 | 4.9 | 3.5 | 3.5 |
| 8pt_6o2r_twl_mwl | 4.3 | 4.6 | 0.8 | 0.4 |
| 8pt_6o2r_two_mwo | 11.8 | 13.1 | 2.0 | 2.0 |
| 12pt_twl_mwl | 1.7 | 1.9 | 0.9 | 1.0 |
| 12pt_two_mwo | 5.3 | 5.9 | 0.9 | 1.0 |
| 4pt_4o_twl_mwl | 2.3 | 2.4 | 1.7 | 1.7 |
| 4pt_4o_two_mwo | 3.6 | 4.2 | 6.3 | 6.4 |
| 6pt_6o_twl_mwl | 2.3 | 2.1 | 1.7 | 1.8 |
| 6pt_6o_two_mwo | 3.2 | 3.6 | 6.3 | 6.3 |
| 6pt_2r4o_two_mwo | 23.2 | 24.9 | 1.3 | 1.3 |
| 4pt_4r_astf_twl_mwl | 1.9 | 1.8 | 4.2 | 1.1 |
| 4pt_4r_astf_two_mwo | 3.1 | 1.9 | 2.2 | 2.2 |
| 4pt_oes_astf_twl_mwl | 1.3 | 1.3 | 0.2 | 0.4 |
| 4pt_oes_astf_two_mwo | 1.6 | 1.2 | 1.6 | 1.6 |
| 4pt_4r_two_mwl | 16.5 | 8.7 | 3.2 | 3.1 |
| 6pt_6r_two_mwl | 14.1 | 8.7 | 3.3 | 3.5 |
| 8pt_4r4o_two_mwo | 5.4 | 3.8 | 0.8 | 0.8 |
| 8pt_4r4o_twl_mwl | 1.4 | 1.4 | 1.5 | 1.6 |

The C^2 value is dependent on the level of vibration absorber effect at the coupled system level, which obviously depends on the stiffness of the test item and the attachment points. As shown in the Figure 3-15, for a 2 d.o.f. system (Figure 1-1), the vibration absorber effect is clearly pronounced with increasing the stiffness of the test item, considering that the effective mass ratio is the same. Therefore it may be concluded that at a constant

mass ratio the C^2 value decreases upon increasing the stiffness of the test item. As mentioned earlier the damping of the structure does not normally affect the C^2 value.

For the same test configuration and considering that the effective mass is the same for both lateral and vertical directions, the stiffness in the lateral direction is usually lower than that in the vertical direction, which is evident from the frequency details of the test item or the mounting structure (table 3-2 and table 3-5).

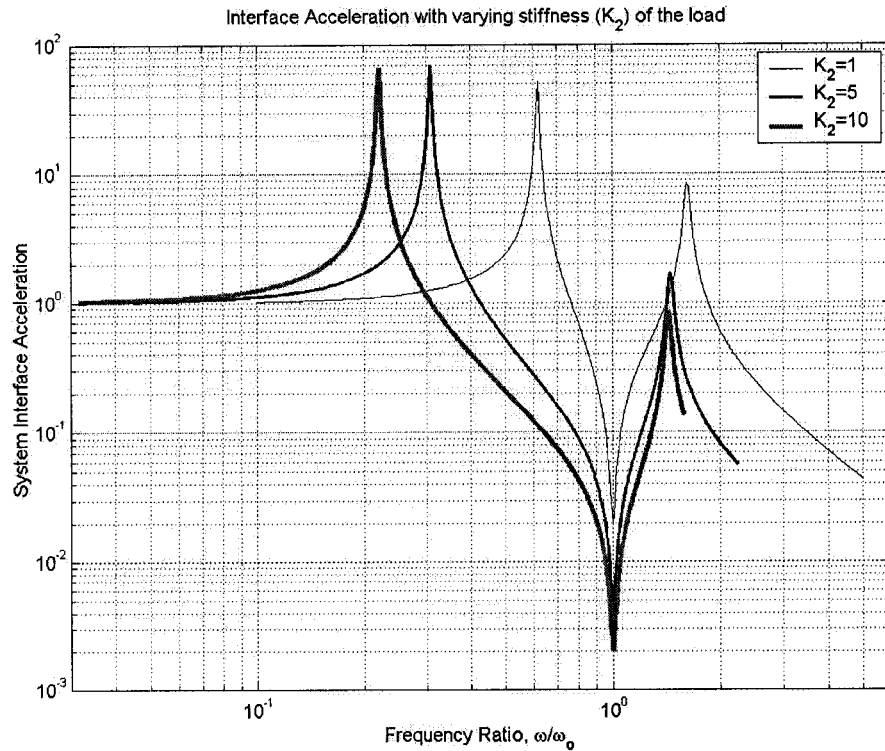


Figure 3-15. System interface acceleration for different stiffness of the load (test item).

3.3.2. Notch Value

Notch value basically depends on the apparent mass, interface acceleration and the interface force at the fundamental frequency of the test item. It might to some extent depend on the number of attachment points and their position. However, it depends significantly on the amplification factor or the damping ratio. This is clearly evident from the results shown in Tables 3-4 and 3-7 confirming the fact that the higher the damping the lower is the notch value.

3.4. Summary and Conclusion

It was shown that most often the values of C^2 fall in the range between 2 and 5 as reported in the literature. However, there are cases when this value is higher than 5 as was reported earlier in the testing of flight hardware [22] and now in the current study. Numerous benchmark case studies were performed and the results of the sensitivity analysis tabulated and plotted to validate the value of C^2 reported in the literature [1,16,22]. The results also indicate the parameters on which value of C^2 depends. To summarize the value of C^2 depends on:

- The number of attachment points,
- Position of attachment points,
- Effective mass ratio of the structures
- Direction of excitation.
- Fundamental frequency of the test structures
- Stiffness of the structures

and it does not depend or not significantly depends on

- Damping of the structures

The notch value for the acceleration specification for testing at the test item level mostly depends on the

- Damping of the structures, and
- Effective mass of the test item

CHAPTER 4

EXPERIMENTAL SENSITIVITY STUDY FOR ESTIMATION OF C^2 PARAMETERS

It can be observed from the analytical sensitivity study of Section 3.3 that, although the C^2 value of the majority of cases falls within the range of 2 to 5 generally found in the literature, there are some cases for which the derived C^2 value was significantly higher than the generally accepted limit of 5. The main objective of the experimental sensitivity study is to validate the procedures, and consequently the derived C^2 values, of the analytical sensitivity study. The experimental validation was performed by testing the test articles designed in Chapter 2 for a few selected cases extracted from Chapter 3.

4.1. Selection of Case Studies

Some of the cases from the analytical study are selected according to the guidelines set to perform the experimental study. Proper guidelines are set for the selection of cases to perform the experimental study. They include:

- i) Minimum number of cases to cover a maximum range of C^2 value.
- ii) Number of force sensors to be used (8 force sensors were available for testing).
- iii) Maximum number of cases possible without changing the configuration of test item in terms of stiffness, i.e., adding or removing of additional stiffening member,
- iv) The cases that simulate the real life structure with respect to the number of attachment points and their location.

- v) The mass ratio of the test structures, i.e., ratio of mass of test item to mounting structure.

Based on these guidelines, 2 sets of cases were selected on the basis of number of attachment points, 3 in terms of mass ratio and 2 in terms of stiffness. According to the number of attachment points, the cases selected are attached at 4 and 8 points. With respect to the mass ratio, the cases selected include i) the test item and the mounting structure without lumped mass, ii) the test item without lumped mass and mounting structure with lumped mass, and iii) the test item and mounting structure with lumped mass. In terms of stiffness, the cases are i) the test item with CPL plate as stiffening member, and ii) the test item with flanges as stiffening member to fix the structure at 4 attachment points in the Ortho direction.

The cases selected are a combination of two or more of the above options. Not all cases are tested in all the directions, i.e., some of the cases are tested only in the vertical direction and some of them only in the lateral direction. In summary, the following cases are selected for the experimental sensitivity study:

- a) 4pt_4r_two_mwo
- b) 4pt_4r_two_mwl
- c) 4pt_4r_twl_mwl
- d) 4pt_4o_two_mwl,
- e) 8pt_4r4o_two_mwo

- f) 8pt_4r4o_two_mwl
- g) 8pt_4r4o_twl_mwl

It is noted that not all of these cases are exactly the same as those investigated in the analytical sensitivity study. They are different in terms of location of lumped mass and/or the type of stiffening member. In order to validate the analytical results and the FEM models, the cases that do not match with the cases in Chapter 3 are analyzed again to compare the C^2 values from experimental and analytical results. The reasons for the experimental cases being different from the analytical cases are because of 1) the guideline (iii) according to which the number of cases should be maximized without changing the stiffening member, and 2) the diameter of the lumped masses overlapped when tried to attach them on the middle plate.

4.2 Test Procedures

There are various steps involved in the test program in both lateral and vertical directions. They include:

- i) Validation of the test fixtures. As mentioned in Section 2.2.3 two different types of fixtures are devised to test in lateral and vertical directions. Validation of fixture involves a low-level testing of the fixture to verify the natural frequency of the structure, mode shape if the frequency is below the specified requirements, and to check the rigidity of the structure at the attachment points of the test item.
- ii) Driven-base modal survey of mounting structures to correlate with the FEM model. A burst random test is performed on the mounting structure in both lateral

and vertical directions for all configurations. Driven-base modal testing is performed to check the analytical frequencies and the mode shapes of the structure.

- iii) Low level random testing of test item is performed to obtain the apparent mass and the fundamental frequency in each configuration and to correlate the mode shape with the FEM model. The low-frequency asymptotic value of the apparent mass of the test item is expected to be 90%-95% of the mass of the structure depending on the direction of excitation. The remaining percentage of the mass (5%-10%) represents the force going through the preloaded attachment bolts; the force sensors and the bolts acting as parallel springs. The value obtained is used to calibrate the force sensors and change the nominal sensitivity of the force sensors if required. The test item configurations used for the experimental testing are:
a) 4pt_4r_cpl_wo; b) 4pt_4r_cpl_wl; c) 4pt_4o_ystf_wo; d) 8pt_4r4o_cpl_wo;
d) 8pt_4r4o_cpl_wl. The mass of the test item without any lumped mass is 16.7 lb (7.58 kg) and with lumped mass is 34.2 lb (15.52 kg) (experimental).
- iv) System level vibration testing at 3.5 g rms for each configuration in X and Z directions. The test item and the mounting structure are designed for 10 g rms input at the test item level and 7 g rms at the system level as mentioned in Chapter 2. For a 3.5 g rms base excitation at the system level, the interface acceleration (acceleration at the test item interface) is varying between 3.5 g to 7 g rms, with a few cases exceeding 8 g rms.
- v) Calculation of the C^2 value based on the system level data as explained in Chapter 3, Section 3.2.

- vi) Demonstration of FLV method in one configuration by conventional random vibration testing (without FLV method) and random vibration testing with FLV method.

4.3. Description of Test Equipment

The experimental part of the project was performed at the CSA, in St-Hubert, Quebec. The equipment used for the tests is part of the Modal Analysis and Vibration Laboratory of the Space Technologies sector of the CSA. The equipment used for the modal and vibration tests is briefly described in this section.

Shaker and Slip Table

All excitation for both vibration and modal testing in the vertical direction is input to the hardware being tested using the shaker model SA15-S202 manufactured by Unholtz-Dickie Co (UD). The shaker capacity is 2000 lbf pk for sine excitation and 2000 lbf rms for random excitation. The excitation signal generated by the vibration system is transmitted to the shaker through a power amplifier system manufactured by UD.

For excitation in lateral directions, the hardware being tested is mounted to the slip table assembly model ST/S202-20-20-4 manufactured by UD. The slip table is basically a 20" x 20" steel plate floating on a thin layer of oil. The slip table is attached to the shaker through a bullnose.

Vibration and Modal Analysis System

Data acquisition and excitation control for both vibration and modal testing is performed using the LMS International (Leuven Measurement & Systems) CADA-X program on an HP 715/50 Unix workstation. An HP 3565 measurement hardware is added as a front-end unit to the workstation. These items constitute an integrated system having the following relevant characteristics:

- 32 measurement channels with sampling rates up to 12.8 kHz per channel;
- 2 source modules for driving independently 2 exciters with random type excitation for modal testing;
- For vibration testing, vibration and control software for performing closed-loop sine sweep and random excitation. Other types of excitation not pertinent to this project are also available;
- For modal testing, data acquisition and averaging software for MIMO (multiple-input-multiple-output) testing, limited to two inputs because of the source modules. The software also generates the time and frequency domain functions (including auto-power spectra, cross-power spectra, coherence functions and frequency response functions);
- Modal analysis software for parameter estimation. The software includes a variety of curve fitting algorithms for SDOF (single-degree-of-freedom), MDOF (multiple-degree-of-freedom), SIMO (single-input-multiple-output) and MIMO; facility for animation of the estimated mode shapes;

- Ability to create various types of Universal Files which are industry standard well-documented ASCII files for transfer of data or modal parameters to other software programs or systems;
- Command mode allowing some mathematical manipulation of time and frequency domain functions;

Triaxial Force Sensors

The force sensors constitutes critical instrumentation for performing FLV vibration testing since they are used in the closed-loop system of the vibration testing for measuring and limiting the reaction force. They are also used in the low-level testing for measurement of the apparent mass. The force sensors used for this project are the triaxial sensor model 9251 manufactured by Kistler. These sensors can measure simultaneously three orthogonal forces at a single point. The measuring range of this model is 1,100 lbf in the axial direction (normally vertical axis) and 550 lbf in the shear direction (normally lateral axis). Eight of such sensors were made available for the tests.

Related equipment for the force sensors includes the summation boxes and charge amplifier, both manufactured by Kistler. The summation box, model 344-107B, adds the charge signal generated by up to four force sensors and produce a charge signal as output. The dual mode charge amplifier, model 5010B1, convert the charge signal generated by the sensor into a voltage signal which is input to the LMS system.

Accelerometers

A variety of accelerometers are used to monitor the input and response accelerations during the test. The model selected at a particular location depends mainly on the level of motion. The accelerometers used during this test program are all manufactured by Endevco and varied sometimes from one test to the other. Their models are: 256-10 or 256HX-10 having a nominal sensitivity of 10 mV/g, and 61-100 having a nominal sensitivity of 100 mV/g.

4.4. Testing in X direction

The testing procedures contain all the following steps summarized in Section 4.2.

a) Validation of the test fixture

The fixture used for the vibration testing in the lateral direction was illustrated in Figure 2-11, and the details of the fixture were also indicated in Table 2-4.

1) Test description and instrumentation

To test the fixture, the shaker is rotated by 90° and is attached to a bullnose, which acts as an interface between the slip table and the shaker to vibrate in the horizontal direction. The test structure (fixture for lateral direction) is fixed to the slip table at its attachment points. The slip table acts as the 'fixture' for the current test, so the vibration is monitored and controlled through the slip table. For the testing of the fixture in the X direction, the required instrumentations are only accelerometers, which are used to monitor and control

the vibration and also to measure the vibration at critical locations (attachment points of test item and mounting structure) in all the directions.

Accelerometers are fixed on either side of the slip table to monitor and control the acceleration input to the test structure. Accelerometers on the fixture are used to get the acceleration response or vibration level at the attachment points of the test item and the mounting structure. Frequencies and mode shapes are extracted from these data. The accelerometers are attached in all three directions at some locations to verify the cross-talk accelerations and their effect on the system level testing (if there is any, there will be no effect of cross talk accelerations on the test item at the system level testing in the excited direction, as the forces get cancelled, or sum of forces in these directions is zero). Low-level sine sweep vibration test with 1 g amplitude as acceleration input is performed on the structure over a frequency bandwidth of 20 Hz to 2000 Hz. The sweep rate of the run is 2 octave/min. Frequency resolution of the data is 2 Hz. The test is controlled with the control accelerometers on either side of the slip table, using the average strategy, meaning that the vibration system controls the test using the average of the two control signals. The fixture used for lateral test and the locations of accelerometers are shown in the Figure 4-1.

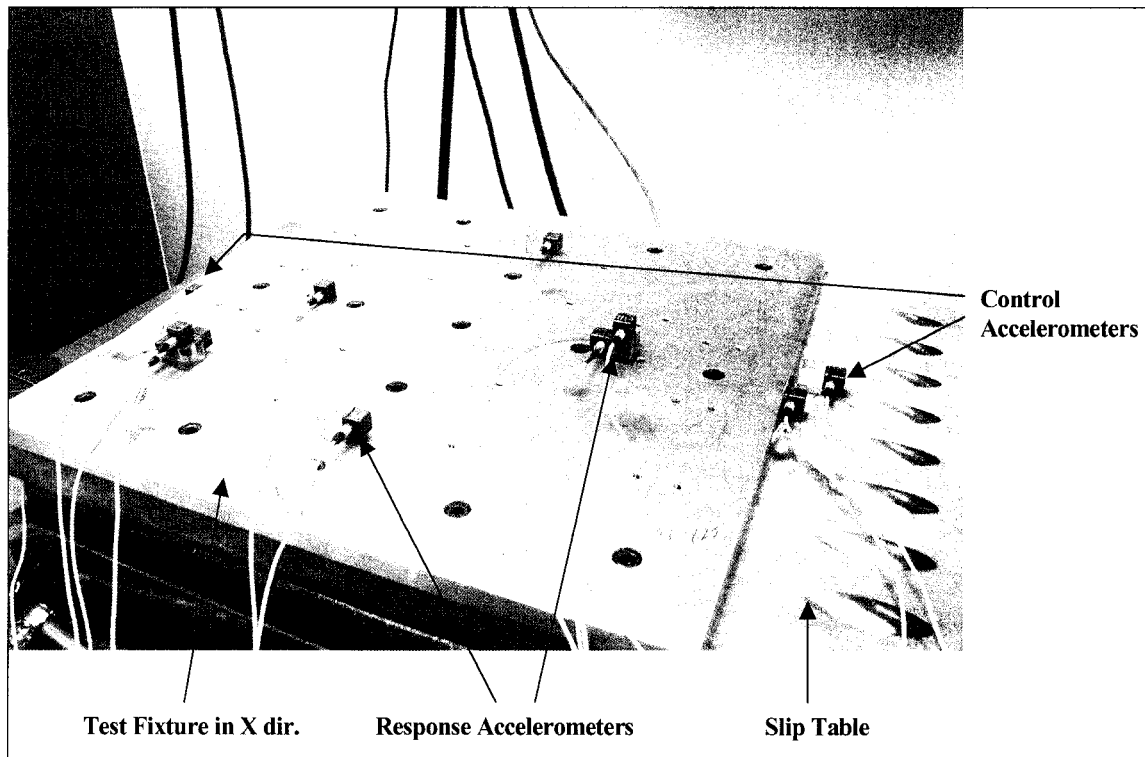


Figure 4-1. Test Fixture for lateral test

2) Test results and comparison with analytical results

The acceleration response of the fixture at the attachment points is shown in the Figure 4-2. It can be observed that there are no modes in the frequency range of interest (up to 2000 Hz) in the direction of excitation (X direction), confirming that the fixture is rigid enough to be used to perform the system level and test item level testing. It is found that there are few modes in the Z direction, however they do not affect the testing in the X direction. Hence the test results agree with the analytical model in the frequency range of interest.

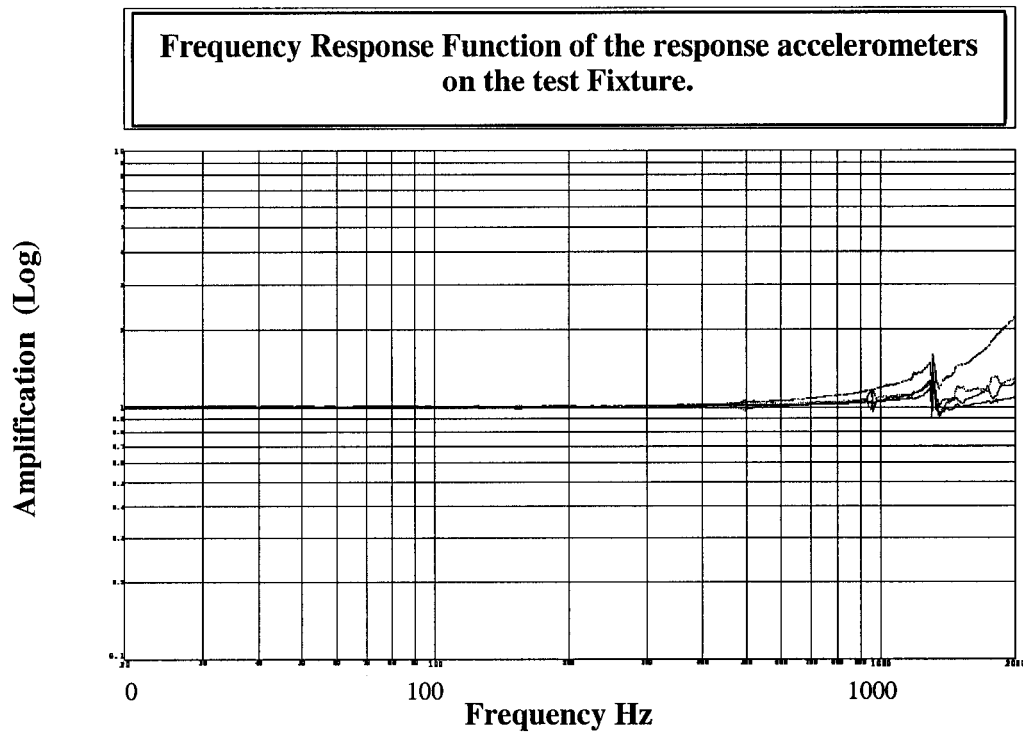


Figure 4-2. Acceleration response at attachment points of the fixture

b) Driven-based modal survey of mounting structure

1) Test description and instrumentation

Modal testing of the mounting structure is performed using burst random excitation process. In this process, the input level is limited to the first part of the measurement time window. In the current case, the random input is applied to the structure for the 50% of the time. Then, for the remaining time, the system is allowed to get to rest and the acceleration response practically approaches to zero by the end of the time. The data acquired by the burst random process will be an average of 40 such samples in order to obtain the vibrations related to the modes of the mounting structure and to phase out the noise that may occur in the process.

For the burst random testing, the mounting structure is attached on the test fixture with M6 Bolts (design requirements 4 and 24). To measure the acceleration response in the frequency bandwidth of 20 to 2000 Hz, accelerometers are attached on both side plates, on the top and the middle plates of the mounting structures as shown in Figure 4-3. The location of each of the accelerometer is noted from a reference point, which would later help in finding the mode shape using the CADA-X software of the LMS system, by creating the nodes representing the accelerometers according to the coordinates noted earlier. In burst random test (as in any other modal testing), there is no closed-loop control of the vibration level. Thus, control accelerometers on the fixture are not required, however two such accelerometers are fixed on either sides of the fixture in the X direction as shown in the Figure 4-3. One of these two accelerometers at the control locations is used as the reference in generating the FRF's (response acc. / reference acc.).

The same procedure as described in the previous paragraph is performed to test the mounting structure with lumped mass in the X direction as shown in the Figure 4-4.

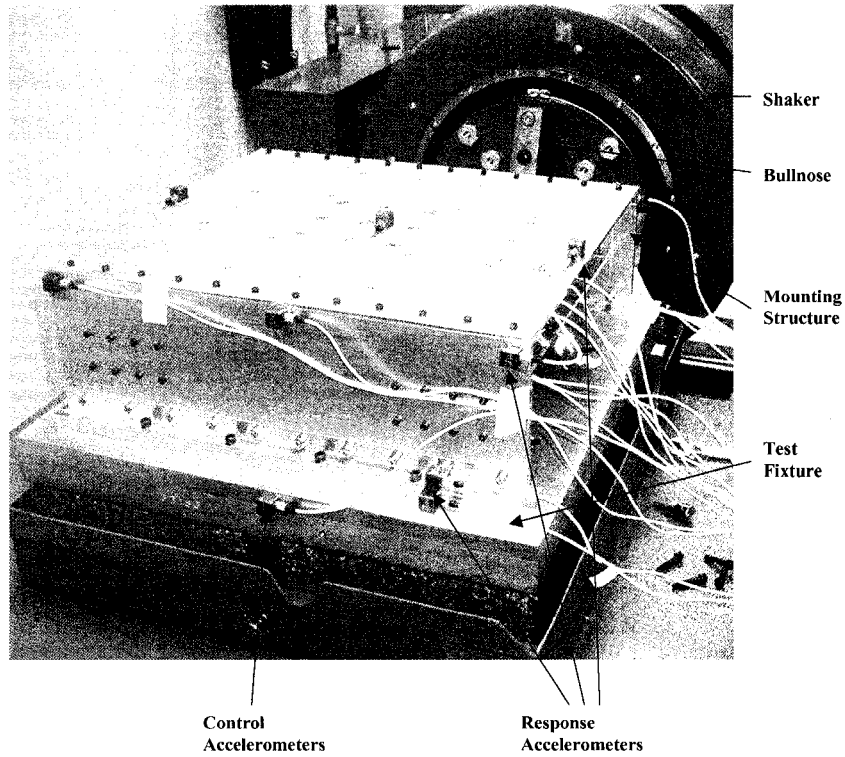


Figure 4-3. Mounting Structure without lumped mass in the burst random testing in the lateral direction.

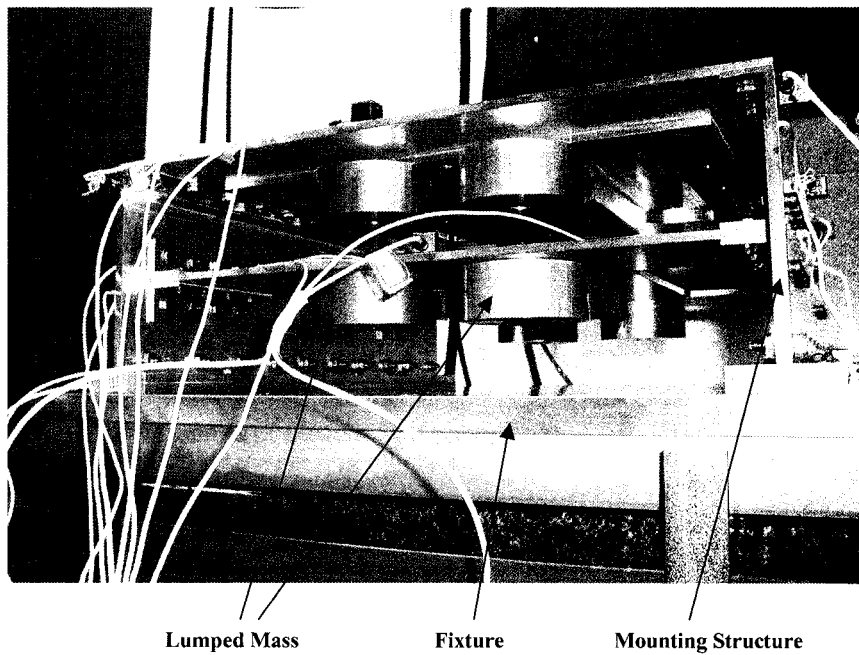


Figure 4-4. Mounting Structure with lumped mass in the burst random testing in the lateral direction.

2) Test results and comparison with analytical prediction.

Once the driven-base modal test is completed on the mounting structure, an FRF plot of the acceleration response of the accelerometers on the side plates is created. This plot can indicate the fundamental frequency of the structure in the X direction and also help to obtain the mode shape (It is noted that CADA-X software can be employed to create a geometry using the accelerometer positions according to the dimensions measured earlier while attaching the accelerometers). The mode shape of the fundamental mode of the mounting structure with or without lumped mass in X direction is compared with the mode shape obtained from the FEM model. The result for fundamental frequency is shown in the Table 4-1.

Table 4-1. Fundamental frequency (Hz) of the mounting structure in X-direction

| Mounting Structure | Experiment | FEM |
|---------------------------|-------------------|------------|
| Without Lumped Mass | 68.3 | 105 |
| With Lumped Mass | 49.5 | 70 |

It is noted that experimental fundamental frequencies are about 30% - 35% lower than the result obtained from FEM. The possible causes of drop in frequency may be attributed to the following points:

1) As mentioned in Chapter 2, the mounting structure is manufactured by joining different parts using bolts and nuts. The point of attachment between the side plate and the legs, where the strain energy is the maximum for the first mode in the lateral direction might not be perfect. This reduction in contact area between the two surfaces might be

the major reason for drop in the fundamental frequency. Had the structure been manufactured as a single part in one piece (which was not possible due to the lack of facilities at CSA) there might not have been much deviation in the natural frequencies of the structure.

2) Another major cause for the discrepancy in the frequency would be the attachment points of the mounting structure. Due to the defect in manufacturing the attachment points of the mounting structure of the two test fixtures, the attachment points of the mounting structure are oval in shape compared to the regular circular cross-section. This might lead to the micro slip in the attachment points during lateral excitation. This will induce flexibility into the attachment points in the lateral directions, and thus reducing the natural frequencies of the mounting structure. The nonlinear micro-slip phenomenon was not modeled in the analysis since it is very complicated to simulate.

3) The thickness at the attachment points of the side plates to the top plate was assumed to be 4.76 mm in analysis, while during the manufacturing this thickness is modified to 6.35 mm mainly due to the manufacturing difficulties in attaching the two plates. It is not a major cause but will increase the effect of the previous two in dropping the frequency.

The FRF of the acceleration response of the accelerometers located on the side plates of the mounting structure without and with lumped mass are shown in the Figures 4-5 and 4-6, respectively.

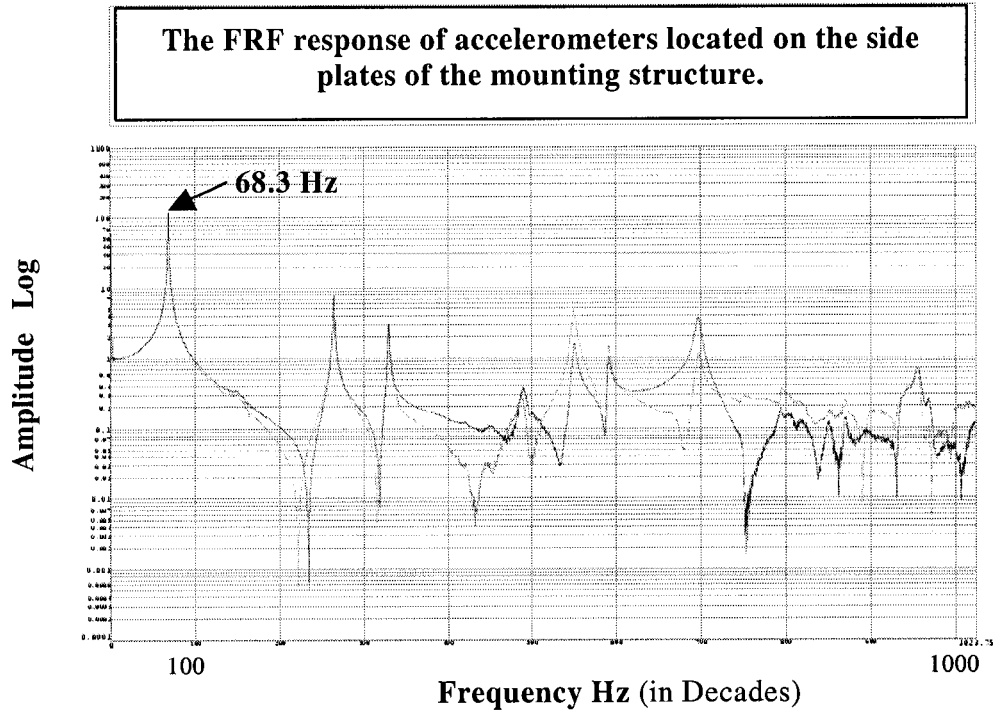


Figure 4-5. The FRF response of accelerometers located on the side plates of the mounting structure without lumped mass.

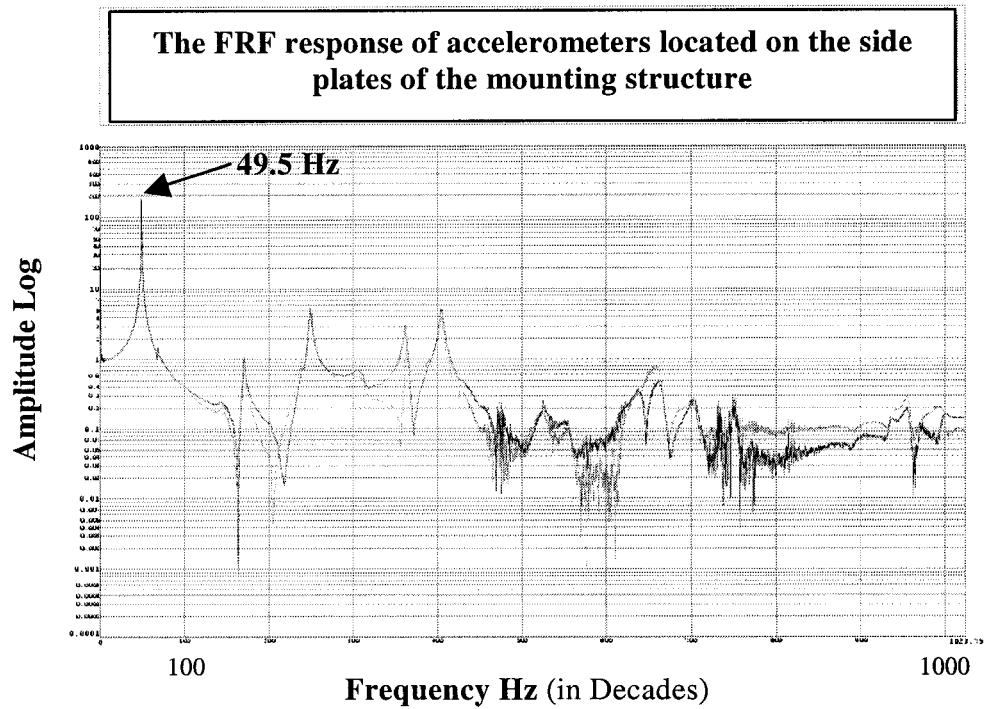


Figure 4-6. The FRF response of accelerometers located on the side plates of the mounting structure with lumped mass.

c) **Low level random vibration testing of test item**

1) *Test description and instrumentation*

A low-level random vibration test with a flat spectrum acceleration input having 1 g RMS was conducted on the test item to obtain the apparent mass of the structure and to compare the asymptotic value of the apparent mass with the actual mass of the test item in order to modify the nominal calibration of the force sensors for the system level testing. The test item without and with lumped mass are shown in the Figures 4-7 and 4-8, respectively.

The force sensors are also required to estimate the apparent mass of the structure. Figure 4-9 illustrates the force sensors used at the attachment points to find the apparent mass of the test item. The vibration level is controlled by two accelerometers on either side of the fixture. The accelerometers attached on the side plates, the top plate and the middle plate are used to find the fundamental frequency of the test item and the part, which is involved in the mode shape. It is not possible to obtain the detailed mode shape due to limited amount of instrumentation; however the part of the structure contributed in the first mode shape can be detected by comparing the FRF response of different accelerometers. Proper care should be taken while attaching the force sensors at the interface points since they should face in the same direction. The total reaction force can be obtained by connecting the force sensors to a summation box whose output is connected to the charge amplifier. In the case of 8 attachment points, 3 such summation boxes should be used as each of them has 4 input points. The figures indicating the test

item with and without lumped mass and the force sensors are shown below. and the force sensors are shown below.

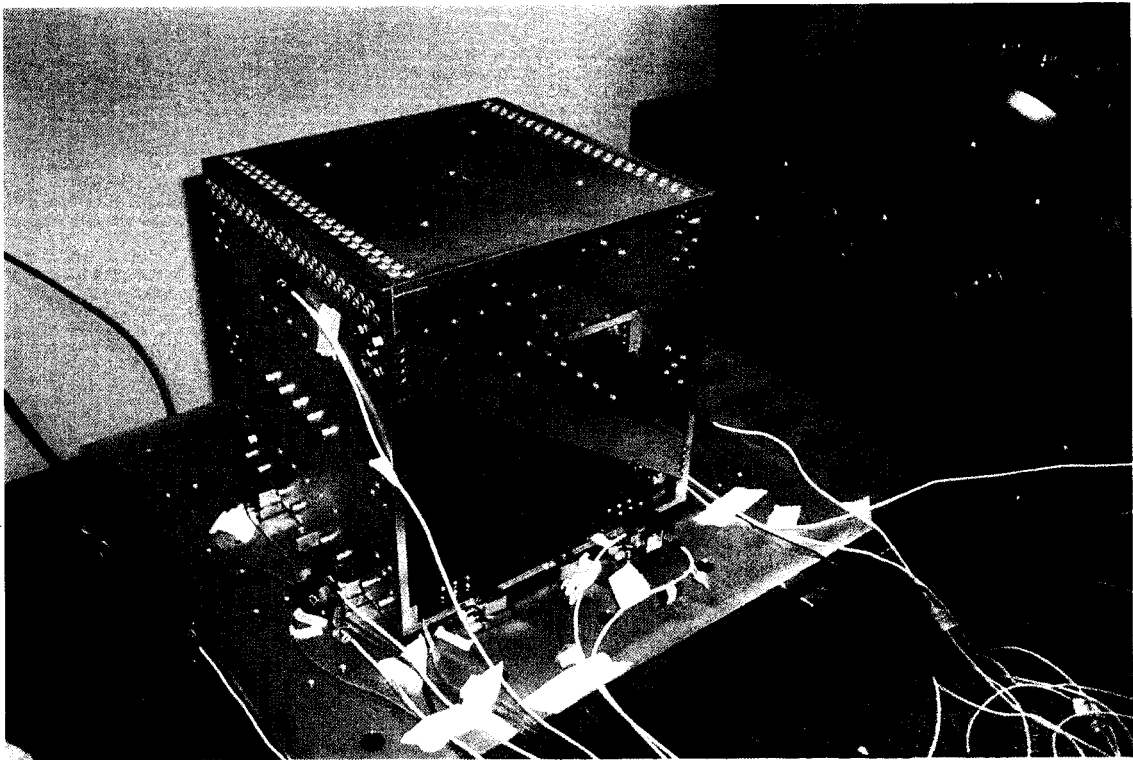


Figure 4-7. Test item without lumped mass and with 8 attachment points for low level random testing in X direction.

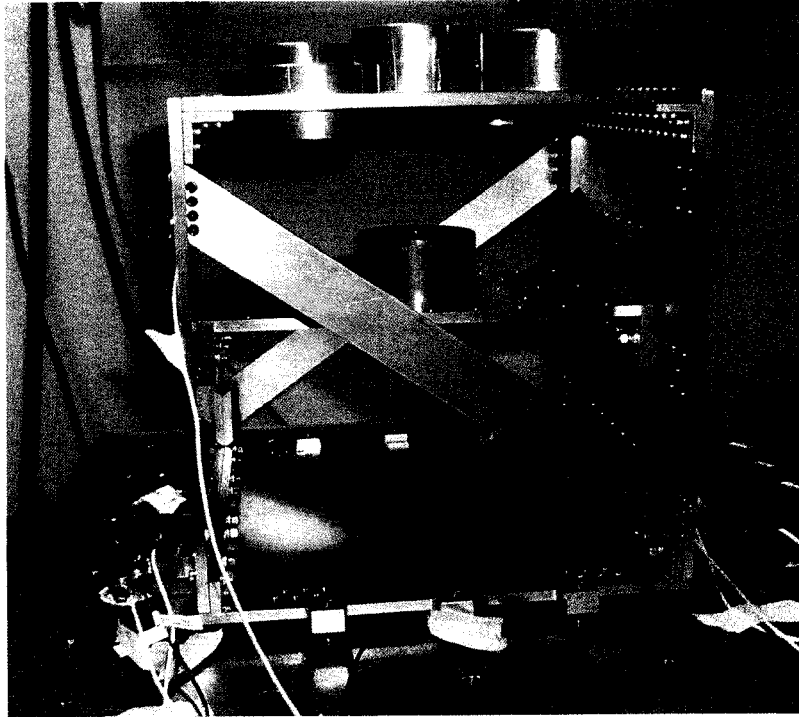
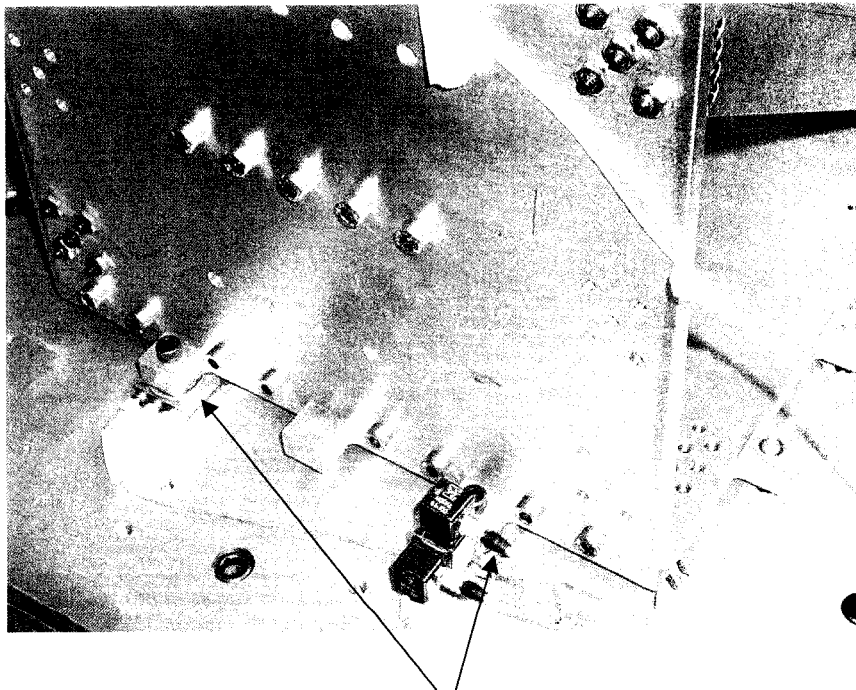


Figure 4-8. Test item with lumped mass and with 4 attachment points for low level testing in X direction.



Force Sensors

Figure 4-9. Force sensors at the attachment points to measure the apparent mass of the test item.

2) Test results and comparison with analytical prediction

Having conducting the low level random vibration test on all considered configurations of the test item, the FRF plot of the total force at the base of the structure can provide the information regarding the apparent mass and the fundamental frequency of the structure. The results for the fundamental frequency and the asymptotic mass for different test items (cases in Section 4.2) are obtained. The asymptotic value of apparent mass for test item 8pt_4r4o_cpl_wo is found to be 16.3 lb (97.7 % of the total mass of the test item has been retrieved). For the test items 8pt_4r4o_cpl_wl, 4pt_4r_cpl_wo and 4pt_4r_cpl_wl, the asymptotic value of the apparent mass have been found to be 33.3 (97.7%), 16.0 (96.0%) and 33.1 (96.7%), respectively. It can be observed that the amount of mass sensed by the force sensors is above 95%; hence it is not required to change the calibration of the force sensors for the testing of test item at the system level in the X direction.

The result for the fundamental frequency and its comparison with the analytical value obtained from finite element analysis for different test item configurations are shown in the Table 4-2. It is noted that good correlation (less than 8% error) between experimental and finite element results exist.

Table 4-2. Fundamental frequency (Hz) of the test item in X-direction

| Test Item | Experiment | FEM |
|-----------------|------------|-----|
| 8pt_4r4o_cpl_wo | 184 | 196 |
| 8pt_4r4o_cpl_wl | 108 | 101 |
| 4pt_4r_cpl_wo | 181 | 190 |
| 4pt_4r_cpl_wl | 106 | 97 |

The Figure 4-10 demonstrates the apparent mass, the fundamental frequency of the test item and the asymptotic value of the apparent mass for the test item 4pt_4r_cpl_wo.

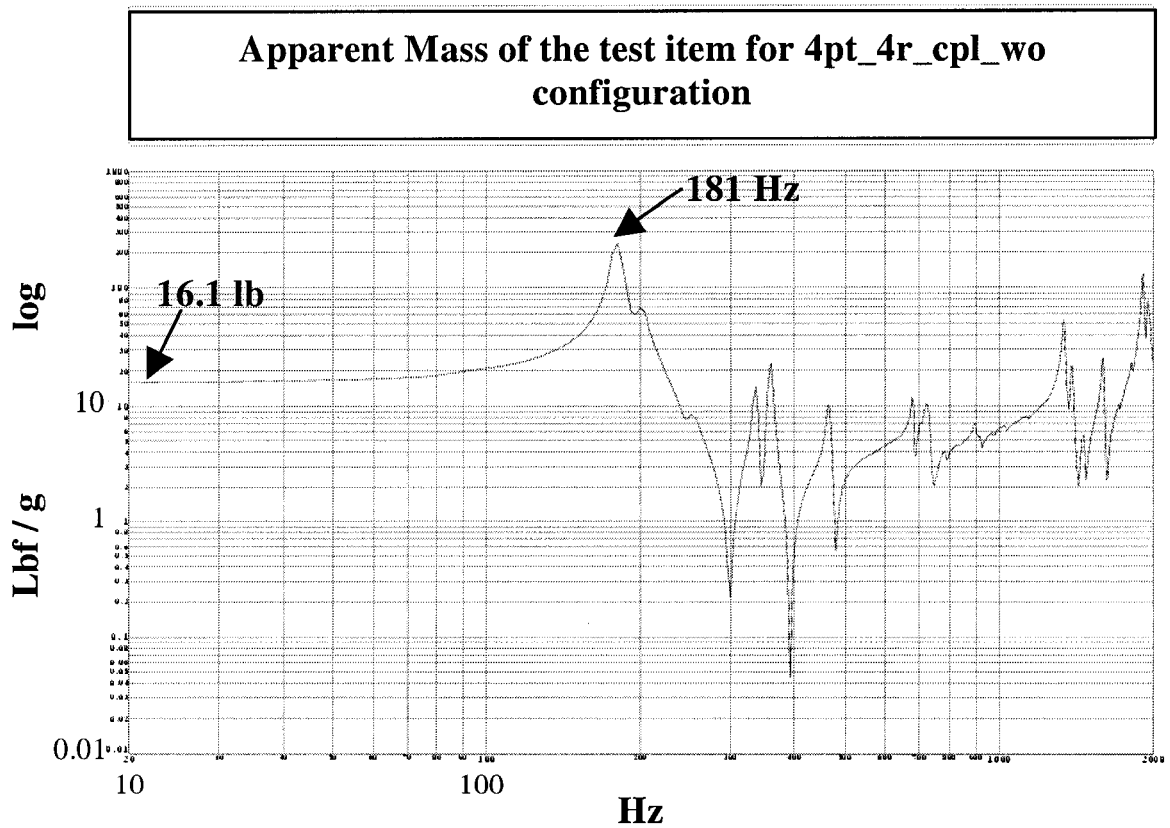


Figure 4-10. Apparent Mass of the test item for 4pt_4r_cpl_wo configuration.

d) System level random vibration testing

1) *Test description and instrumentation*

For the system level testing, all the structures are mounted one on top of the other. First the mounting structure is attached to the fixture, and then the test item is mounted on the mounting structure. The input acceleration at the base of the mounting structure is controlled by the accelerometers attached to the fixture on either side of the mounting structure. Accelerometers are placed at the interface locations in order to measure the acceleration at the interface points between the mounting structure and the test item. The number of accelerometers depends on the test configuration, i.e., 8 and 4 for 8 attachment points and 4 attachment points respectively. Some response accelerometers are also attached to the critical locations of the mounting structure and the test item, i.e., on the side plates of both test structures. The response of these accelerometers will be used to identify the frequency in which the interface acceleration is computed for the calculation of C^2 parameter. Force sensors are sandwiched between the test item and the mounting structure to measure the reaction force at each interface point, which will subsequently be used to evaluate the apparent mass of the test item. Acceleration input spectrum with level of 3.5 g RMS is applied to the structures and monitored through the control channels. The input spectrum is a scaled-down version of the GEVS spectrum shown in Figure 3-8 of Chapter 3. Abort and alarm levels are set for the input acceleration so that if at any time the acceleration exceeds the abort level the test is terminated in order to prevent any probable damage to the system. Similar to the previous tests, the frequency bandwidth of excitation is 20 to 2000 Hz with frequency resolution of 4 Hz. It should be noted that modern-day control systems such as the one used for the present test program

allows higher frequency resolution. However, the bandwidth of 4 Hz was still selected since, for operational reasons, it is the one still most frequently applied for vibration testing of space flight hardware. The test consists of three levels starting at -12 dB, where it is run at this level until the input acceleration is controlled. Then the input level is increased to -6 dB and then to 0 dB (full level) where the test is run for 60 sec. The test setup and the instrumentation involved in the test are shown in the Figures 4-11 and 4-12.

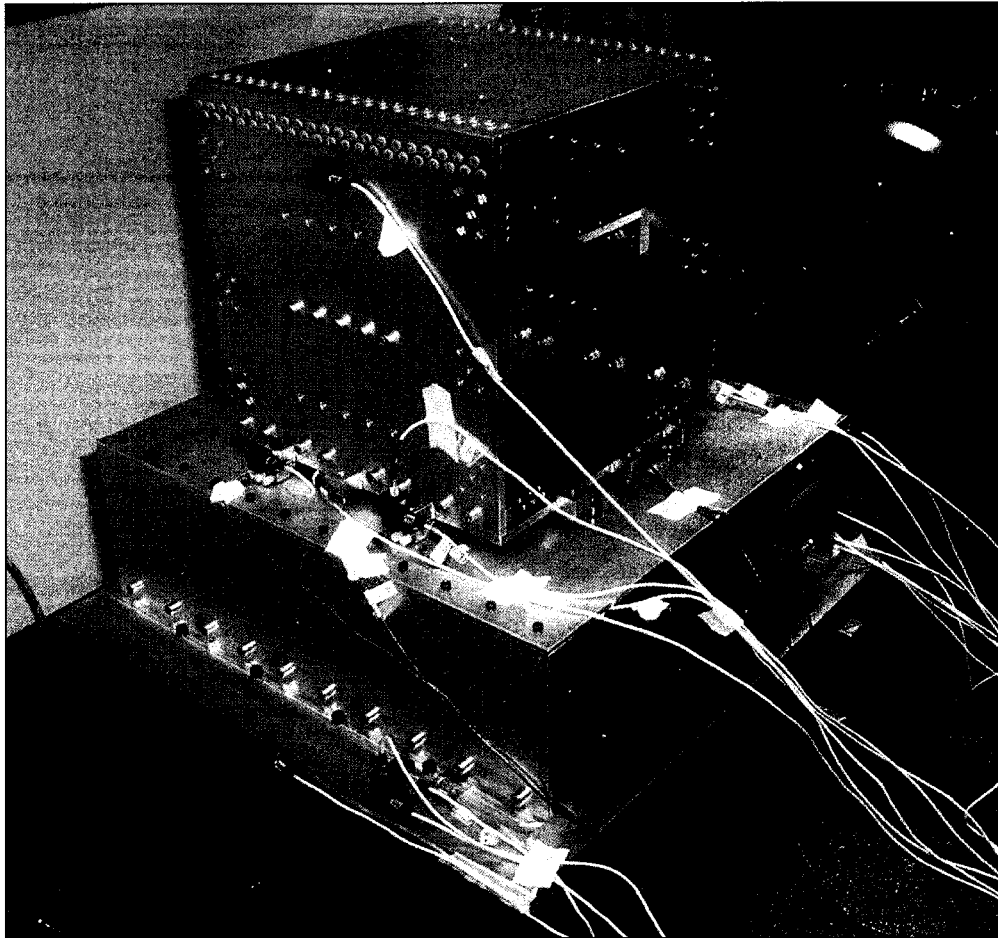


Figure 4-11. System level testing of test item fixed at 4 attachment points in X direction.

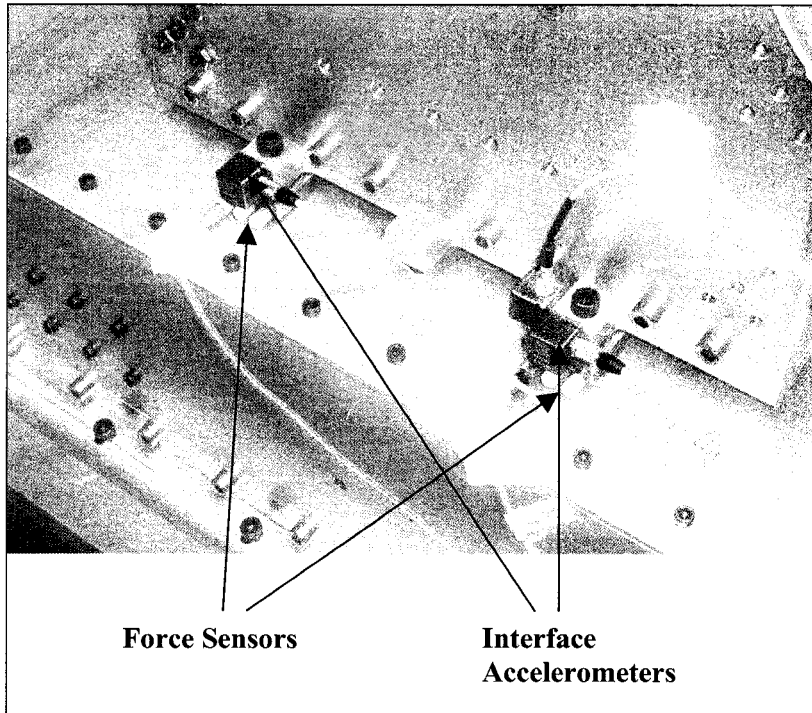


Figure 4-12. Force sensors and the interface accelerometers at the system level testing in X direction.

2) Test results and calculation of C^2 value

Once the system level testing is performed, the C^2 value for the corresponding configuration will be evaluated using the interface data (acceleration and the force). As it was explained in Chapter 3, the C^2 value is evaluated using the peak acceleration at the system level adjacent to the fundamental frequency of the test item by itself and the corresponding force. It may not be necessary that the maximum force and the maximum acceleration occur at the same frequency or even peak. In such cases, the maximum force and maximum acceleration are used to find the corresponding C^2 value. For most configurations, the maximum acceleration and force occurred at the same peak.

For instance, let us consider the case where the test item without any lumped mass is attached at 4 points all in the real direction to the mounting structure with lumped mass

on top, middle and the side plates i.e., 4pt_4r_two_2mwl (it is noted that 2 is added to the last term since there are cases where the mounting structure has lumped mass only on top and middle plate which is named as mwl. 2 indicates the 2nd possible case of mounting structure with lumped mass). For this configuration, the test results reveal a maximum acceleration of 0.0141 g²/Hz at 132 Hz and the maximum force of 17.2 lbf²/Hz at 136 Hz. Thus, the C² can be evaluated as:

$$C^2 = \frac{17.2}{16.7^2 \times 0.0141} = 4.4$$

where 16.7 lb is the physical mass of the test item without any lumped mass.

The Figures 4-13 and 4-14 indicates the four-interface acceleration and force for 4pt_4r_two_2mwl configuration.

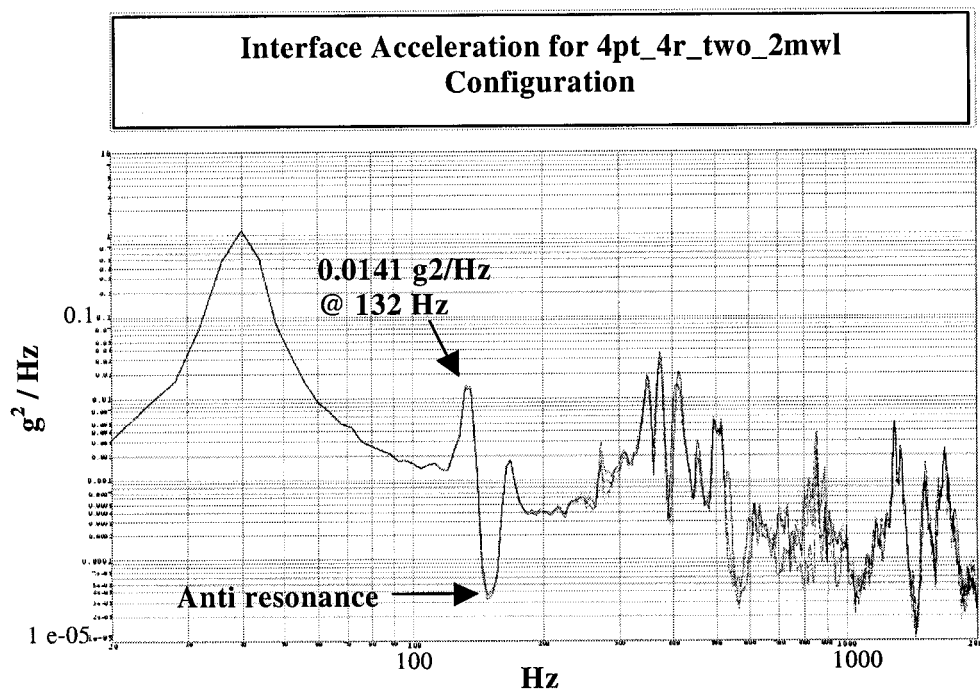


Figure 4-13. Interface acceleration for 4pt_4r_two_2mwl configuration.

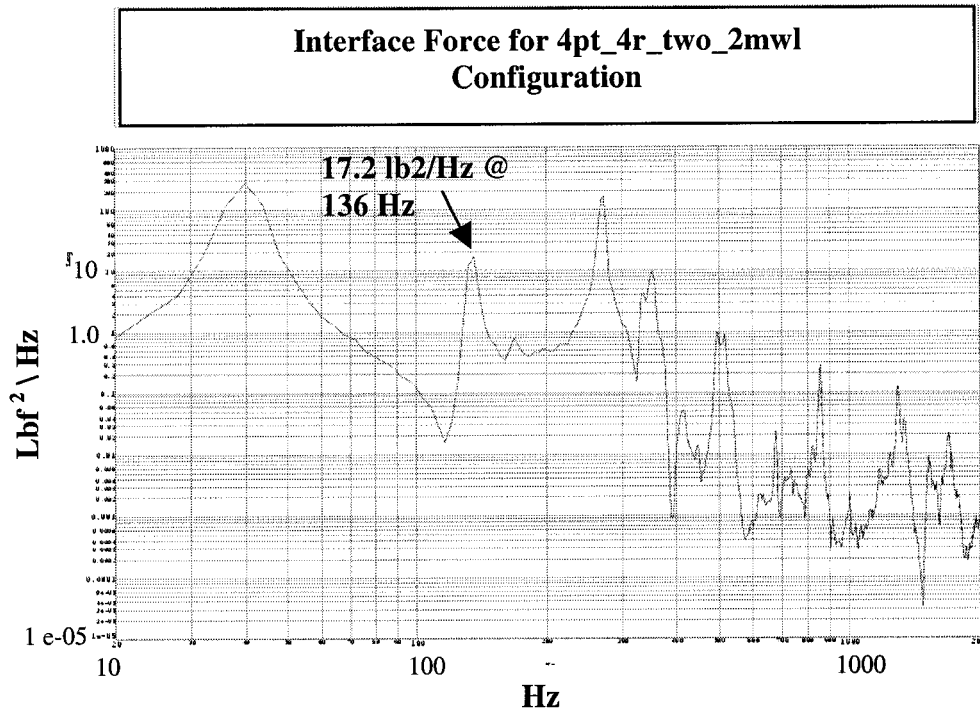


Figure 4-14. Interface Force for 4pt_4r_two_2mwl configuration.

4.5. Testing in Z direction

a) Validation of the fixture

The fixture used for testing at the system and the test item levels is shown in Figure 2-10 of Chapter 2, and the details of its dynamics are indicated in Table 2-4.

1) Test description and instrumentation

To test the test fixture in the vertical direction, the fixture is directly mounted on the shaker with 3/16" alloy steel bolt. Low-level vibration testing of the fixture is performed by exciting it with a flat acceleration spectrum having a 1 g RMS value. The two control accelerometers are attached on the shaker for controlling the input acceleration. Several

accelerometers are mounted on the fixture to monitor its response at critical locations. The test set up and the location of the response and control accelerometers are shown in Figures 4-15 and 4-16.

Driven-base modal testing is also performed on the vertical fixture to find the mode shape of the structure at the natural frequencies. The procedure employed is similar to the one employed for the mounting structure in the lateral direction. The details of the frequencies of the fixture obtained are explained in the next section.

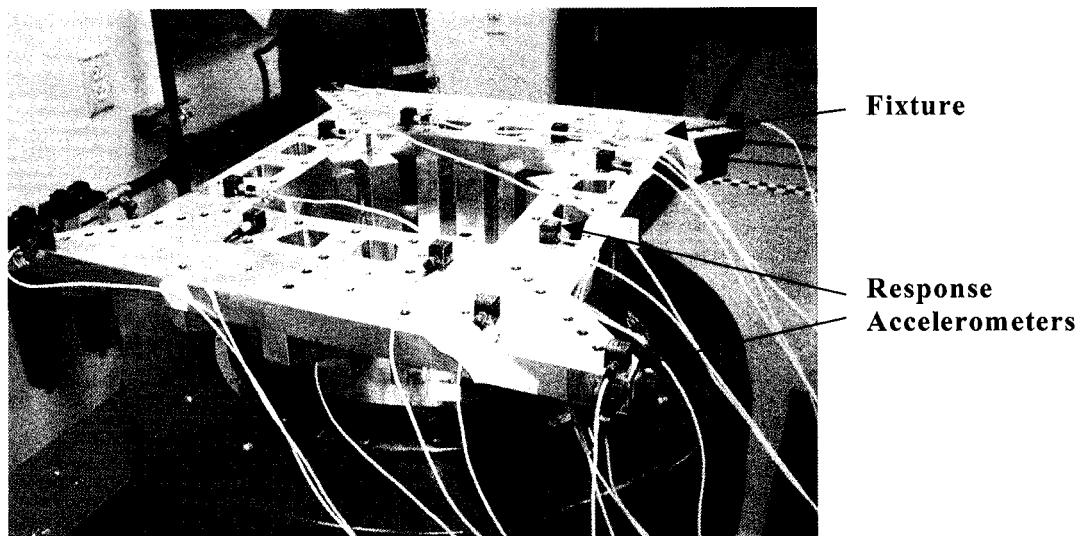


Figure 4-15. Test fixture for Z direction and the response accelerometers.

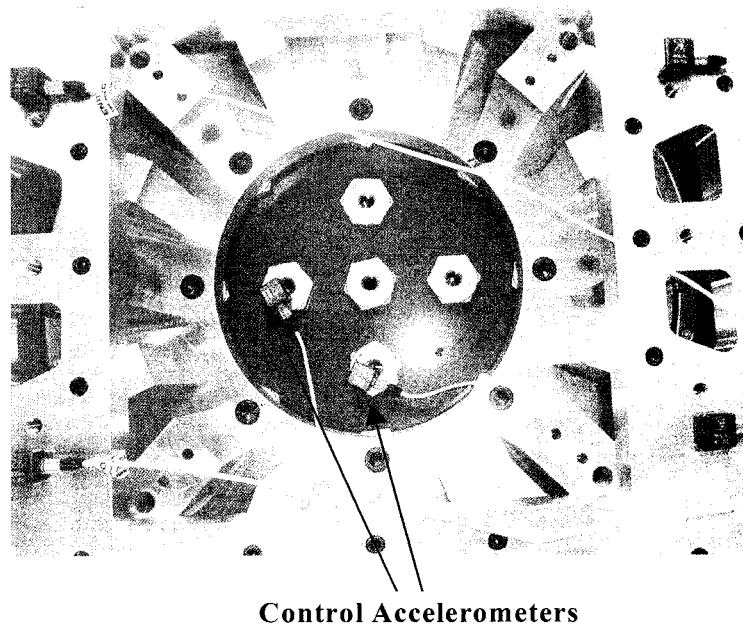


Figure 4-16. Control accelerometers location on the shaker.

2) Test results and comparison with analytical results

It is found that the fixture has modes at 978 Hz and 1545 Hz, the fundamental frequency of the structure is below the predicted analytical results of 1185 Hz. These modes appear in the FRF's shown in Figure 4-17. Since All the parts of the fixture such as the flanges, bottom plate and top plate are manufactured separately and assembled by the alloy steel bolts, the possible cause of reduction in frequency may be attributed to the micro-slips accruing at the contact area between each part. This will induce some flexibility at the contact areas between different parts, causing reduction of frequency. However, in the finite element analysis, the fixture has been modeled as a single unit and no flexibility exists at the contact areas. It is noted that the structure is manufactured in different parts, since the cost involved in manufacturing the fixture as a single part was very high and the facility was not available at CSA St-Hubert.

The mode shapes of the structure are extracted from the results of the burst random testing and they are in good agreement with those obtained from the FEM analysis. These mode shapes are basically the bending of large flanges located at the four corners of the top plate. Although the fundamental frequency of the fixture was below the expected value, the vibration level or response measured at the attachment points of the test item and mounting structure was very small in the frequency bandwidth of interest for deriving the C^2 values (below 300 Hz), confirming that the fixture is rigid enough to perform testing at the system and test item level.

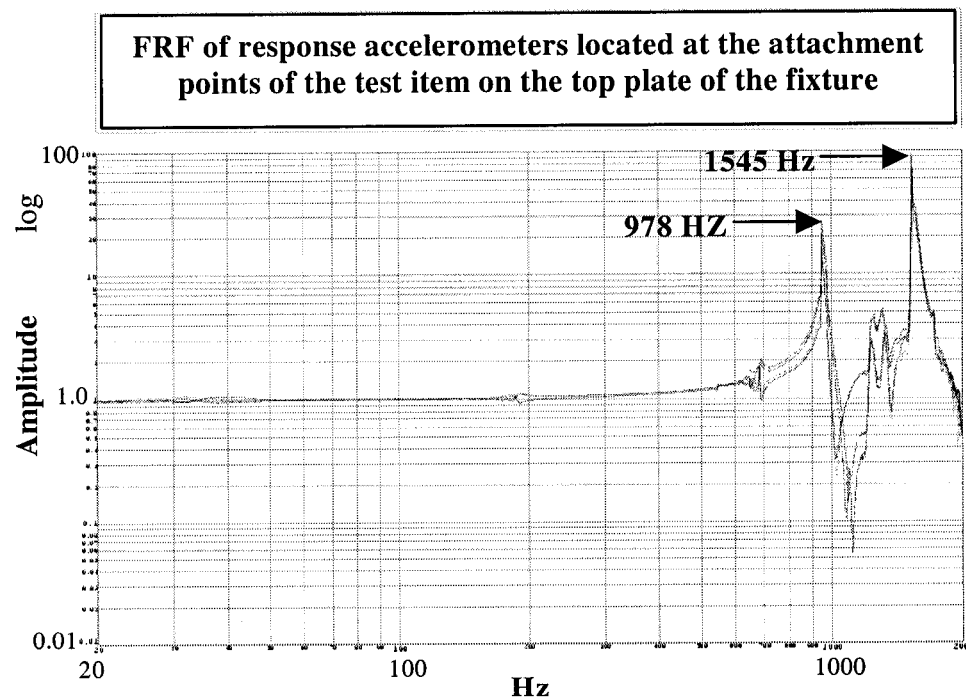


Figure 4-17. FRF of response accelerometers located at the attachment points of the test item on the top plate of the fixture.

b) Driven-base modal survey of mounting structure

1) *Test description and instrumentation*

The test procedure and instrumentation involved in testing of mounting structure in the Z direction is similar to the testing procedure in X direction, except that the response accelerometers are located on the top and the middle plate which are the active participants in the vibration of the structure in the vertical direction. One of the two so-called 'control' accelerometers attached to the fixture is used as the reference for the derivation of the response FRF's. The test setup for the mounting structure in the Z direction and the location of the control and response accelerometers are shown in Figures 4-18 and 4-19.

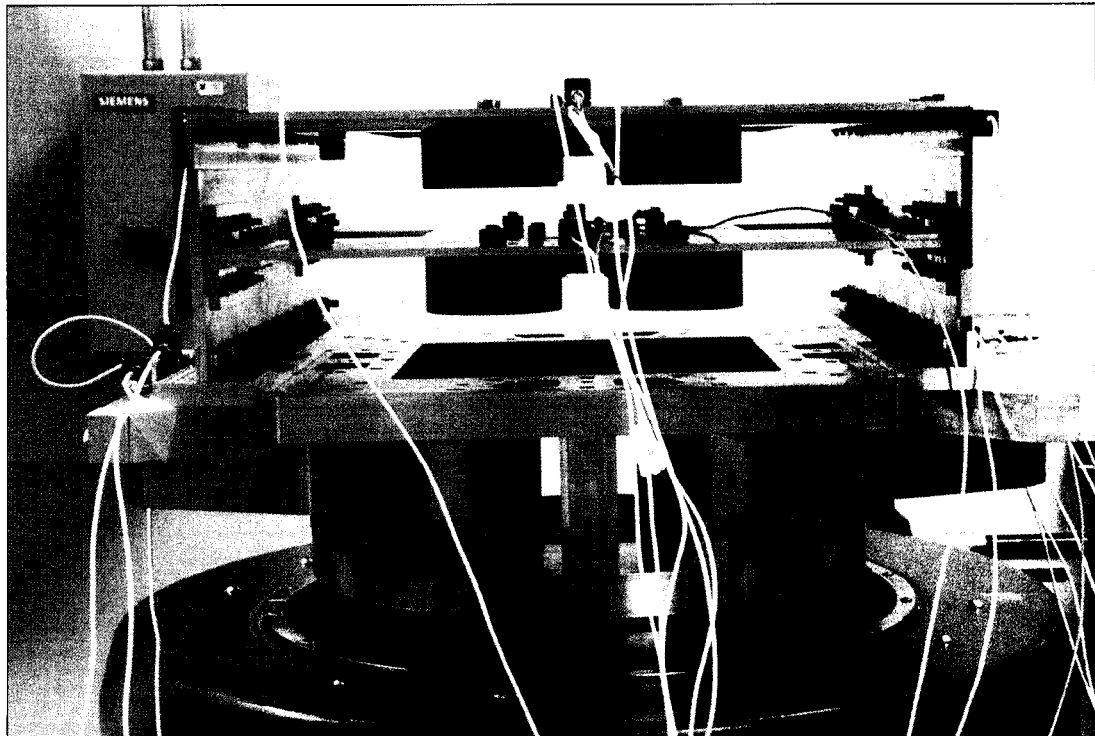


Figure 4-18. Mounting Structure with lumped mass in driven-base burst random testing configuration for Z direction.

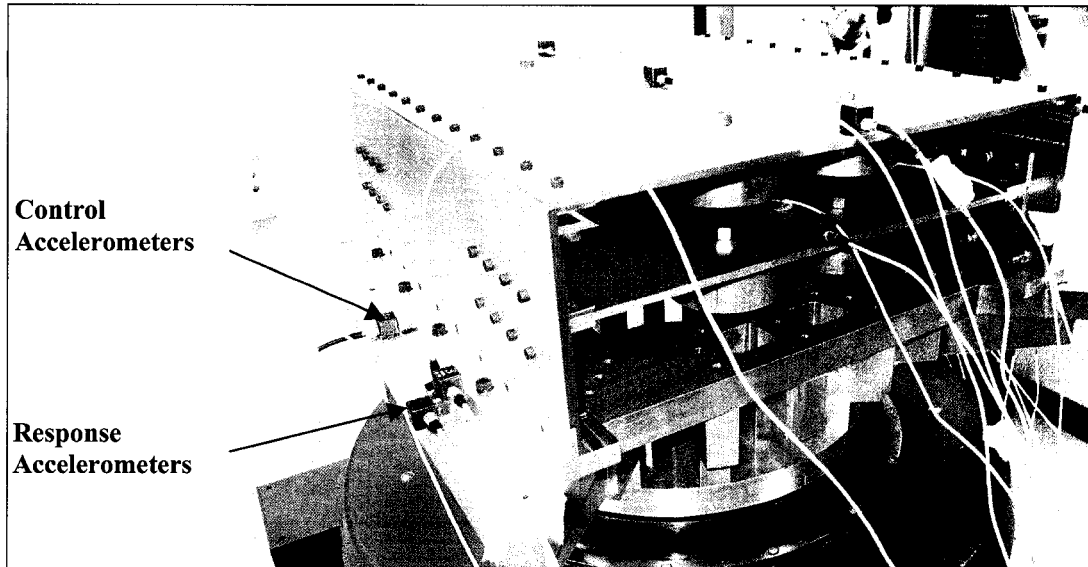


Figure 4-19. Control and response accelerometers for burst random testing of mounting structure for Z direction.

2) Test results and comparison with the analytical prediction

The fundamental frequency of the mounting structure obtained by burst random testing in the vertical direction and its comparison with FEM are shown in Table 4-3. It is noted that excellent agreement exists between experimental and finite element results.

Table 4-3. Fundamental frequency (Hz) of the mounting structure in Z-direction

| Mounting Structure | Experiment | FEM |
|---------------------------|-------------------|------------|
| Without Lumped Mass | 85.4 | 83 |
| With Lumped Mass | 68.4 | 62 |

The FRF of acceleration response of accelerometers located on the top plate of the mounting structure without and with lumped mass are illustrated in Figures 4-20 and 4-21.

FRF of acceleration response of the accelerometers located on the top plate of the mounting structure

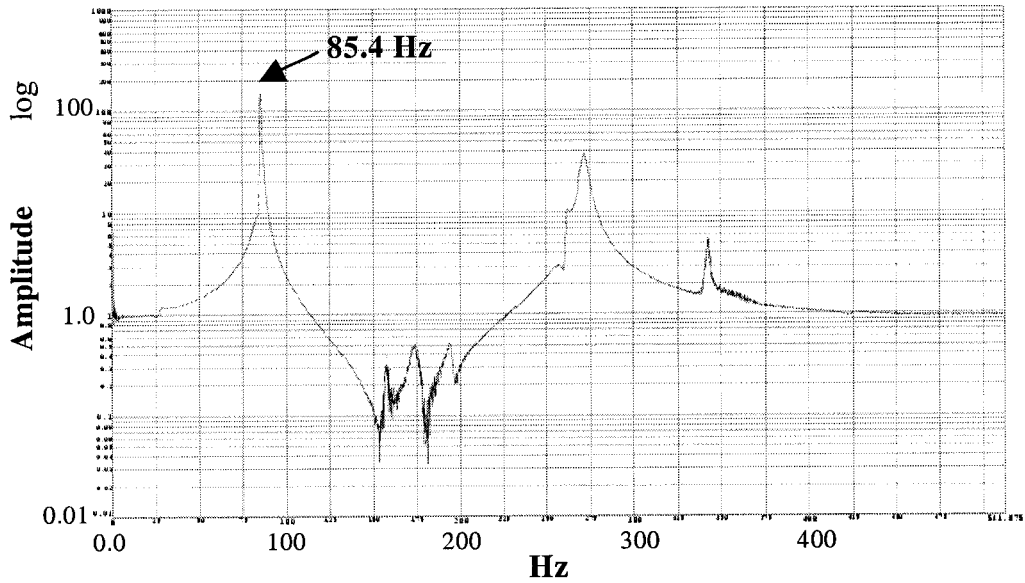


Figure 4-20. The FRF of acceleration response of the accelerometer located on the top plate of the mounting structure without lumped mass.

The FRF of acceleration response of the accelerometer located on the top plate of the mounting structure

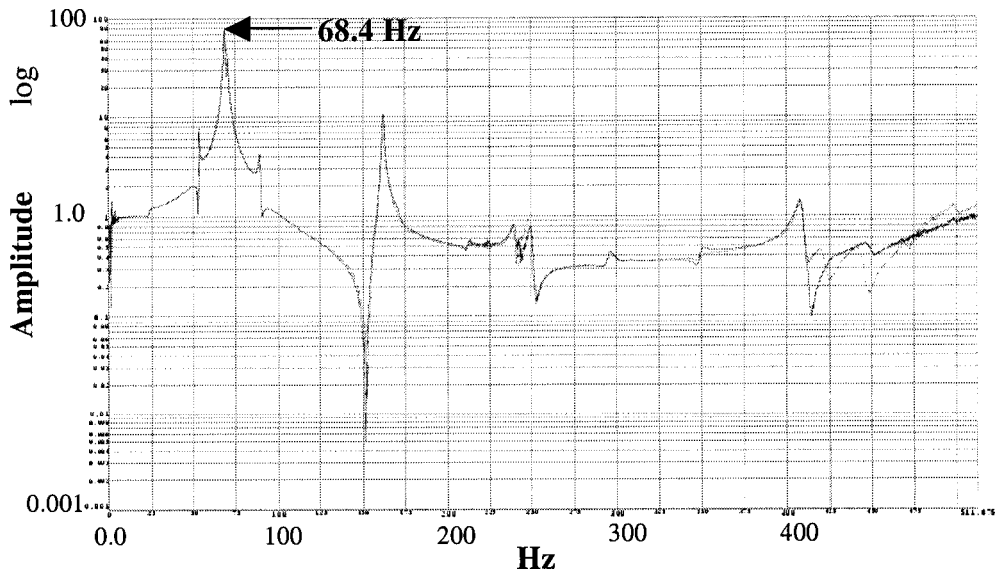


Fig 4-21. The FRF of acceleration response of the accelerometer located on the top plate of the mounting structure with lumped mass.

c) Low level random testing of test item

1) *Test description and instrumentation*

The low-level random test procedure employed is similar to the testing procedure in the X direction. The test setup indicating the instrumentation and the test item are shown in Figures 4-22 and 4-23.

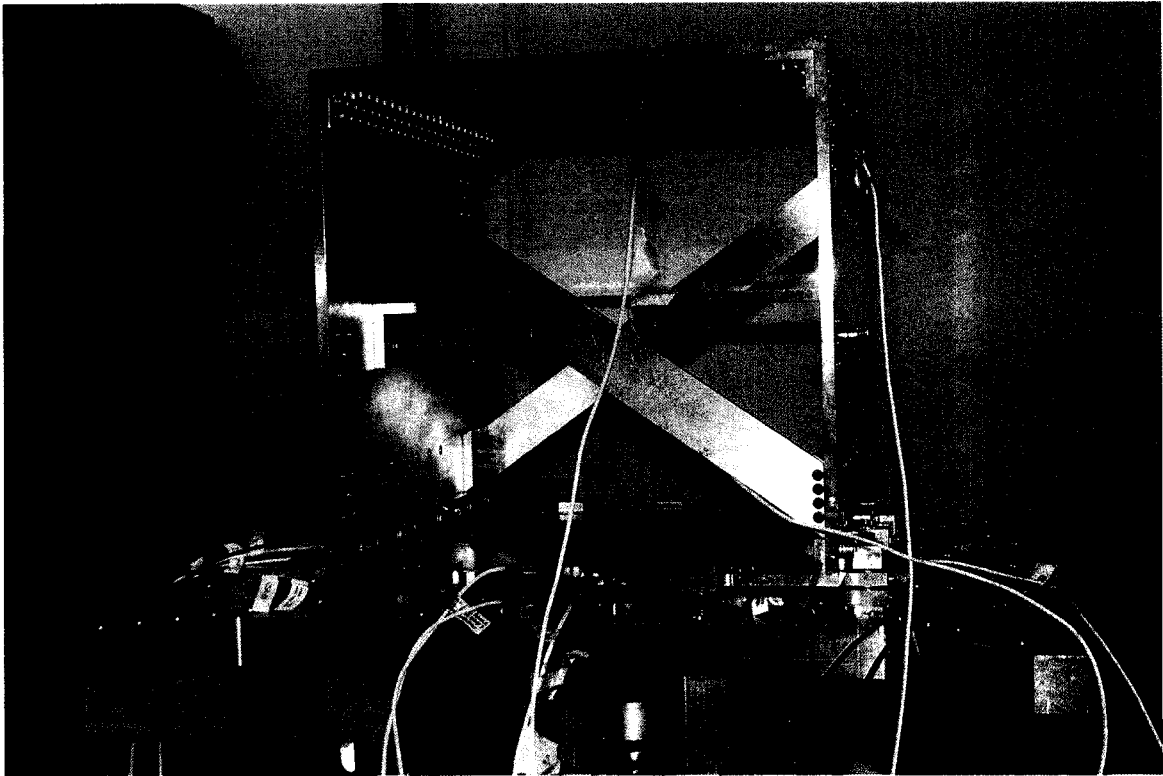


Figure 4-22. Test item attached at 8 attachment points without lumped mass for low level random testing in Z direction.

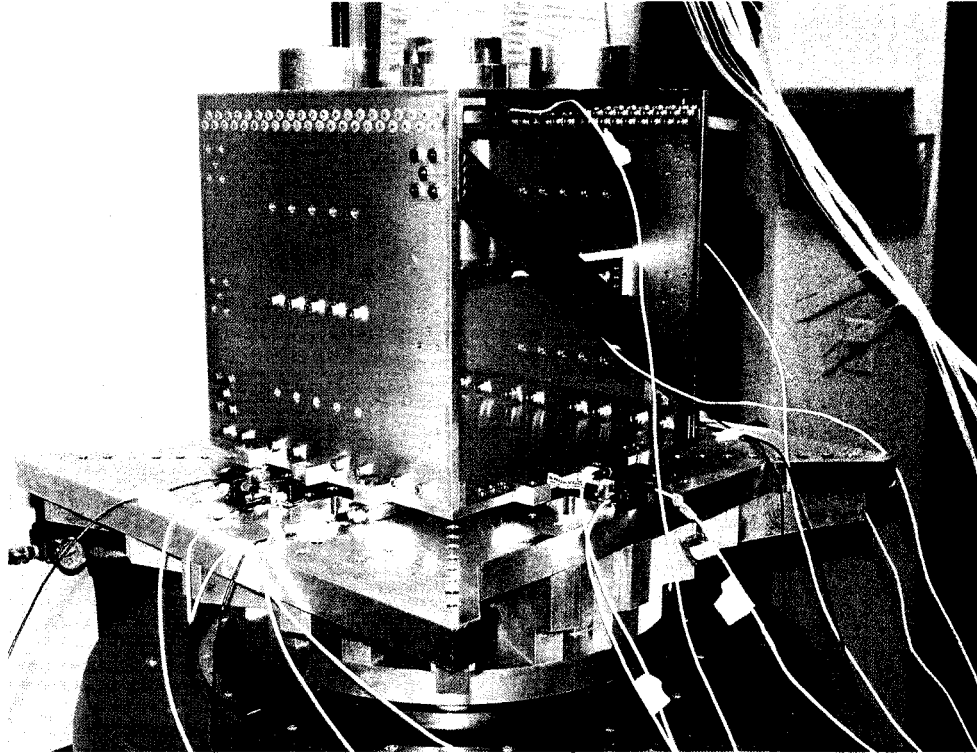


Figure 4-23. Test item with lumped mass and attached at 4 attachment points for low-level random testing in Z direction.

2) Test results and comparison with analytical prediction.

The result for fundamental frequency obtained by the low-level test on the test item in the Z direction and its comparison with the FEM are shown in the Table 4-4 for different test item configurations. It can be observed that there is a better agreement between experimental and FEM results for 8 attachment points than those for 4 attachment points configurations. The possible reason is that the analysis is conservative in terms of the frequency i.e., the test item is attached in 4 DOF during the analysis while the structure is fixed in 6 DOF because of the torque applied on the alloy steel bolts. It is also verified by rerunning the analysis of 4-point attachment without lumped mass case with 6_DOF attachment and the frequency was found to be 310 Hz, which is in excellent agreement with the experimental value.

The asymptotic value of the apparent mass for different test configurations are obtained. This asymptotic value for the test item 8pt_4r4o_cpl_wo is found to be 14.9 lb (90% of the total mass of the test item has been recovered. For the test items 8pt_4r4o_cpl_wl, 4pt_4r_cpl_wo, 4pt_4r_cpl_wl and 4pt_4o_ystf_wo, the asymptotic value of the apparent mass have been found to be 30.8 (90%), 14.9 (90%), 30.8 (90%) and 17.3(99.9%) respectively. It can be observed that the asymptotic value in the Z direction is about 90% of the total mass of the structure. The 10% 'lost' in term of mass is significant; therefore the force sensor calibration is changed accordingly by modifying its nominal sensitivity as input to the charge amplifier to obtain the entire mass of the structure, which can be verified for 4pt_4o_ystf_wo configuration in which the test has been performed after calibration of the force sensors. Figure 4-24 demonstrates the apparent mass, the fundamental frequency and the asymptotic value of the test item for 4pt_4r_cpl_wo configuration in Z direction.

Table 4-4. Fundamental frequency (Hz) of the test item in Z-direction

| Test Item | Experiment | FEM |
|-----------------|------------|-----|
| 8pt_4r4o_cpl_wo | 328 | 299 |
| 8pt_4r4o_cpl_wl | 153 | 140 |
| 4pt_4r_cpl_wo | 316 | 264 |
| 4pt_4r_cpl_wl | 152 | 120 |
| 4pt_4o_ystf_wo | 252 | 224 |

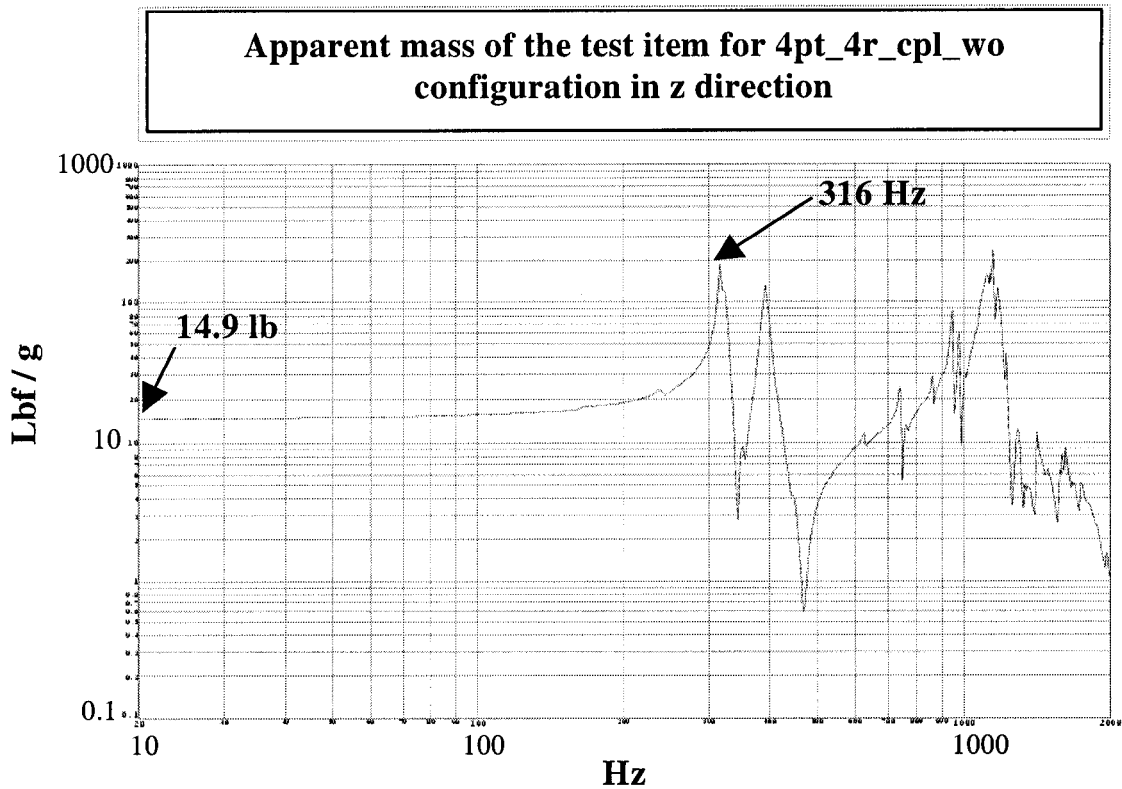


Figure 4-24. Apparent mass of the test item for 4pt_4r_cpl_wo configuration in Z direction.

d) System level random vibration testing

1) *Test description and instrumentation*

The test procedure and the instrumentation for the system level testing in Z direction are similar to those in X direction. However, as explained in the test item section, the force sensor sensitivity or calibrations are modified in order to retrieve the entire mass of the structure. The test setup and the instrumentation for 4pt_4r_two_mwl configuration in the Z direction are shown in Figure 4-25 and 4-26.

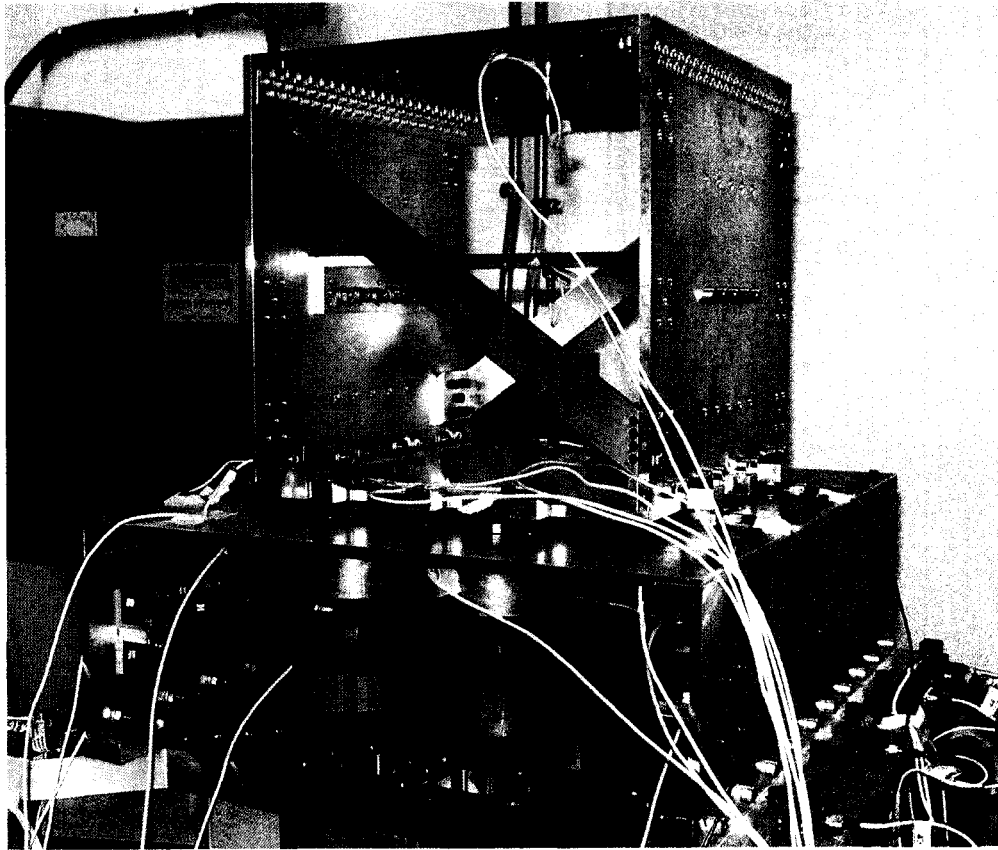


Figure 4-25. Test setup and instrumentation for system level testing of 4pt_4r_two_mwl configuration.

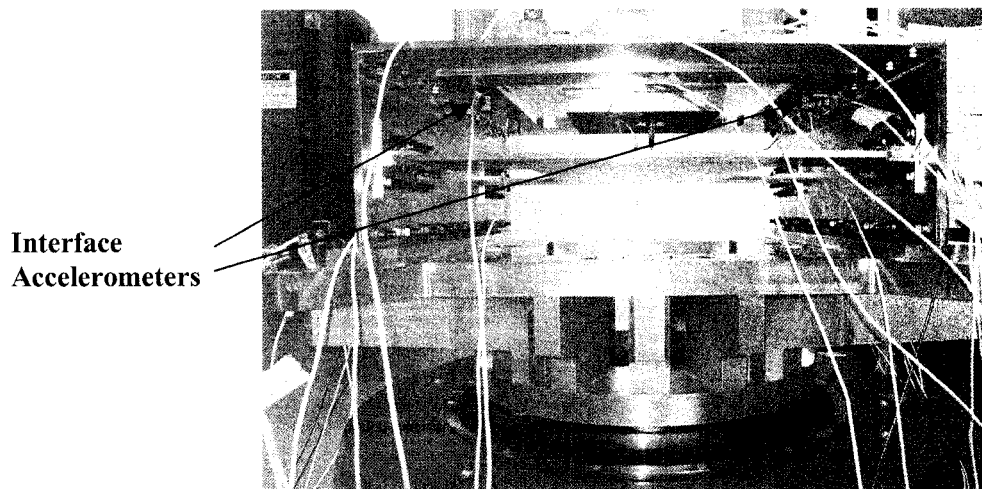


Figure 4-26. Interface accelerometers at 4-point configuration (4pt_4r_two_mwl).

2) Test results and calculation of C² value

For calculating the C² value in the Z direction, the 4pt_4r_two_2mwl configuration (the same as X direction) has been selected and the procedure is similar to that of X direction. Since the fundamental frequency of the test item in the Z direction is 316 Hz (Table 4-4), the maximum value of acceleration adjacent to the anti-resonance in the interface acceleration is selected as the input level for testing the test item by itself, which for the current configuration is 0.839 g²/Hz at 260 Hz. The corresponding interface force (total reaction force) is 710 lbf²/Hz, which also occurred at 260 Hz. Hence the C² value for the current example is

$$C^2 = \frac{710}{16.7^2 \times 0.84} = 3.0$$

The interface acceleration and the interface force for the 4pt_4r_two_2mwl configuration are shown in Figures 4-27 and 4-28, respectively.

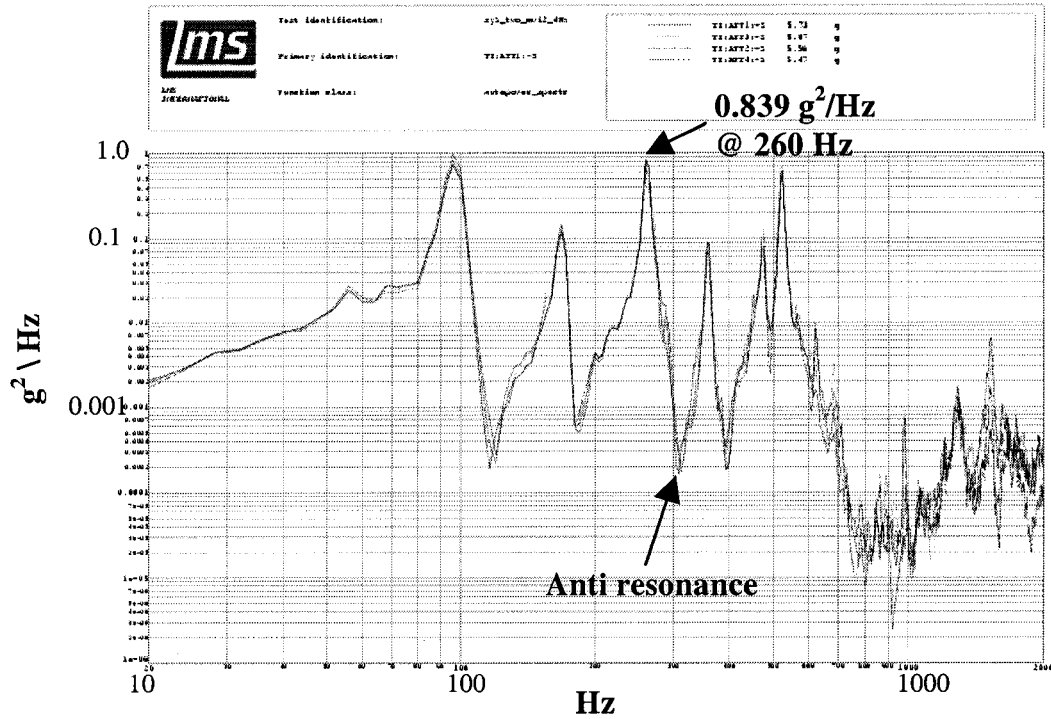


Figure 4-27. Interface acceleration for 4pt_4r_two_2mwl configuration.

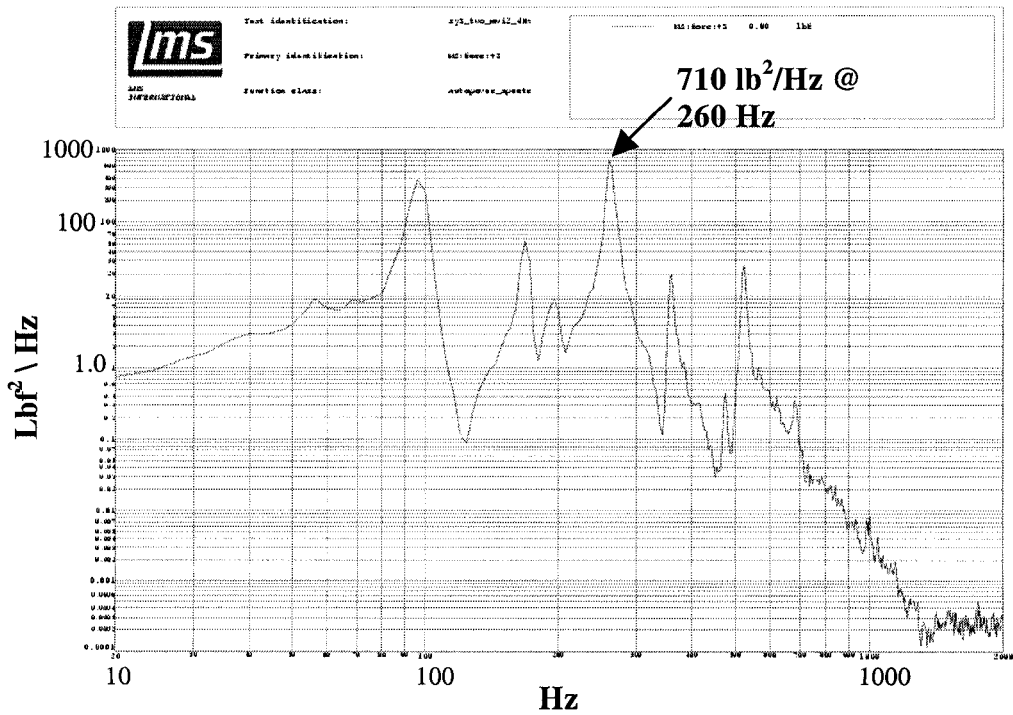


Figure 4-28. Interface force for 4pt_4r_two_2mwl configuration.

4.6. Demonstration of FLV Notching

Once the system level information (acceleration and force) is obtained, the input PSD for the test item by itself is derived. It is defined by simply enveloping the interface acceleration curves between the test item and the mounting structure. According to NASA Handbook 7005 [18], there are many ways of enveloping the acceleration curves. They include 1) Normal Tolerance Limits, 2) Distribution – Free Tolerance Limits, 3) Empirical Tolerance Limits, 4) Normal Prediction Limits and 5) Simple Envelope of accelerations. In this study, the accelerations are enveloped by simple envelope of accelerations being less conservative of all the above-mentioned techniques. This is accomplished by enveloping the peak values of accelerations by the horizontal lines and maintaining the slope as a multiple of ± 6 dB between two adjacent horizontal lines and at the two edges of the curve.

To demonstrate the FLV notching, the configuration of 4pt_4o_two_2mwl t at the system level is considered. There is no particular reason for selecting this case, except that it was the last case to be tested at the system level. The configuration of the test item is 4pt_4o_ystf_wo, i.e., test item is without lumped mass, has Y – Stiff as the stiffening member and is attached at 4 attachment points all in Ortho direction. The mounting structure has lumped mass on all the plates (top, middle and the side plates). Since there is not much variation in the acceleration peaks at the interface points they are enveloped by a straight line.

The interface acceleration and the envelope spectrum are shown in the Figure 4-29. It

was found that the acceleration envelope accounts for 23.0 g RMS, which is way above the 10 g RMS that test item was designed for. Hence the input level is dropped to 5.8 g RMS maintaining the slopes of the curve and reducing by 16 the height of the horizontal lines. This corresponds to scaling down the original envelope spectrum by -12 dB.

Using the relevant maximum interface accelerations and interface force measured at system level, and the procedure shown in the previous section, the C^2 value is estimated. In real-life situation, one does not have system level data for deriving this critical parameters; the C^2 value is thus derived based on one or several of the guidelines discussed in Section 3.2.

Based on the apparent mass of the test item obtained from the low level vibration testing, the roll-off ratio 'n' is estimated by fitting a straight line having the proper slope between the resonances and the anti-resonances above the fundamental frequency. This is achieved using a custom-made Matlab program, called 'softflv', developed by the Space Technologies Sector of CSA for simplifying the implementation of FLV. Implementing the two relations for the semi-empirical method of FLV shown as Eqs. (1-9) and (1-10) in Chapter 1 and using all required parameters now known, softflv computed the force limits at the frequencies where the force limits change slopes. The force limits and the corresponding acceleration input values are given in Table 4-5. These values are input to the vibration control system so that the input acceleration is notched whenever the force at the interface increases more than the limit specified in the frequency range. Proper

abort and alarm level are set for the input acceleration so as to control the maximum input acceleration to the test item.

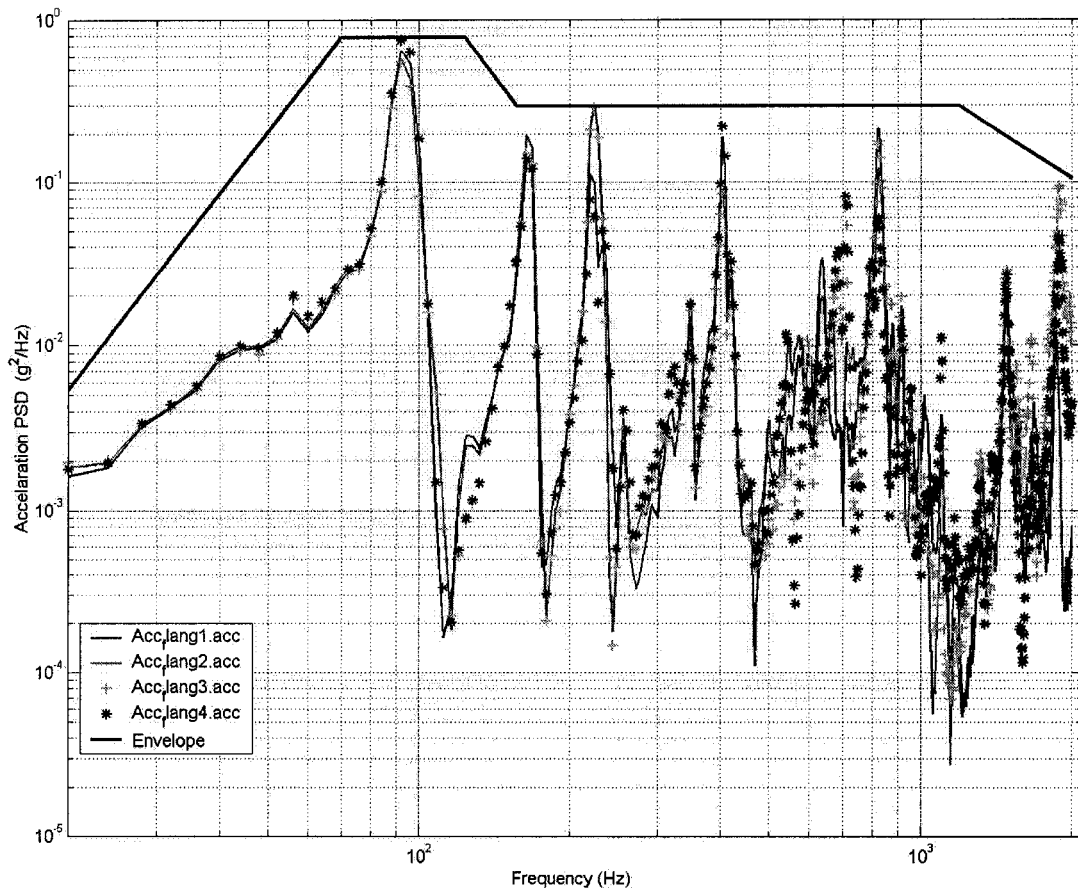


Figure 4-29. Interface accelerations for 4pt_4o_two_2mwl and the input acceleration (envelope) for testing of test item by itself.

Table 4-5. The acceleration input and corresponding force limit for testing of test item with FLV procedure.

| Frequency (Hz) | Acceleration Input (g²/Hz) | Force limit (lbf²/Hz) |
|---------------------------|--|---|
| 20 | 3.32×10^{-4} | 0.636 |
| 70 | 49×10^{-3} | 103. |
| 125 | 49×10^{-3} | 103. |
| 158 | 19×10^{-3} | 40.2 |
| 256 | 19×10^{-3} | 40.2 |
| 1200 | 19×10^{-3} | 1.83 |
| 2000 | 6.86×10^{-3} | 0.24 |

The interface force obtained at the system level testing is shown in Figure 4-30.

The input acceleration and forces to the test item with and without FLV are shown in Figures 4-31 and 4-32, respectively.

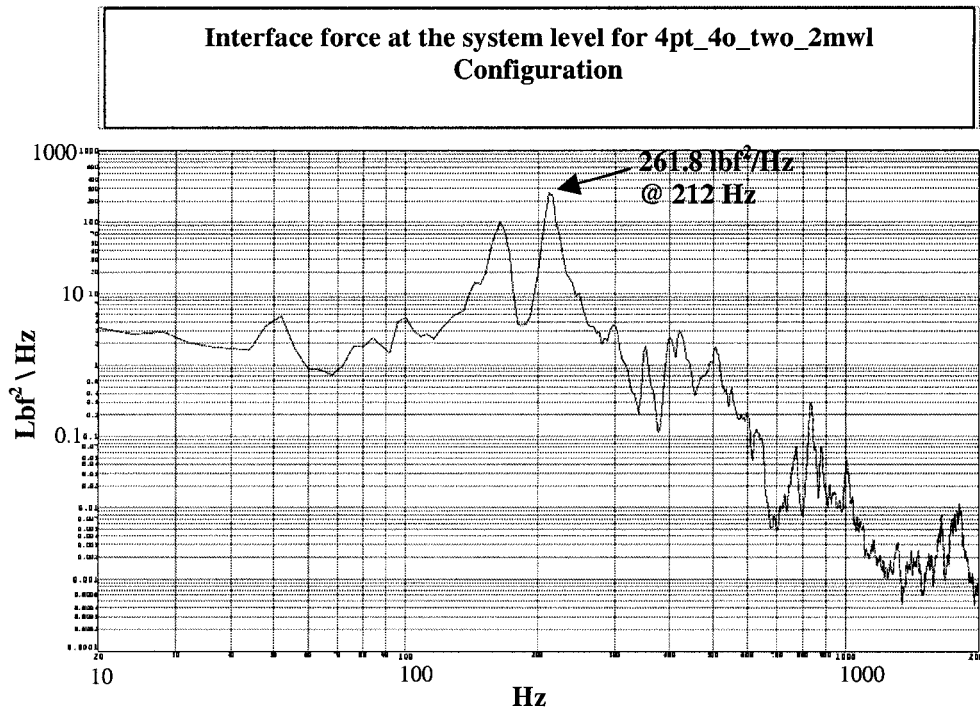


Fig 4-30. Interface force at the system level for 4pt_4o_two_2mwl configuration.

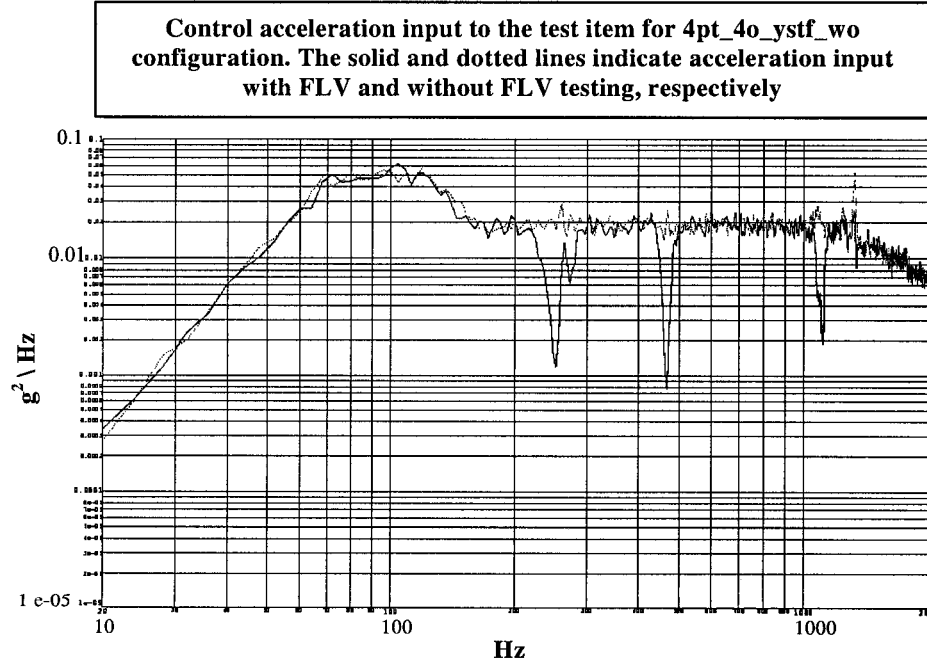


Figure 4-31. Control acceleration input to the test item for 4pt_4o_ystf_wo configuration. The solid and dotted lines indicate acceleration input with FLV and without FLV testing, respectively.

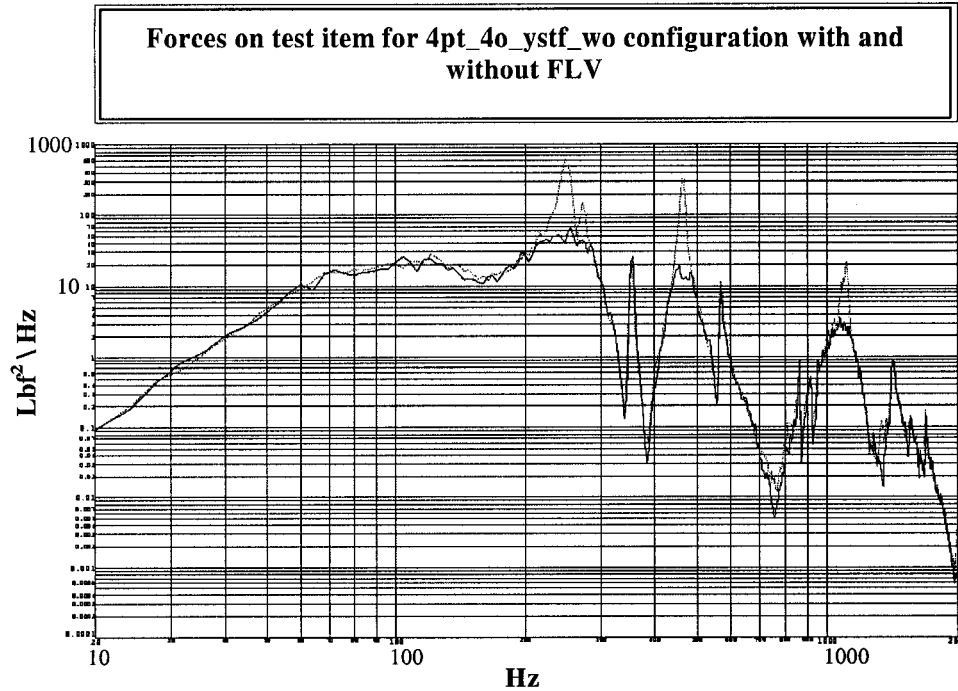


Figure 4-32. Forces on test item for 4pt_4o_ystf_wo configuration. The solid and dotted lines indicate acceleration input with FLV and without FLV testing, respectively.

The notching in the acceleration input for test implementing FLV is controlled by the force limit specified earlier, which is obtained from the interface force shown in the Figure 4-30.

The input acceleration PSD at the fundamental frequency of the test item is reduced by – 15 dB and the force RMS value (between 20 to 2000 Hz) at the base of the structure has been reduced by about 50% by implementing the FLV testing.

4.7. Results and Conclusions

The structures used for the experimental sensitivity study are not exactly the same as the ones used for analytical sensitivity study in terms of the location of attachment point of lumped masses. Hence to compare the results, the FEM is modified accordingly for all the cases.

The results (C^2 value) obtained by both the experimental and analytical sensitivity study are tabulated in Tables 4-6 and 4-7 for X and Z direction, respectively. The values in the last column indicate the range of analytical values with damping. The first value is obtained when the test item and mounting structure are assumed to have an amplification factor of 50, and the second values is obtained for an amplification factor of 20. The cases in the Z direction where the range of C^2 is not indicated, the value accounts for an amplification factor of 50.

Table 4-6. The C^2 values in X direction.

| Case No. | Case Name | Experiment | FEM |
|----------|-------------------|------------|------------|
| 1 | 4pt_4r_two_mwl | 3.87 | 10.2 - 9.1 |
| 2 | 4pt_4r_two_2mwl | 4.37 | 16.5 - 8.7 |
| 3 | 4pt_4r_two_mwo | 1.82 | 5.6 - 4.7 |
| 4 | 8pt_4r4o_two_mwo | 1.46 | 5.4 - 3.8 |
| 5 | 8pt_4r4o_twl_2mwl | 0.76 | 1.4 - 1.4 |
| 6 | 8pt_4r4o_two_mwl | 5.74 | C.N.E |

Table 4-7. The C^2 values in Z direction.

| Case No. | Case Name | Experiment | FEM |
|----------|-------------------|------------|-----------|
| 1 | 4pt_4r_two_mwl | 3.1 | 3.8 |
| 2 | 4pt_4r_two_2mwl | 3.0 | 3.8 - 3.2 |
| 3 | 4pt_4r_two_mwo | 3.0 | 3.6 - 3.4 |
| 4 | 4pt_4r_twl1_2mwl | 11 | 14 |
| 5 | 4pt_4r_twl2_2mwl | 2.7 | 7.0 |
| 6 | 8pt_4r4o_two_mwl | 1.1 | 0.8 |
| 7 | 8pt_4r4o_two_2mwl | 0.92 | 0.86 |
| 8 | 8pt_4r4o_two_mwo | 1.6 | 0.8 - 0.9 |
| 9 | 8pt_4r4o_twl_mwl | C.N.E | C.N.E |
| 10 | 4pt_4o_two_2mwi | 7.2 | 6.4 - 6.5 |

It can be observed from Table 4-6, that the experimental value of C^2 is at most half of the analytical value. The reason for such discrepancy between experimental and FEM results in C^2 value in the X direction can be attributed to the fact that the experimental fundamental frequency of the mounting structure by itself is about 30% - 35% lower than the result obtained from FEM.

It can be noted from the values of C^2 in the Z direction that the FEM models of the test structures represent the manufactured structures to a greater extent than in the X direction. However for the case 5, there is a large variation of C^2 value. The reason for this particular variation is the way the middle plate is attached to the side plates in the

manufactured part. In this particular case, the lumped mass is distributed evenly on top plate and the middle plate. The fundamental mode of the test item by itself was due to the middle plate (which was the same in both the analytical and experimental study). On the other hand, at the system level, the mode corresponding to the peak adjacent to the anti-resonance (corresponding to the fundamental frequency of the test item by itself) was due to top plate in the analysis and middle plate in experimental study. Hence in general sense, the results of the case cannot be compared.

The cases with C.N.E indicates that the interface accelerations and the forces could be extracted from the response at the interface as the mode corresponding to the peak adjacent to the anti resonance got mixed with the system level modes. Hence the value of C^2 is not evaluated for these cases. The cases 4 and 5 in the Z direction are named in a different form as they both have the lumped mass on the test item, but the location is different from each other. In case 4, most of the mass is added on the top plate; while in case 5, the mass is distributed more evenly on top and middle plate than in case 4. As mentioned earlier, the mounting structure with lumped mass only on top and middle plate is named as mwl, while the structure with lumped mass on top, middle and side plates is named as 2mwl.

In summary, the experimental sensitivity study validates the procedures and results of the analytical sensitivity study since the results of the experimental C^2 values are in agreement with their analytical counterparts for the cases for which the excitation is in the vertical direction. The case for which the experimental C^2 value is 11 is of particular

interest since it confirms experimentally that this parameter can be above 5 which is the maximum limit normally found in the literature. It is found that when the excitation is in the horizontal direction, $C2$ values for the experimental study are at most half of the values obtained in the analytical study. However, this discrepancy may be attributed to shortcomings in the FE model of the test structures

CHAPTER 5

SUMMARY, CONCLUSIONS AND RECOMMENDATIONS

5.1. Summary

In conventional vibration testing of aerospace hardware, the acceleration input to the base of the test item is controlled to the specifications, namely the envelope of the acceleration peaks of the flight environment. This conventional approach to testing has been known for over forty years to greatly overtest the test item at its own natural frequencies. This is caused by impedance differences of the mounting structure between the flight and the testing environments. The penalty of overtesting with conventional vibration test appears in design and performance compromises, as well as in the high costs and schedule slippage associated with recovery from artificial test failures that would have not occurred in a flight environment.

The purpose of Force Limited Vibration (FLV) testing developed at NASA JPL is to reduce the overtesting occurring during conventional vibration testing. In addition to controlling the input acceleration, the FLV testing measures and limits the reaction force between the test item and the shaker. This force limiting technique results in acceleration notching at predominant natural frequencies of the test item. The semi-empirical method is presently the approach most widely applied to derive the force limits between the test item and the shaker, due to its advantages over the previously developed more analytical simple and complex TDFS methods. Although the semi-empirical method is very powerful and has been applied successfully on numerous space missions, there is still

some work to be done to make everyone comfortable with its use. Due to its partly empirical nature, the crucial C^2 parameter which sets the force limits throughout the complete frequency bandwidth of excitation is based either on the extrapolation of interface forces for similar mounting structures and test items, or on comparison with results of techniques such as the TDFS methods or the limit load factors. Based on limited number of flight data, it has been observed that, in normal conditions, C^2 value as low as 2 might be chosen for complete spacecraft or strut-mounted heavier equipment, C^2 value as high as 5 might be considered for directly mounted lightweight test items. This range of 2 to 5 for adequate selection for the C^2 value is what is generally mentioned in the literature on FLV.

The objective of the present thesis is to present a comprehensive and complete analytical and experimental investigation on the semi-empirical method. More specifically, the present work investigates the range of C^2 values which might be expected for space hardware and the parameters on which it depends. The present study provides a platform to acquire a better understanding of the semi-empirical method so that it can be used in aerospace community more comfortably.

The analytical sensitivity study was performed to cover (1) a large range of effective mass ratio (which is considered a major factor for defining the force limits, according to TDFS techniques), (2) several numbers of attachment points, (3) different directions of excitation, and (4) different damping of the test structures. To perform the analytical and experimental sensitivity studies, very versatile test structures (test item and mounting structure) and related test fixtures were designed based on pre-defined design

requirements. Finite-element (FE) models of the test structures and the fixtures were developed for the design and analysis of the structures and the sensitivity studies. The test items, mounting structures and fixtures were later manufactured to be used in the experimental sensitivity study.

More than 70 cases were selected to perform the analytical sensitivity study on the basis of (1) number of attachment points for each structure, (2) position of attachment points, (3) fundamental frequency of the test structures, (4) stiffness of structures, (5) damping of structures, (6) direction of excitation, and (7) mass ratio of both structures.

The experimental sensitivity study was performed on the manufactured structures to validate the procedures and results obtained in the analytical sensitivity study. This experimental work was done on 16 selected cases of the analytical sensitivity study. The selection of the test cases was based on pre-defined guidelines.

5.2. Conclusions

The following important conclusions can be drawn from the analytical and experimental sensitivity studies undertaken in this research. Based on the analytical sensitivity study:

1. It has been observed that most often the range of value of C^2 range is between 2 and 5, as reported in the literature. However, there are several cases when this value is higher than 5 (between 10 and 17).
2. The results indicate that the C^2 value depends mainly on the number and position of the attachment points, the effective mass ratio between the test item and the

mounting structure, the direction of excitation, the fundamental frequency of the test structures, and the stiffness of the test structures. However, the factors such as fundamental frequency and stiffness of the structures are inter-dependent.

3. For all cases, except for three exceptions, the C^2 value does not depend on the damping in the structure.
4. The notching of input acceleration PSD at the fundamental mode of the test item, due to the force limits, covered a broad range of -9 to -30 dB. The main parameters affecting the notching level are the damping in the structures and the effective mass ratio.

The experimental sensitivity study validated the procedures and the results of the experimental C^2 values were in agreement with their analytical counterparts for the cases for which the excitation was in the vertical direction. It was found that, when the excitation was in the horizontal direction, C^2 values for the experimental study were approximately half of the values obtained in the analytical study. However, as explained in details in Chapter 4, this discrepancy may be attributed to shortcomings in the FE model of the test structures.

5.3. Recommendations for Future Work

Although this thesis has taken an important step towards the understanding of semi-empirical method, other numerous and interesting aspects are identified to complement and improve the results of the sensitivity studies performed to evaluate the C^2 parameter

of the semi empirical method, and the parameters on which it depends. These thoughts for future work are summarized as follows:

1. Improving the FEM of the mounting structure to account for the drop in fundamental frequency of the structure and the stiffness at different locations on the structure.
2. Comparing the results obtained from the sensitivity study with the more analytical simple and complex TDFS methods.
3. Increasing the range of effective/physical mass ratio of the test structures. A solution would be to design a smaller test item with the least possible mass, so that the current test item can also act as mounting structure if the stiffness members are removed.
4. Obtaining flight level data in order to compare the input level where the test items are tested to the actual vibration level felt during the actual launch.

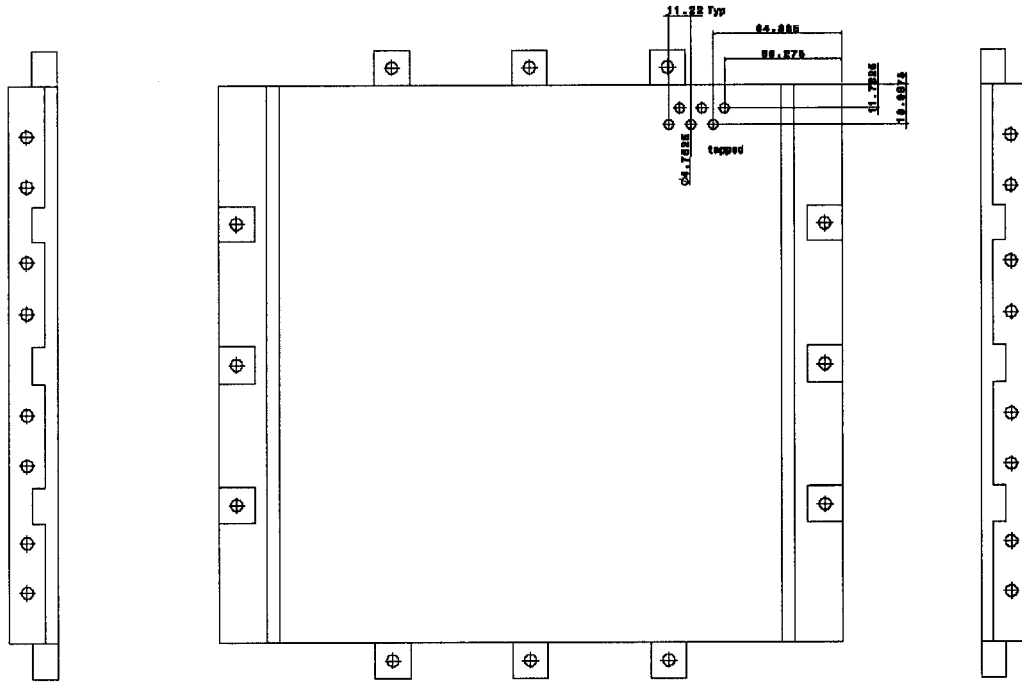
REFERENCES

1. Scharton, T.D., "Force Limited Vibration Testing Monograph", NASA Reference Publication RP 1403, JPL, Pasadena, Ca. May 1997, 117 pages.
2. Soucy, Y. et al., "Force Limited Vibration Testing Applied to the FTS Instrument of SCISAT-1", Proceedings of the ASTRO-2002, 12th Conference on Astronautics, Ottawa, ON, Nov 2002.
3. Blake, R.E., "The need to control the output impedance of vibration and shock machines", Shock and Vibration Bulletin, No.23 June 1956, pp. 59-64.
4. Morrow, C.T., "Application of Mechanical Impedance Concept to Shock and Vibration Testing", Los Angeles, CA, TRW Report AD-608030, 1960.
5. Slater, J.P., "Taming the General-Purpose vibration Test", Shock and Vibration Bulletin, No.33, Pt.3, March 1964, pp. 211-217.
6. Ratz, A.G., "An Impedance Compensated Random Equalizer", Proceedings of the Institute of Environmental Sciences 12th Annual Technical Meeting, San Diego, April 1966, pp. 353-357.
7. Painter, G.W., "Use of Force and Acceleration Measurements in Specifying and Monitoring Laboratory Vibration Tests", Shock and Vibration Bulletin, No. 36, Pt.3, Jan. 1967.
8. Murfin, W.B., "Dual Specification in Vibration Testing", Shock and Vibration Bulletin, No.38, Pt.1, 1968.
9. Witte, A.F. and Rodeman, R., "Dual Specification in Random Vibration Testing, An Application of Mechanical Impedance", Shock and Vibration Bulletin, No 41, Pt.44, 1970, pp. 109-118.

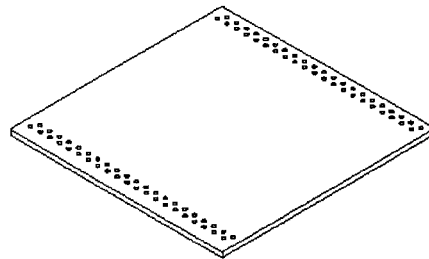
10. Hunter, N.F. and Otts, J.V., "The Measurement of Mechanical Impedance and Its Use in Vibration Testing", Shock and Vibration Bulletin, No.42, Pt.1, 1972, pp. 79-88.
11. Wada, B.K., Bamford, R. and Garba, J.A., "Equivalent Spring-Mass System: A Physical Interpretation", Shock and Vibration Bulletin, No.42, Pt.5, 1972, pp. 215-225.
12. Scharton, T.D., "Force Limited Vibration testing at JPL", Proceeding of the Institute of Environmental Sciences 14th Aerospace Testing Seminar, 1993, pp. 241-251.
13. Scharton, T.D., "Vibration-Test Force Limits Derived From Frequency Shift Method", AIAA Journal of Spacecraft and Rockets 32(2), 1995, pp. 312-316.
14. Scharton, T.D. and Chang, K., " Force Limited vibration Testing of the Cassini Spacecraft and Instruments", IES 17th Aerospace Testing Seminar, Los Angeles, Ca., Oct. 14, 1997.
15. Scharton, T.D., " In-Flight Measurements of Dynamic Force and Comparison With Methods Used to Derive Force Limits For Ground Vibration Tests", Proceedings of European Conference on Spacecraft Structures, Materials and Mechanical Testing, Braunschweig, Germany, 1998, pp. 583-588.
16. Worth, D.B. and Kaufman, D.S., " Validation of Force Limited Vibration Testing", Journal of the IEST 41(3), May/June 1998, pp. 17-23.
17. Scharton, T.D., "Force Limits Measured on a Space Shuttle Flight", Proceedings of the European Conference on Spacecraft Structures, materials, and Mechanical Testing, Nov 2000, Noordwijk, NL.

18. Chang, K.Y., "Force Limit Specifications VS Design Limit Loads In Vibration Testing", Proceedings of the European Conference on Spacecraft Structures, materials, and Mechanical Testing, Nov 2000, Noordwijk, NL.
19. Scharon, T.D., "Force Limited Vibration Testing', NASA Technical Handbook, NASA-HDBK-7004A, Nov. 2002, 30 pages.
20. Kaufman, D.S. and Worth, D.B., " Follow on Validation of Force Limited Vibration Testing", Proceedings of 19th Aerospace Testing Seminar, Manhattan Beach, Ca. 2000, pp. 338-351.
21. Amato, D., Pankow, D. and Thomsen, K., "Force Limited Vibration Test of HESSI Imager", Presented at the IIAV's ICSV7, Garmisch, Germany, July 2000..
22. Chang, K.Y., "Deep Space 1 Spacecraft Vibration Qualification Testing", Journal of Sound and Vibration 35(3), March 2001, pp. 14-17.
23. Soucy, Y. and Coté, A., "Reduction of Overtesting During Vibration Tests of Space Hardware", CASI Canadian Astronautics and Space Journal 48(1), March 2002, pp 77-86.
24. Soucy, Y., Rao, V. and Sedaghati, R., "Investigation of Semi-Empirical Method for Force Limited Vibration Testing", Proceedings of the ASTRO-2002, 12th Conference on Astronautics, Ottawa, ON, Nov 2002.
25. Wirsching, P.H., Paez, T.L. and Ortiz, H., "Random Vibrations Theory and Practice", textbook of random vibrations, Wiley-Interscience, 1995.
26. Soucy, Y., "Design Requirements for the test articles for collaborative project Between CSA and Concordia University on Force Limited Vibration Semi-Empirical Method", CSA Internal Report Jan. 2002.

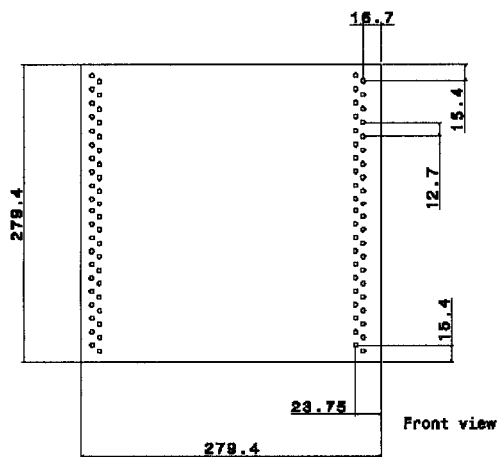
27. Sweitzer, K.A., "A Mechanical Impedance Correction Technique for Vibration Tests", Proceedings of Institute of Environmental Sciences, 1987, pp. 73-76.
28. Sedaghati, R., Yvan, S. and Etienne, N., "Efficient Estimation of Effective Mass for Complex Structures under Base Excitations", CASI Canadian Astronautics and Space Journal, to be appear in Sept. 2003 issue.
29. NASA GSFC, "General Environmental Verification Specification for STS and ELV, Payloads, Subsystems, and Components", June 1996.



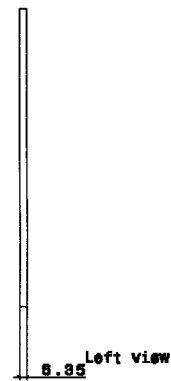
Top Plate:



Isometric view

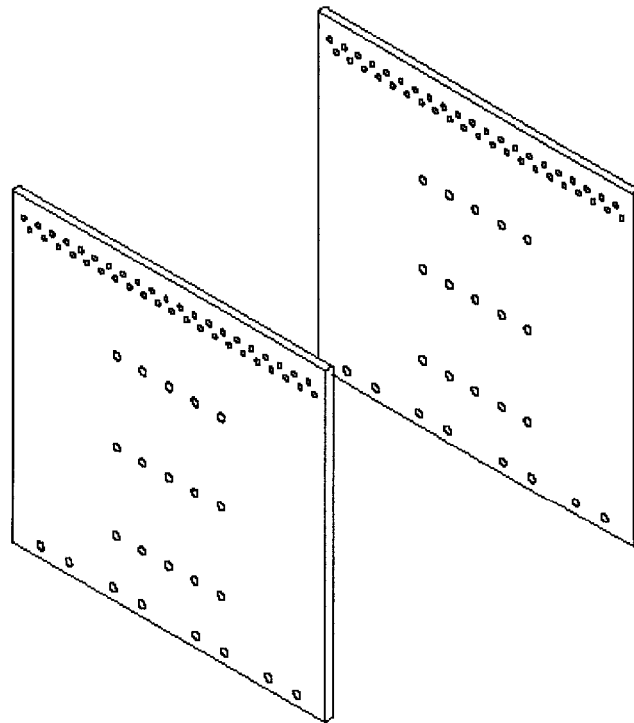
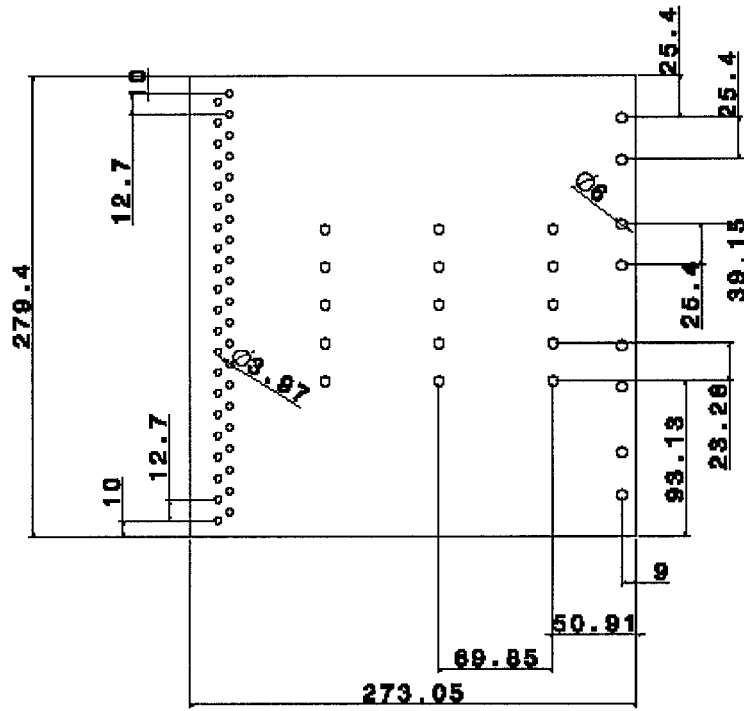


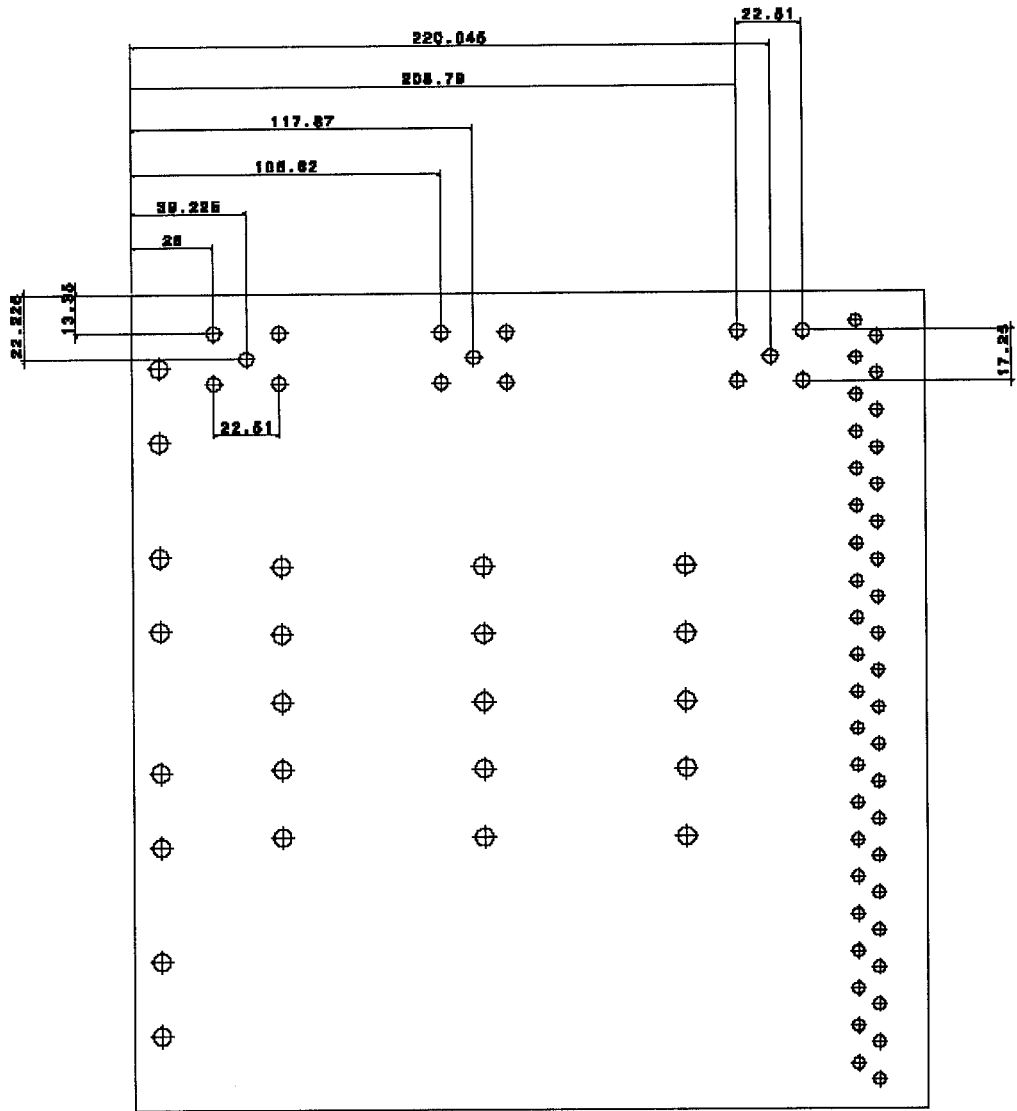
Front view



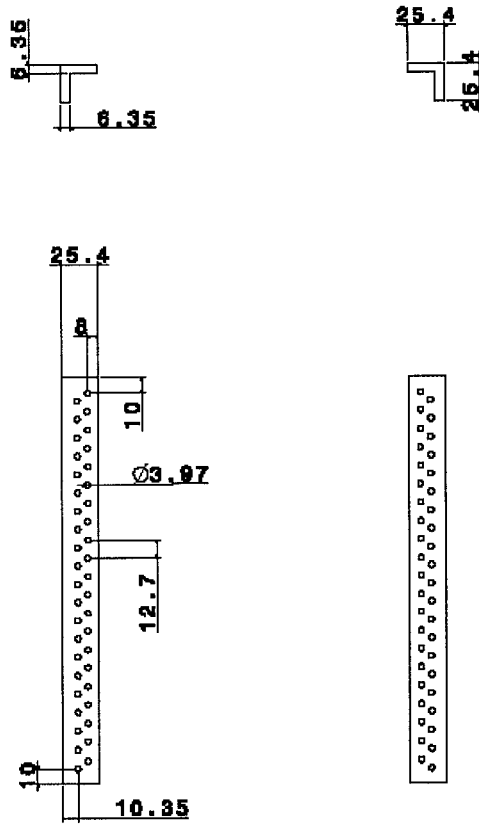
Left view

Side Plates:

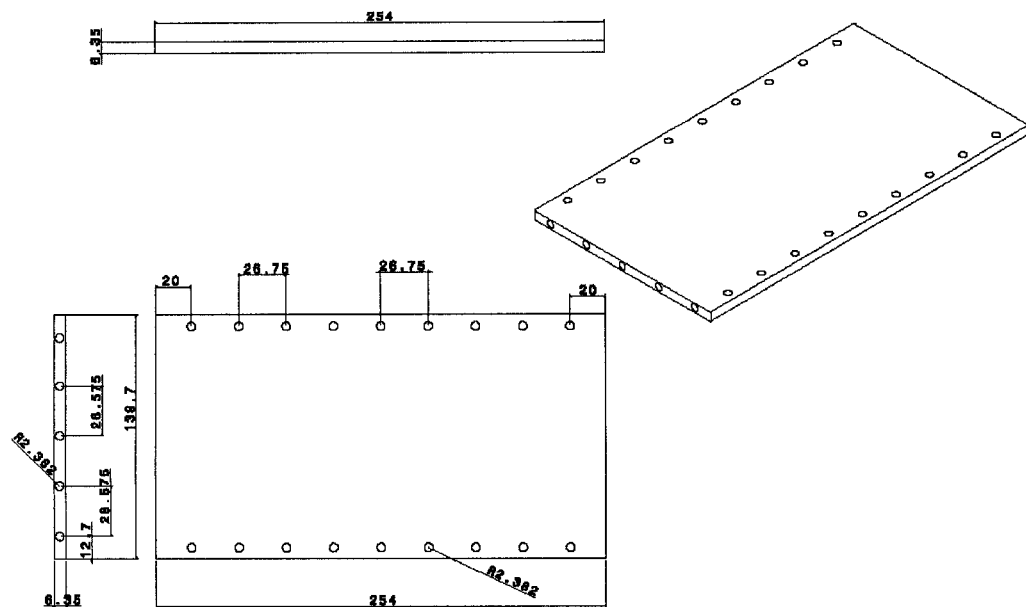


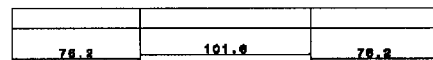
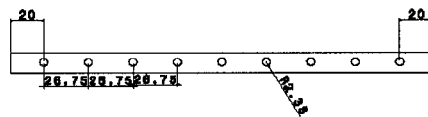
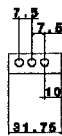
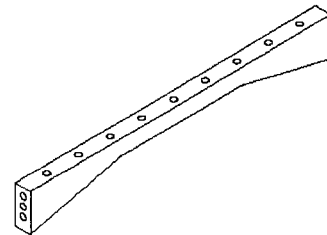
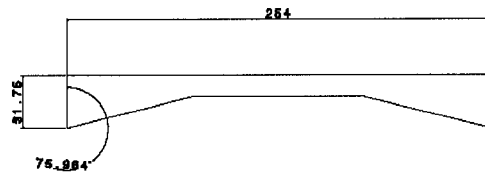
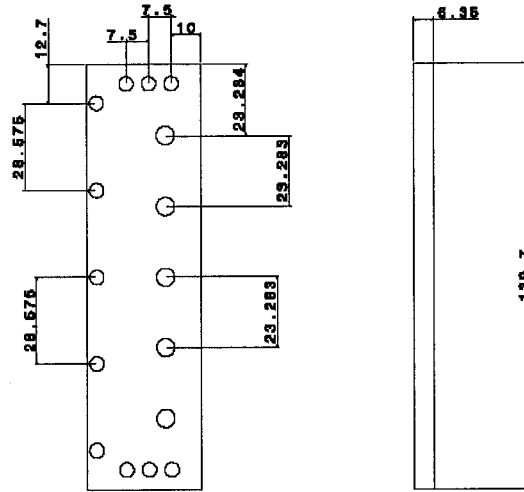
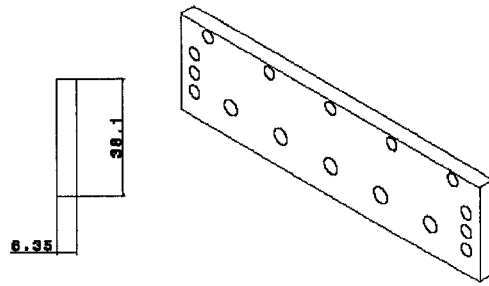


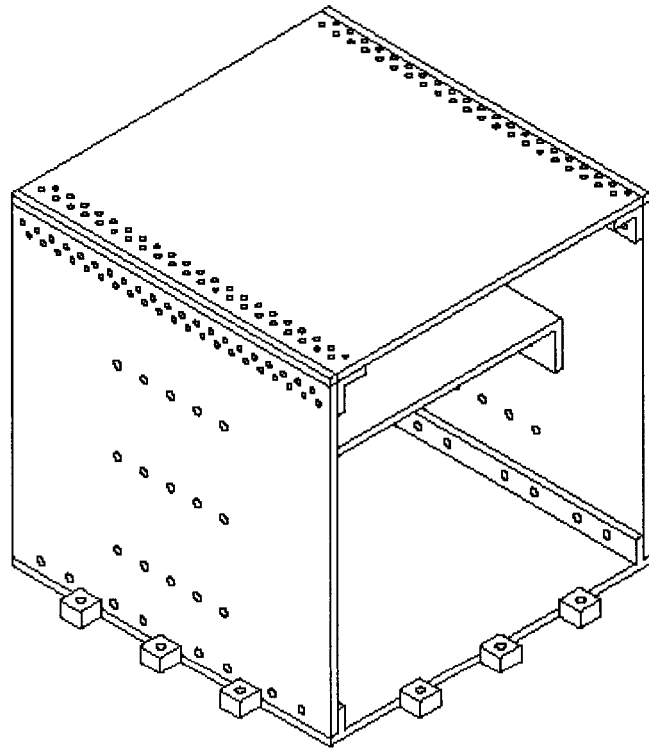
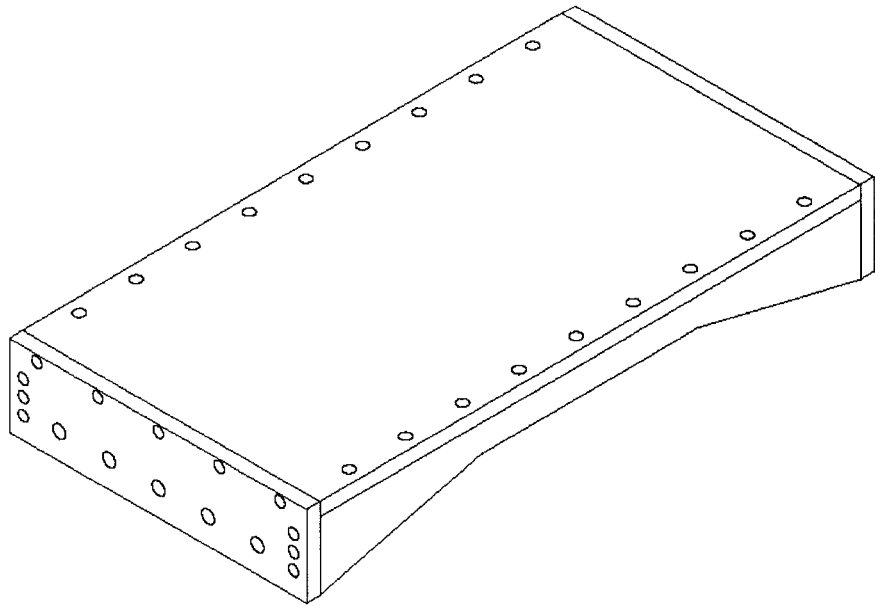
L-Beam:



Middle Plate:

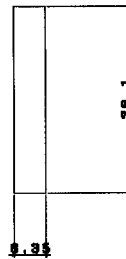
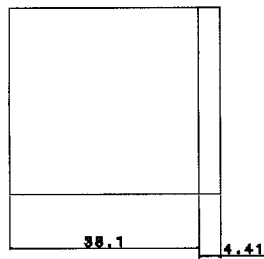
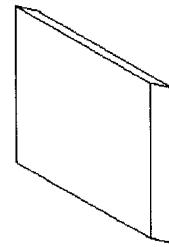
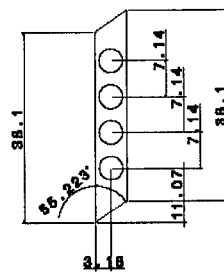
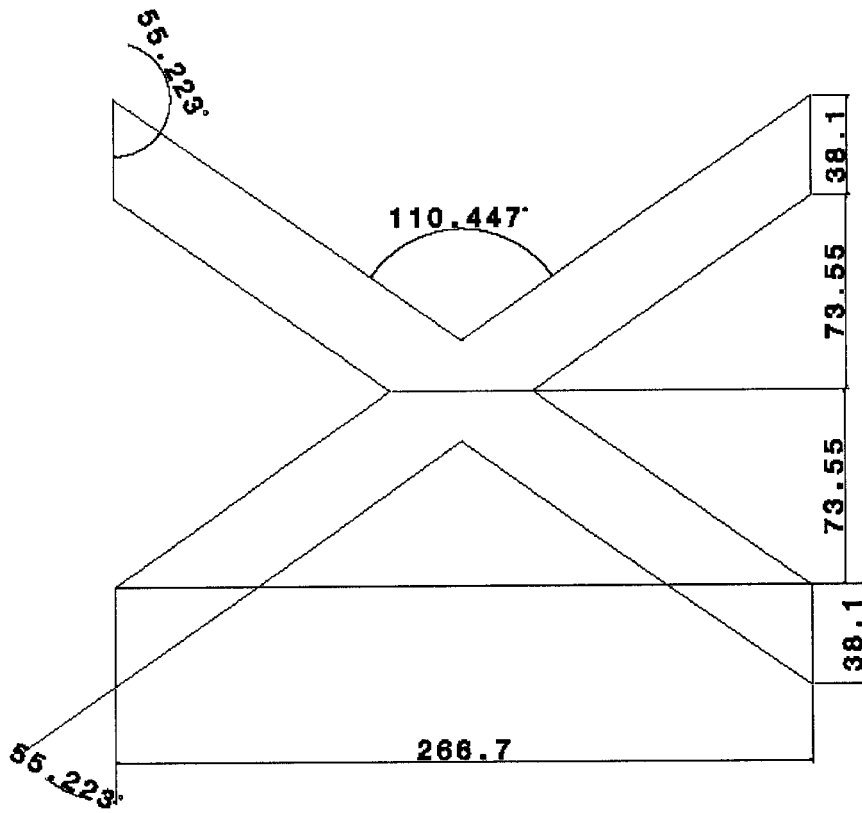


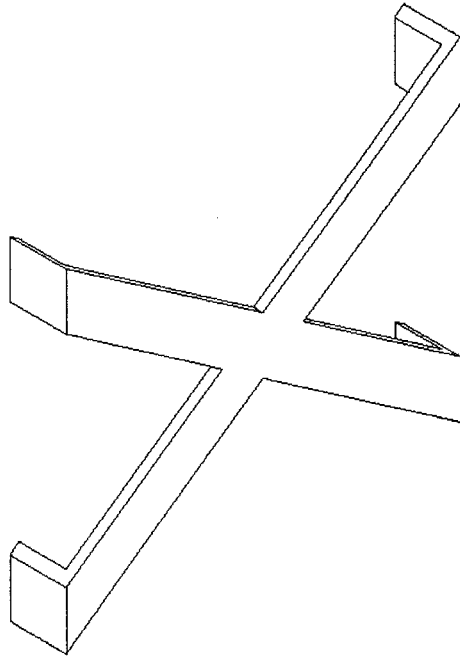
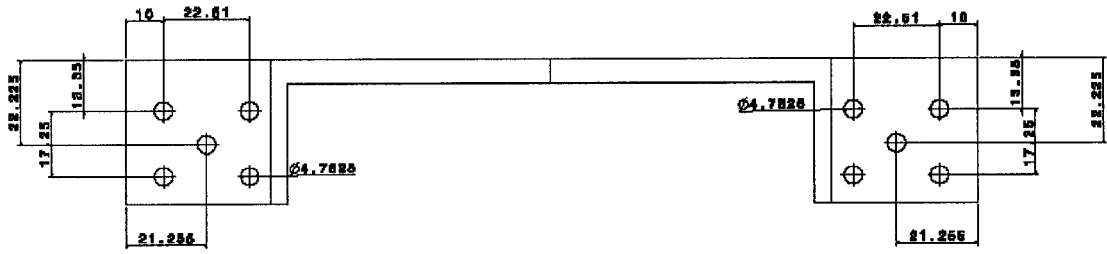




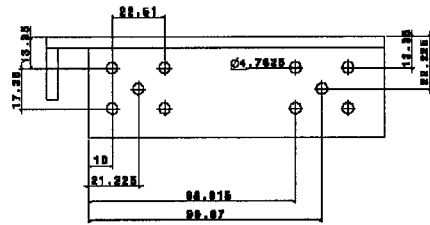
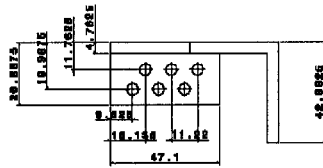
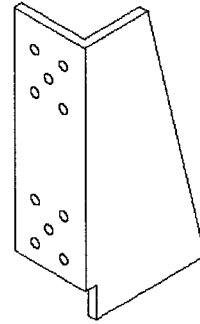
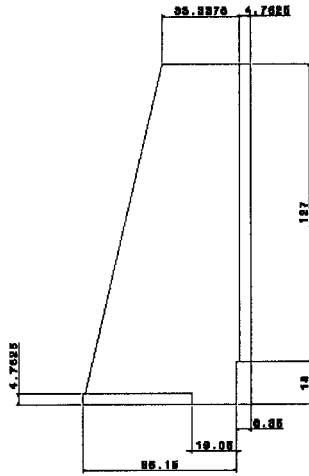
Stiffening Members:

X plate:

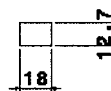
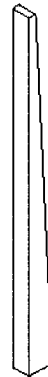
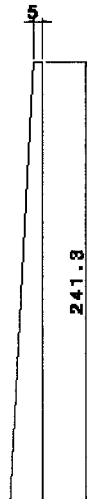




Y – Stiff:

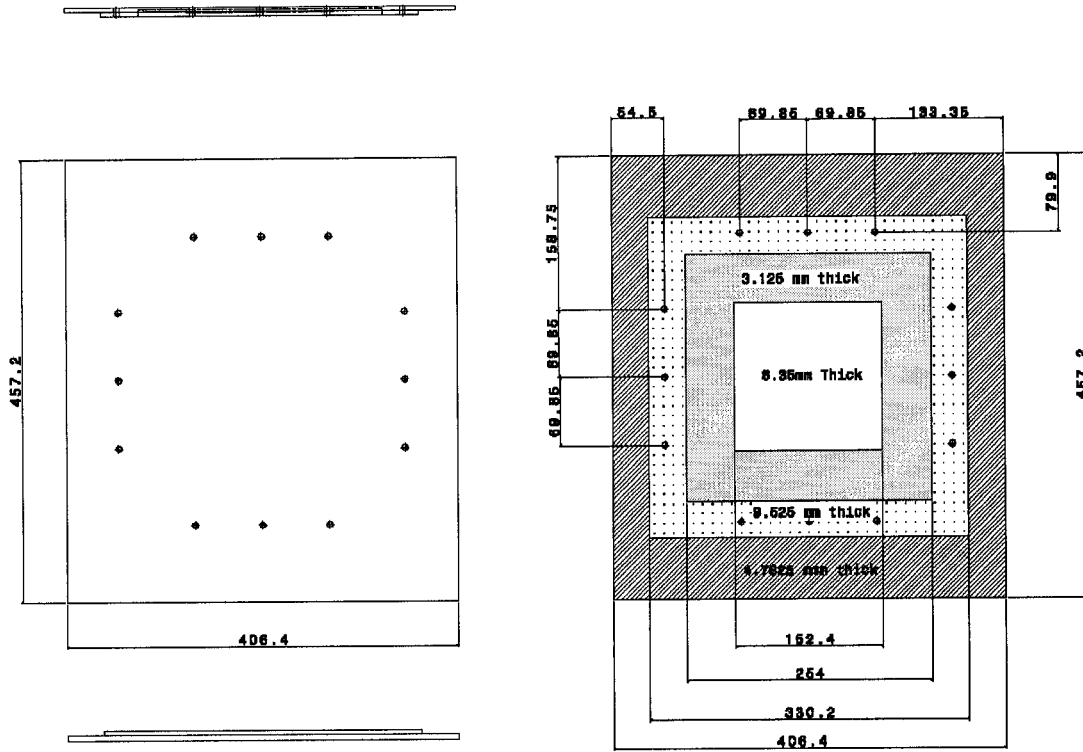


End Stiff:

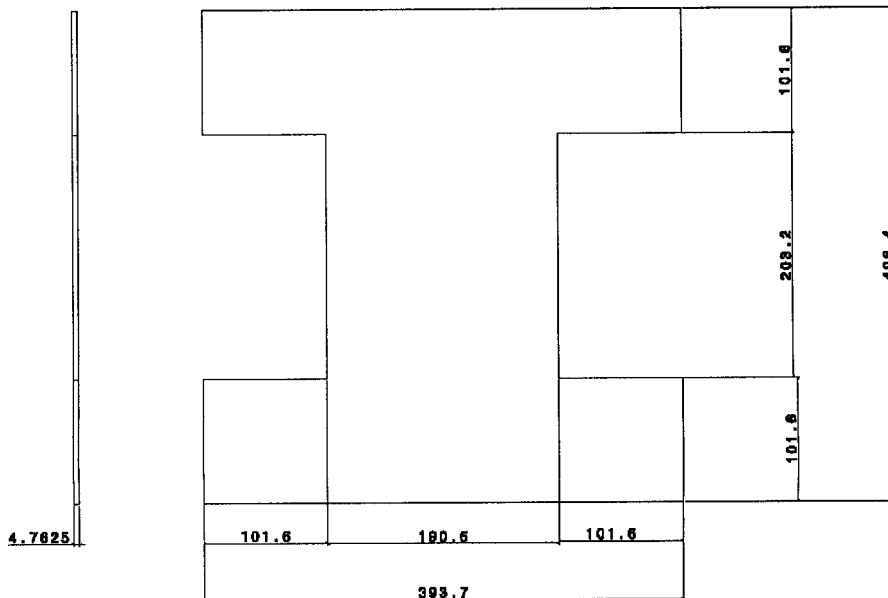


Mounting Structure

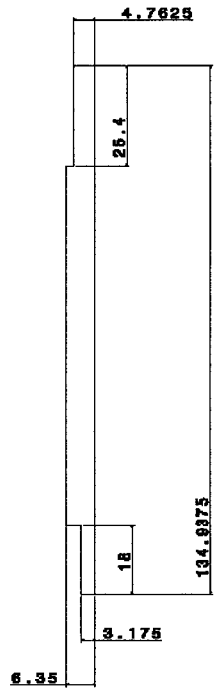
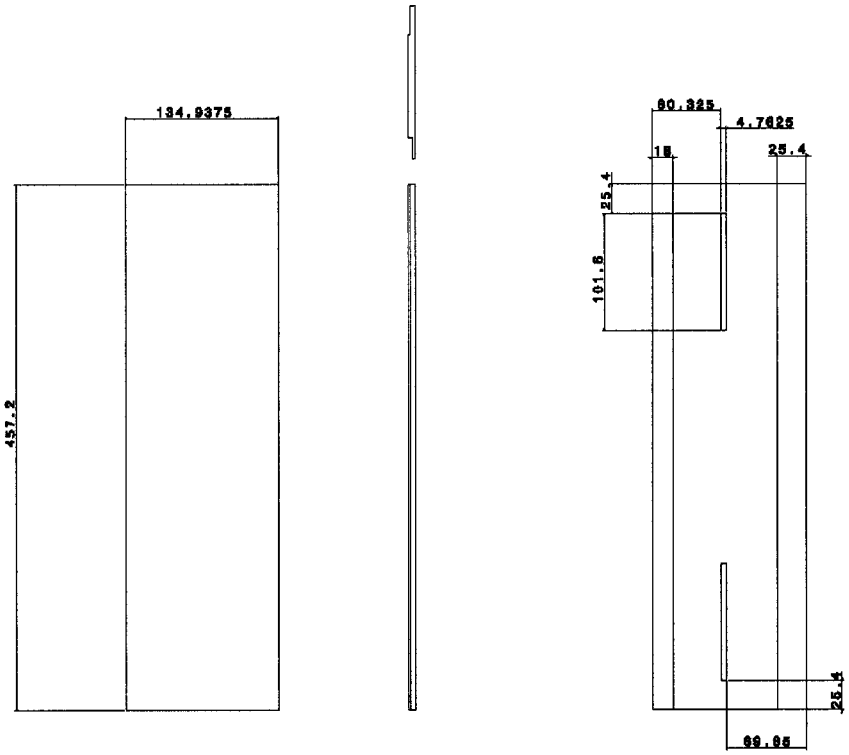
Top Plate:



Middle Plate:

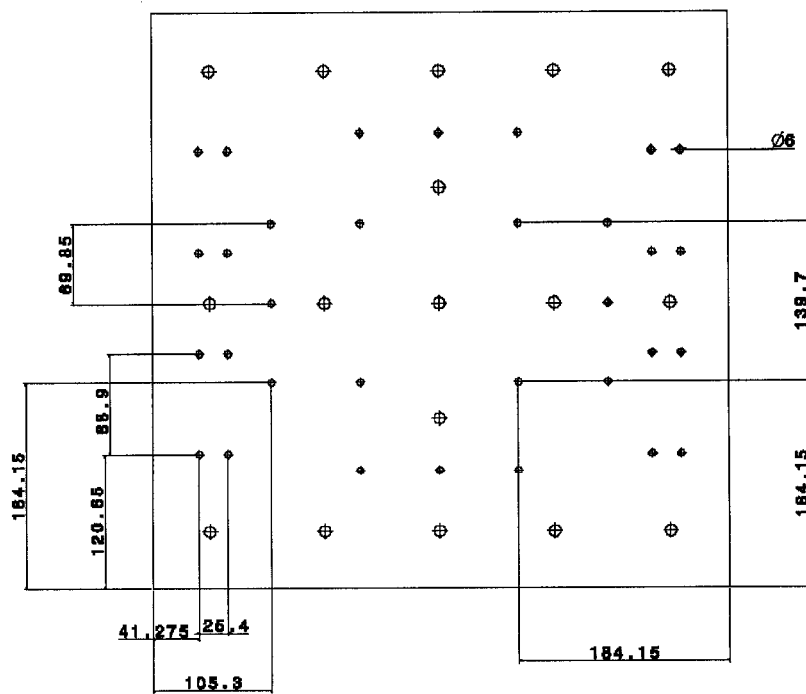
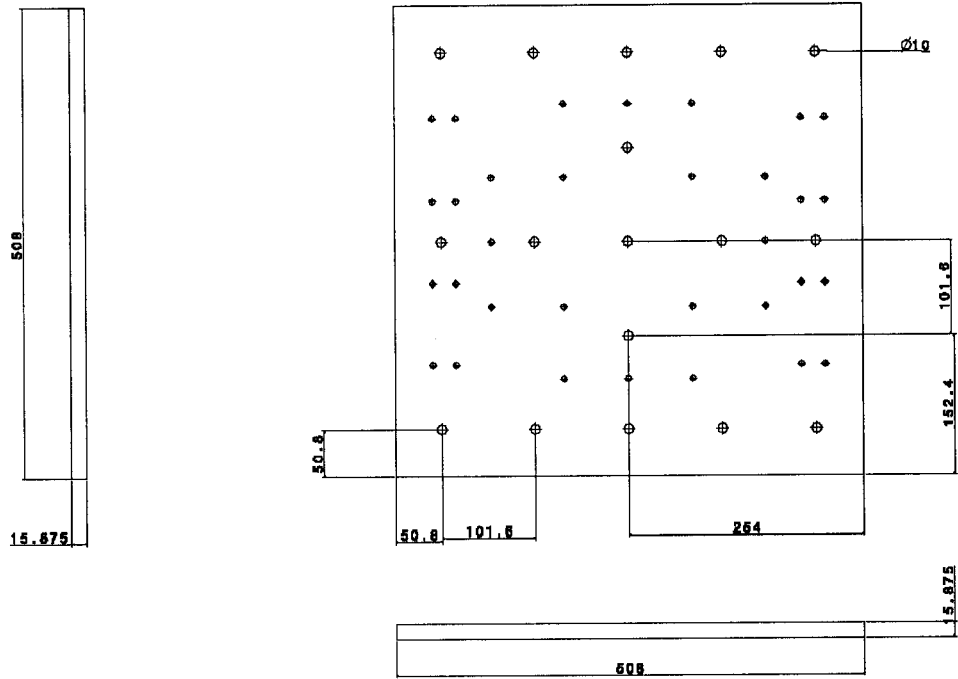


Side Plates:



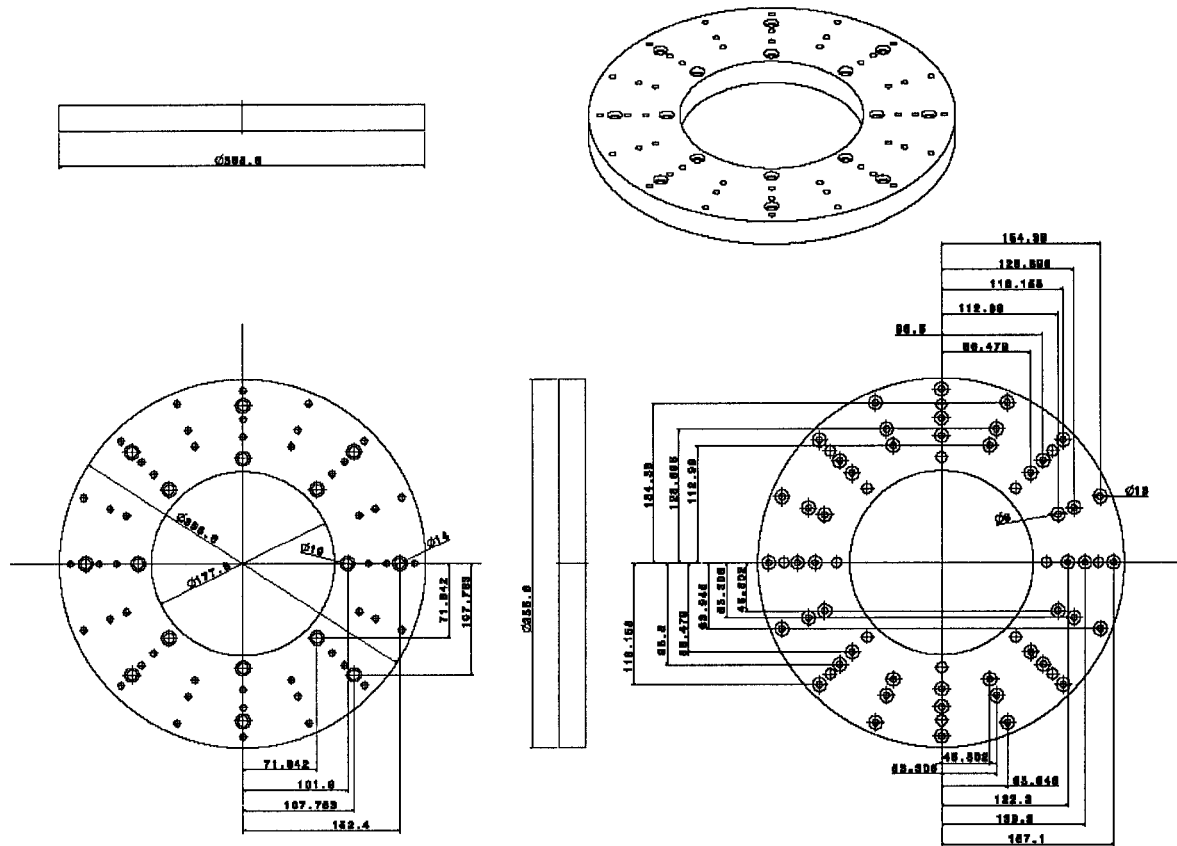
Fixtures

Horizontal Fixture:

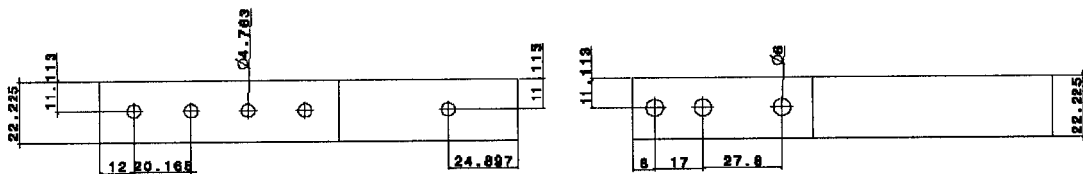
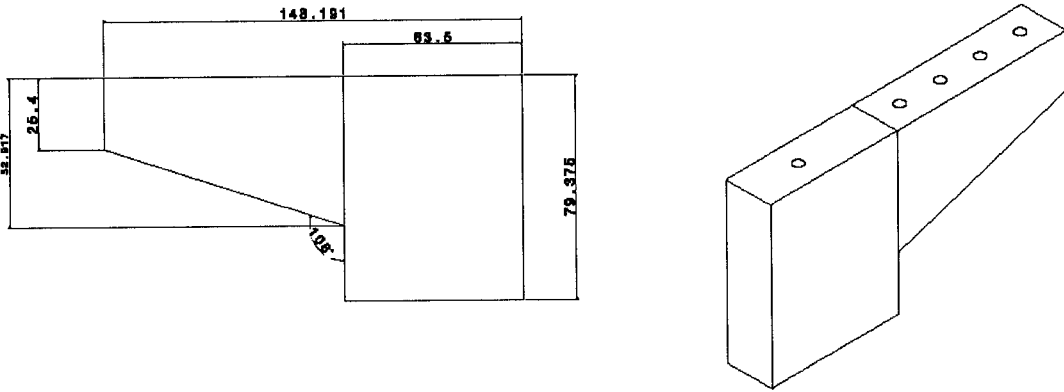
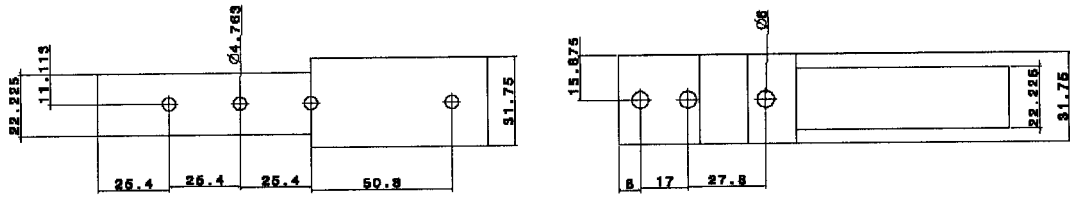
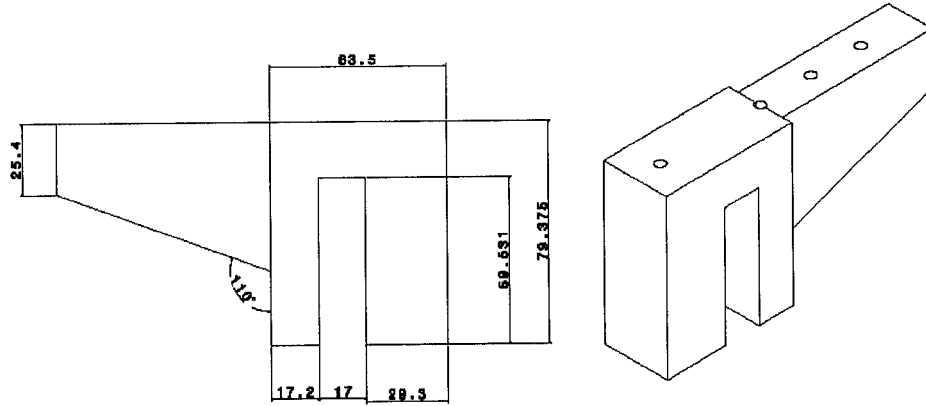


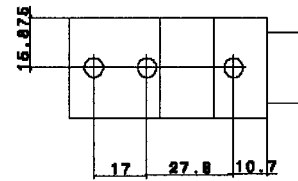
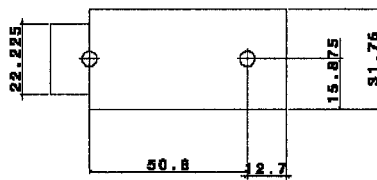
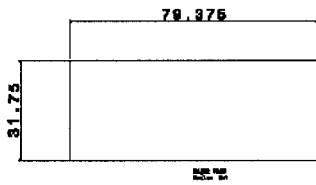
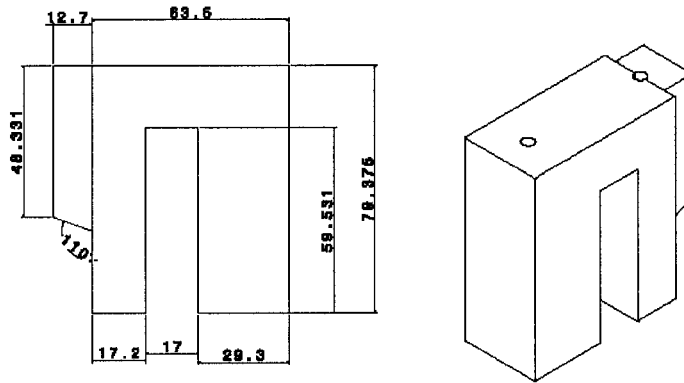
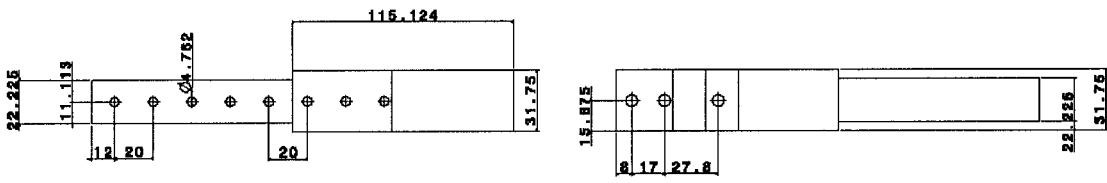
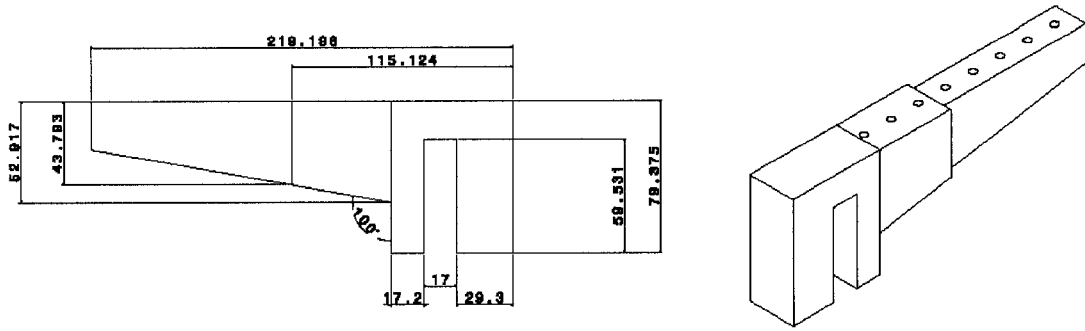
Vertical Fixture:

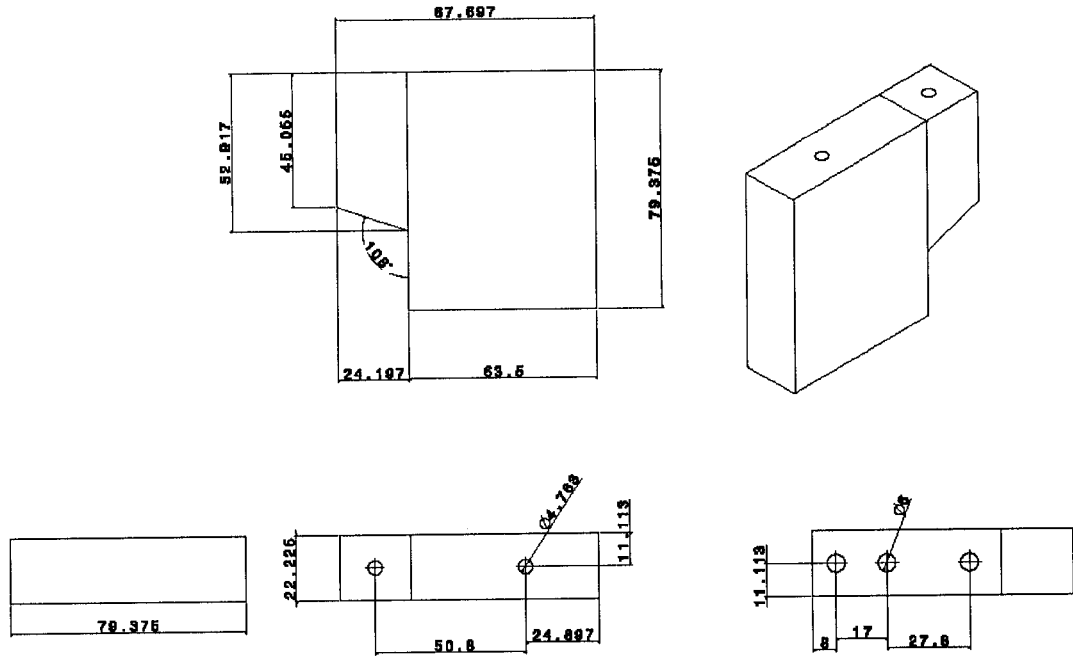
Bottom Plate:



Flanges:







Top Plate:

